Fisheries Research Report No. 205, 2010

Coastal and Marine Resource Condition Monitoring – Scoping Project

Final NRM Report – Project 073007

Part 2 – Field trial of potential resource condition indicators, and an exploration of the utility of remote sensing, for mangroves and intertidal mud flats in the Pilbara – Pilot study

Brett A Human, Katherine Murray,
Katherine Zdunic, and Graeme Behn

Government of **Western Australia**
Department of **Fisheries**

Australian Government

This project is funded by the Australian Government and the Government of Western Australia

Department of
Environment and Conservation

Our environment, our future

Fisheries Research Division
Western Australian Fisheries and Marine Research Laboratories
PO Box 20 NORTH BEACH, Western Australia 6920

Fish for the future

Fisheries Research Reports

Titles in the Fisheries Research Report series present technical and scientific information for use in management processes. Research Reports are subject to full internal refereeing by senior scientists of the Fisheries Research Division, and in many cases, elements of the work are published in international scientific literature.

Correct citation:

Human, B.A., Murray, K., Zdunic, K., and Behn, G. 2010. Field trial of potential resource condition indicators, and an exploration of the utility of remote sensing, for mangroves and intertidal mud flats in the Pilbara – Pilot study. Coastal and Marine Resource Condition Monitoring – Scoping Project. Final NRM Report, Project 073001 – Part 2. Department of Fisheries, Government of Western Australia. 104 pp.

Enquiries:

WA Fisheries and Marine Research Laboratories, PO Box 20, North Beach, WA 6920
Tel: +61 8 9203 0111
Email: library@fish.wa.gov.au
Website: www.fish.wa.gov.au
ABN: 55 689 794 771

A complete list of Fisheries Research Reports is available online at **www.fish.wa.gov.au**

Brett Human is from the Biodiversity and Biosecurity Branch,
Department of Fisheries, Government of Western Australia.

Katherine Murray, Katherine Zdunic, and Graeme Behn, are from the Remote Sensing Unit,
Department of Environment and Conservation, Government of Western Australia.

Cover image: Kathy Murray measuring canopy cover with a densiometer. Photo: Brett Human

ISSN: 1035 - 4549 ISBN: 1 921258 80 2

Contents

List of Figures

List of Tables

Abbreviations

ALOS AVNIR-2 - Advanced Land Observing Satellite (ALOS) contains the instrument Advanced Visible and Near Infrared Radiometer type 2 (ANVIR-2)

CALM - Department of Conservation and Land Management, Government of Western Australia (currently DEC)

DCC - Department of Climate Change, Australian Government

DEC - Department of Environment and Conservation, Government of Western Australia

DEWHA - Department for the Environment, Water, Heritage and the Arts, Australian Government

DMSI - Digital Multi Spectral Imagery

DoE - Department of Environment, Government of Western Australia

DoF - Department of Fisheries, Government of Western Australia

EQC - Environmental Quality Criteria

PFC - foliage percentage cover

GPS - Global Position System

NCAS–LCCP - National Carbon Accounting System Land Cover Change Project

NDVI - normalised difference vegetation index

NRM - natural resource management

PFC - percentage foliage cover

PFC(cc) - percentage foliage cover representing the canopy cover estimate;

PFC(i) - percentage foliage cover image index

PFC(f) - percentage foliage cover derived from field estimates

PFC(p) - percentage foliage cover representing the average photo canopy estimate

PFC(pvc) - percentage foliage cover representing the average photo estimate with average site vegetation cover

PFC(vc) - percentage foliage cover representing the average site vegetation canopy estimate

QB2 – Quickbird 2, satellite

RCI - resource condition indicator

RCM - resource condition monitoring

TM - Thematic Mapper, Landsat image sensor

WAFMRL - Western Australian Fisheries and Research Laboratories, Department of Fisheries, Government of Western Australia

WALIA - Western Australian Land Information Authority

Executive summary

This pilot study investigated potential resource condition indicators, remote sensing, and ground truthing methodologies, for their use in long term monitoring of mangroves and intertidal mudflats in the Pilbara and Kimberley.

This study found that from the many potential resource condition indicators that are available, few are truly indicative of the resource condition, and even fewer are practical to implement. Of the potential resource condition indicators trialled here, approximately half of them were found to be useable.

Biological measurements that can be used as resource condition indicators tend to be complex, due to the complex nature of the environments examined here, and simplistic measures were found to be misleading of the true resource condition, in most instances. Remote sensing was shown to be a successful tool for estimating canopy density and habitat extent. However, this study also showed that it is essential to define appropriate spatial scales and select the appropriate remote sensing imagery resolution in order to use remote sensing successfully. Also apparent from this study, is the need to collect on ground measurements from the target area to be monitored, to correctly calibrate the remote sensing imagery. Site sampling replication needs to be relatively high in order to capture the high variability of the mangrove habitat.

Logistical issues of sampling in mangrove habitats are discussed, as are the issues of being familiar with field data collection techniques, prior to collecting important data. Advanced planning is needed for coordinating field data collection with imagery capture, as well as consideration for tides, season, and other environmental factors, particular to a given habitat or environment.

Overall, remote sensing can be used as an appropriate tool for long term resource condition monitoring, given that such data is appropriately calibrated with on ground measurements with sufficient replication to capture the heterogeneity of a particular habitat, or in this instance, mangroves and intertidal mudflats.

Key findings

The results of this pilot study are highlighted by the following key findings:

1. Remote sensing is a cost effective and efficient tool for long term monitoring of mangrove and intertidal mudflat habitats in the Pilbara.
2. Remote sensing is only effective and efficient if appropriately calibrated with on ground field measurements.
3. In a highly variable environment, such as mangrove habitat, relatively large numbers of replicate sampling sites are needed to capture the variability adequately.
4. Acquiring baseline data in a pilot study will increase the efficiency of a long term monitoring program from the outset.
5. Simplistic biological measures of resource condition are usually ineffective in complex environments, such as mangrove habitat, and are often misleading. Complex measures, requiring expert data collection and analyses, in some instances, are required to monitor such complex habitats.
6. Setting appropriate values that indicate significant change, for measures that will be used for monitoring, is essential prior to the commencement of a long term monitoring program. Baseline data will assist in this process. Also essential, is determining appropriate spatial scales and choosing remote sensing imagery with the resolution to suit that spatial scale.

Project aims and background

A large coastal and marine resource condition monitoring (RCM) project was developed for the Pilbara and Kimberley regions. Unfortunately this larger project did not eventuate. However to continue with developing our understanding of RCM in this region a smaller scoping study was developed.

This scoping study has three primary aims:

1. Knowledge review and gap analysis - undertake a desktop study of the current coastal and marine resource condition monitoring.
2. Undertake a short field program to inform the development of monitoring protocols in two intertidal environments.
3. Develop a Strategic Framework with recommendations and a suggested approach to inform and guide a future Coastal and Marine RCM Program for the Pilbara and Kimberley Regions.

This document addresses the second aim of the project, conducting a pilot field survey to trial potential resource condition indicators of mangrove and intertidal mudflat habitats to develop standardised monitoring protocols for use in future long term resource condition monitoring program for the Pilbara and Kimberley region.

An earlier report (Human & McDonald, 2009) satisfied the first aim of the project with an extensive literature review of the research and monitoring that has been undertaken in the Pilbara and Kimberley marine and coastal environments, and a further report will provide a strategic framework for resource condition monitoring of the Pilbara and Kimberley regions, satisfying the third aim of the project.

Pilot study aims

This pilot study intends to satisfy the second aim of the Coastal and Marine Resource Condition Monitoring - Scoping Project. Several aims were conceived for the pilot study to inform the development of monitoring protocols in two intertidal environments. The habitats of choice were mangroves, which are considered to be a primary ecological driver (Semeniuk *et al*., 1978; and Duke, 2006), and widely encountered along the Pilbara and Kimberley coasts, therefore are an obvious target for resource condition monitoring; and intertidal mudflats adjacent to mangrove habitats. Using two habitats that are closely associated with each other, and generally in close proximity to each other, lessens the logistic burden of monitoring these habitats. Additionally, over time, the synergistic effects of the two habitats may become apparent and useful as an indicator in itself.

This pilot study has three primary aims:

1. Conduct a field survey to ground truth remote sensing data for mangrove habitats and adjacent inter-tidal mud flat habitats.
2. Use high spatial resolution satellite imagery to map the extent/location of coastal mangrove within the study area.
3. Field trial potential resource condition indicators, such as number of trees per transect, tree heights, leaf health, water quality, and soil quality, among others.

1.0 Introduction

Habitat loss and its effects on biodiversity are a growing global concern. Loss of habitat is a major cause of the decline of coastal species (DEH, 2008). Changes in distribution, such as range extensions or reductions, are also of interest, especially during times of climate change, as they may be indicators of significant ecological changes underway. If pressures or threats are left unchecked, serious damage or irreversible loss is likely to occur. However, we currently know little about the characteristics of key habitats or how they might respond to any stressors. There is a significant lack of monitoring at unimpacted reference sites in Western Australia (WA), and there is a need for natural resource monitoring to gauge natural variability, inform target setting, and differentiate between the effects of human and natural influences.

The WA coastal and marine environment is a vast area with 20,800km of coastline, including islands (Trewin, 2006) and spans both tropical and temperate climates. With the exception of Ningaloo Marine Park, we know almost nothing of the condition of the marine resources of the arid tropical Pilbara and Kimberley regions, yet the high marine biodiversity and recreational values of these areas are recognised at a national and international level. The need for critical baseline information of natural resource condition in the region is urgent.

The Pilbara is of great strategic and economic importance for the State and Commonwealth. The area supports a wealth of offshore oil and gas resources; for example, the recently approved Gorgon project will target a gas reserve of 40 trillion cubic feet, and is expected to boost Australia's gross domestic product (GDP) by AU$64.3 billion (http://www.gorgon.com.au). The Pilbara has the country's largest export ports, some of which are currently expanding or have proposals to expand. There are also a number of new large scale industrial activities proposed throughout the region, most of which will rely on large marine infrastructure to facilitate export. The region also has great tourism potential. It is also an area that supports some of the country's most unique and highly biodiverse marine habitats (e.g. nearshore coral reefs develop due to the limited run off from the land, and arid zone tropical mangrove communities are also present) (CALM, 2005; DoE, 2006; NWSJEMS, 2007; DEWHA, 2008; and Wood & Mills, 2008).

The Kimberley is one of the most remote and uninhabited stretches of the Australian coastline. Apart from a few indigenous communities, the only coastal settlements are the small ports of Derby and Wyndham. Despite this remoteness, the remarkable natural beauty of the coastal environment means that commercial tourism operations are already well established, and major development applications by oil and gas industries are currently being planned. Assessment of the potential impact of all of these activities is hampered by the paucity of baseline environmental data for any of the marine communities in the Kimberley. What little is known of these habitats indicates that they tend to be locally very complex and diverse, and frequently not found elsewhere in Western Australia (NWSJEMS, 2007; DEC, 2008; DEWHA, 2008; Fry *et al.*, 2008; NDT, 2008a,b; and Wood & Mills, 2008).

1.1 Mangroves of the Pilbara and Kimberley

Mangroves and inter-tidal mudflats are dominant coastal habitats of the Pilbara and Kimberley (Semeniuk *et al.*, 1978; Pedretti & Paling, 2000; and Lyne *et al.*, 2006). Mangrove communities consist of a taxonomically heterogeneous community of hypersaline tolerant flowering plants that are generally greater than half a meter tall and normally occur above the mean sea level of the intertidal zone in coastal and estuarine zones (Semeniuk *et al.*, 1978; and Duke, 2006).

However, there are numerous species of epiphytic plants and fungi that are found in mangrove communities also (Duke, 2006). In some instances, the term mangrove refers specifically to individual trees or plants, whereas a mangal is the term used to describe the entire mangrove community (Semeniuk *et al.*, 1978). Here the term mangrove is equivalent to the term mangal, referring to a mangrove community, unless otherwise stated. Hypersaline tolerant plants less than half a meter tall are generally classified as saltmarsh plants and are recognised as a separate ecological community (Duke, 2006).

The mangroves of the Kimberley are the most diverse and luxurious in Western Australia, with decreasing complexity and diversity along a southward longitudinal gradient (Semeniuk *et al.*, 1978; and Duke, 2006). The Kimberley coast provides environments that are protected from strong wave action, favouring complex mangrove systems. The Pilbara coast however, is more exposed resulting in less complex mangrove communities (Semeniuk *et al.*, 1978), and mangroves here are often bordered by geological barriers to their landward side resulting in fringing stands of mangrove (Duke, 2006). The mangrove systems in northern Western Australia are relatively unimpacted compared to those found in eastern and southern Australia, and remain in pristine, or near pristine condition (Duke, 2006). However, where mangroves have been affected by human activity, the impact tends to be severe (Duke, 2006).

Mangroves are important habitats for numerous reasons. Mangroves slow currents sufficiently for sedimentation to occur, thereby stabilising coasts by slowing sediment transportation (Semeniuk *et al.*, 1978; Duke, 2006). Mangroves provide nursery habitat for numerous species of fishes and crustaceans, as well as many other aquatic organisms including crocodiles and turtles, predatory fishes such as sharks and stingrays, molluscs, polychaetes and other worms, and many more invertebrate groups (Semeniuk *et al.*, 1978; and Duke, 2006). Mangroves support a diverse canopy fauna, providing both refuge and habitat. Such canopy animals include mammals (possums, rats, and bats), reptiles (snakes and lizards), birds, spiders, insects, crustaceans (crabs) and molluscs (snails) (Duke, 2006).

The benefits that mangroves provide to humans are mostly perceived to be limited to the commercially exploitable fishes and crustaceans that utilise mangroves as nurseries. However, other benefits from mangroves include shoreline protection, nutrient uptake, carbon sequestering, and more recently, an awareness of the ecological role played by mangroves has made them a target habitat for ecotourism and school group tours, as well as an increased appreciation of their aesthetic value (Duke, 2006).

1.2 Burrup Peninsula

The target area for this pilot study was the Burrup Peninsula in the Pilbara (Fig. 1), which was chosen as the study site for several reasons. Its proximity to large towns (Karratha and Dampier) makes the peninsula relatively easily accessible, and the study sites used here are generally around one to two hours drive from Karratha. It is hoped that the relative accessibility of the study sites will promote their use in future long term monitoring programs. There are many mangrove sites around the Burrup peninsula, and mangroves are found in every bay on the peninsula, therefore there was ample choice for choosing study sites. As mentioned previously, the peninsula is also host to significant industrial activity, including a major liquid natural gas (LNG) hub, iron ore mining, salt mining, and is home to the worlds largest bulk export port, therefore, having mangroves located so close to such large scale industry makes them desirable for monitoring for impacts (or lack thereof) that may be associated with these industries.

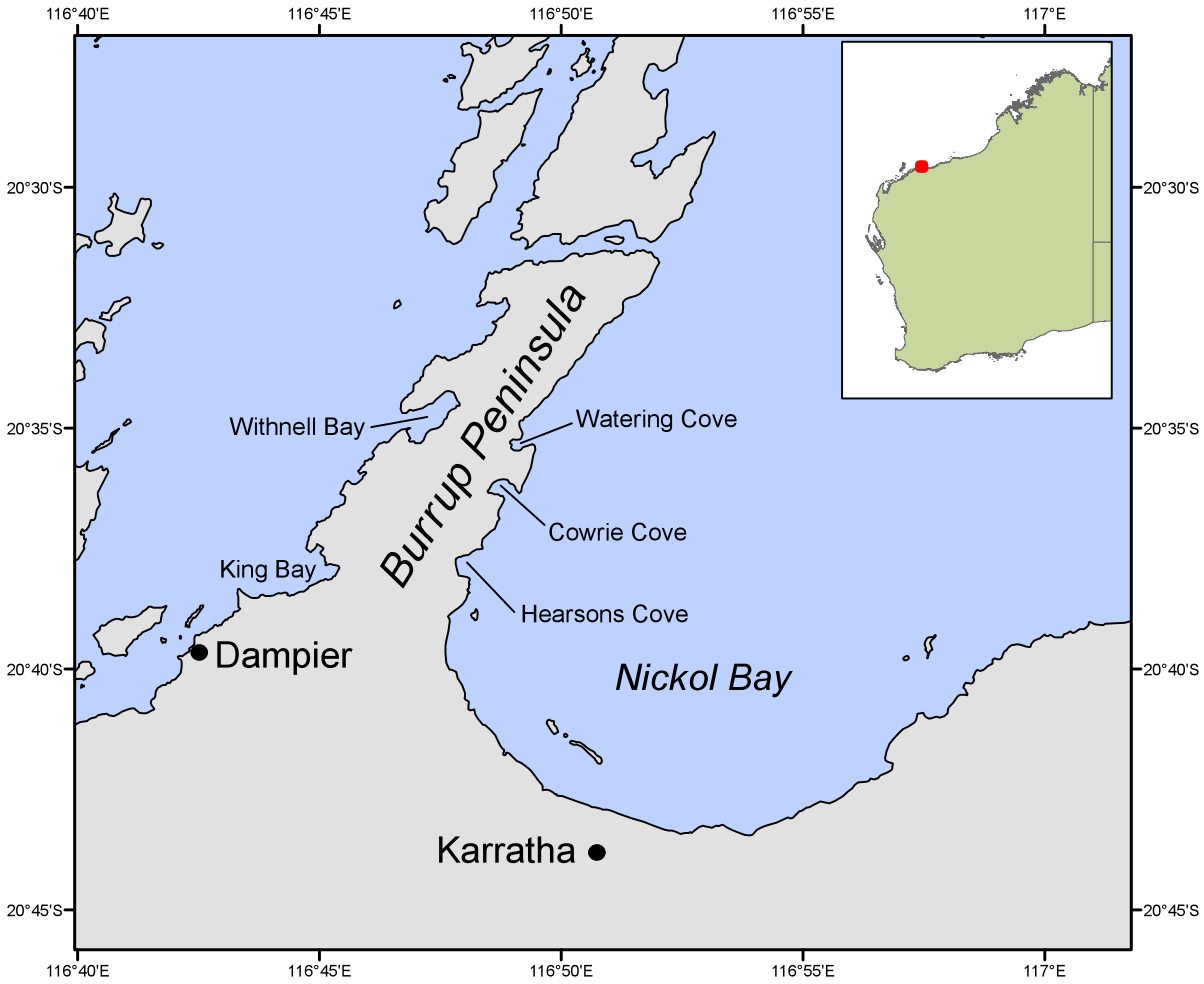

Figure 1. The Burrup Peninsula and surrounds, showing the study sites used in this pilot study. Dampier Port encompasses the majority of the area west of the peninsula shown on this map, and extends northwards and westwards.

1.3 Remote sensing

Remote sensing techniques developed for vegetation condition monitoring of Australian forest, rangeland, and agricultural environments, have been proven as an important conservation tool (Wallace *et al.*, 2006). Applying remote sensing technologies to detect mangrove extent is a cost effective alternative to traditional methods of mapping the extent with aerial photography and ground truth mapping methods from a single survey (Behn *et al.* 2004; Behn, 1999; and Kimber *et al.*, 1991*)*.

Ortho-rectified and calibrated multi-spectral imagery, and the application of remote sensing techniques, can provide a measure of vegetation change that is consistent, repeatable, reliable, and deliver a robust long term monitoring tool. Multi-spectral imagery can be captured with both satellite and airborne sensors. The spectral variation across the visible, near infrared and short wave infrared spectrum captures wavelength ranges (bands) that can be used to detect different aspect of land cover, such as vegetation cover.

1.3.1 Discriminant analysis of spectral data

The reflectance (ie. spectrum) displayed by any pixel representing natural vegetation is a combination of the relative spectral combinations from tree canopy, understorey, ground cover, and exposed soil, within the pixel. When the canopy or tree crowns are not dense, the spectral reflection from soil and understorey vegetation can dominate the spectral influence of the trees on the pixel characteristics. The analysis of remotely sensed data in such environments involves understanding the spectral responses, variation of the numerous components, and developing techniques that explain these variations.

The crucial factor in producing spectral maps or enhancements which reliably display vegetation status, such as biomass levels, is that the spectral separation of the biomass classes, for example, dense vegetation cover from sparse vegetation cover, is large compared to the vegetation variation within classes. If this can be established, then important band combinations, which provide the vegetation biomass discrimination, can be identified, and appropriate enhancements produced. A classification-mapping approach can also be adopted, and pixels can be allocated with confidence to one or other of the classes (Behn *et al.*, 1990).

1.3.2 Normalised difference vegetation index (NDVI)

Indices, or mathematical combinations of spectral bands, are derived to express spectral anomalies that are diagnostic of specific target materials. The most commonly used is based on normalised ratios, and can very effectively measure the amount of green vegetation cover over the soil. This index is commonly referred to as NDVI (normalised difference vegetation index), was developed with Landsat Multispectral Scanner (MSS) and Thematic Mapper (TM) sensors, and is described by Tucker (1979) as relating to the proportion of photosynthetically absorbed radiation.

NDVI measures the differential reflection of green vegetation in the visible and infrared portions of the spectrum and provides a basis for monitoring vegetation. Satellite imagery is well suited for this monitoring with its spectral and spatial resolutions and NDVI is commonly used in such applications. This index is defined as:

$$NDVI = \frac{R_{nir} - R_{vis}}{R_{nir} + R_{vis}}$$

where R_{vis} is the land surface reflectance in the visible waveband (0.58 - 0.68 μm; TM band 3) and R_{nir} is the land surface reflectance in the near infrared waveband (0.725 - 1.1 μm; TM band 4). The principle behind this is that the visible region is a part of the spectrum where there is considerable absorption of incoming solar radiation by chlorophyll, and the near infrared is a region where spongy mesophyll leaf structure leads to increased reflectance (Tucker and Sellers, 1986).

The NDVI is affected by the degree of absorption by chlorophyll in the red wavelengths, which is proportional to leaf chlorophyll density, and by the reflectance of near-infrared radiation, which is proportional to green leaf density. Therefore, NDVI is likely to correlate well with green leaf biomass, and can be related to healthy vegetation. The NDVI is generally related to both green biomass and leaf area index (LAI) of plants, and is a very good measure of plant

health and vigour. However, this relationship can vary with the structure of the vegetation type, and different relationships for major vegetation types are required to account for dry biomass (Bellairs *et al.*, 1994). The colour and brightness of the soil also affect NDVI values.

1.3.3 Landsat imagery as a monitoring tool

The multi-spectral sensor, Landsat Thematic Mapper (TM), provides suitable imagery for mapping and monitoring vegetation over regional areas because a single scene covers an area of 185km by 185km with 30m (resampled to 25m) pixel resolution, and has a revisit cycle of 16 days. Landsat imagery has eight bands with which to discriminate land cover.

Continental Australian summer coverage of Landsat TM and ETM+ imagery has been ortho-rectified and calibrated over the last 20 years, with near annual coverage. This archive provides a monitoring tool that can be calibrated with on ground measurements and used to construct a historical timeline. This dataset was created to archive an annual snapshop of the continent for the National Carbon Accounting System (NCAS) project (Caccetta *et al.*, 2003). The dataset also allows the detection of dynamic change on a regional scale.

Historically, ortho-rectified Landsat imagery has been utilised in Western Australia by the Department of Environment and Conservation (DEC) to map and monitor terrestrial vegetation change and condition. This technique has been developed by calibrating Landsat imagery with on ground assessments (ground truthing), such as foliage percentage cover (PFC) estimate, which is traditionally a forestry technique used to predict canopy closure (Behn *et al.,* 2001; and Behn, 1999). This technique has been successfully applied to different terrestrial vegetation cover types in Australia to derive extent, and act as a surrogate of vegetation condition (Behn, 1999; Behn *et al.*, 2001, 2003; Kullnell *et al.,* 1998; and Zdunic and Behn, 2009).

Within DEC, the same technique has also been used to demonstrate the feasibility of detecting and classifying mangroves using on ground assessment and aerial photography to determine PFC values and calibrate ortho-rectified Landsat satellite imagery within the Kimberley and the Pilbara (Kay *et al.*, 1991; and Behn, 1999). The combination of datasets to estimate mangrove resources and the associated influential ecological conditions was also recommended by Blasco *et al.* (1998).

Monitoring mangrove extent change over time with the NDVI and Landsat TM has been made possible by using a combination of ground truth data, aerial photography and multiple dates of ortho-rectified and calibrated Landsat TM imagery. These combinations of data have been used to define the variation in mangrove canopy closure, as an indication of density and condition (Giri *et al.,* 2007; and Paling *et al.*, 2007).

1.3.4 Spatial resolution

When detecting narrow fringing mangroves, the spatial resolution limitations of Landsat imagery were highlighted in the Kimberley (Manson *et al.*, 2001) and the Northern Territory to Shark Bay (Behn, 1999), where assessing mangrove extent was restricted by the 25m by 25m pixel size. Manson *et al.* (2001) found that a mangrove stand must be at least 50m across to be identified with Landsat. Hence Landsat is considered more appropriate for broad scale mapping and monitoring. In the Pilbara region of Western Australia, many of the mangrove stands are narrow and fringing, including the mangrove habitats of the current study sites. Landsat was not considered in this study because the pixel resolution is too coarse (25m) for areas where the mangroves extent is narrow (<20m).

Utilising higher resolution imagery with on ground assessments of canopy cover to calibrate NDVI for detecting mangrove extent and variation in canopy cover, was noted to achieve greater accuracy (Blasco *et al.*, 1998). A comprehensive study by Green and Clark (2000) assessed the accuracy of this technique with different resolution imagery, two multi-spectral satellite sensors - Landsat TM (30m pixel) and SPOT XS (20m); and airborne capture imagery CASI (1m pixel). They found that all sensors could provide useful forestry management information, but the higher resolution, the greater the sensitivity and accuracy of the sensor (Edwards, 2000; Green and Clark, 2000; and Green *et al.,* 1998).

This pilot study employs a similar technique previously used with Landsat and higher resolution imagery, to detect mangrove locations and characteristics. This includes discriminating vegetation from other land types using the spectral response, and calibrating imagery with mangrove canopy cover field measurements, to create a resource condition index. The objective of this part of the study are summarised below:

- To build on previous research in this field by exploring the suitability of two high and one medium resolution multi-spectral sensors, to monitor mangrove forest.
- Utilisation of NDVI, or indices derived from band 3 or 4, to define the variation in mangrove density.
- Evaluate various field methods to measure the canopy cover density to determine the most efficient technique for monitoring in the mangrove environment.

The successful application of remote sensing techniques can provide a cost-effective method of mapping and monitoring of the mangroves at a finer spatial resolution across the landscape than is possible with current techniques. This will have a variety of benefits for many agencies interested in coastal zone management and monitoring.

2.0 Methods

2.1 Experimental design and pre-analyses

2.1.1 Strategy

The aim of the pilot study was to field trial potential resource condition indicators in mangrove and intertidal mudflat environments. Remote sensing is considered to be the primary tool for long term monitoring (Behn, 2001; and Wallace *et al.*, 2006) particularly when considering both the remoteness and spatial extent of the Pilbara and Kimberley marine and coastal environments, therefore the sampling strategy used here focussed on ground truthing remotely sensed data. The pilot study employed a non-random stratified design. The sampling method was stratified by selecting areas of mangrove vegetation with a range of different canopy cover. This approach was essential to locate a range of canopy density ground measurements suitable for imagery calibration. Each of the study sites had a mangrove and an intertidal mud flat associated with it.

2.1.2 Season and tide

The Pilbara is an arid tropical region, with the dry season starting at the beginning of April and the wet season beginning at the start of October. Sampling occurred from 11-15 May, 2009, which was approximately one month into the dry season.

The field schedule of the pilot study was constrained due to the limited timeline of the project, and requirements of other activities relating to the project, and thus sampling dates unfortunately coincided with spring high tides. The tide heights for King Bay during the sampling period are given in Table 1. Sampling of the study sites was undertaken from first light in the mornings (approx. 0700hrs), with sampling continuing until approx. 1100hrs, or until the water line was seen approaching the transect area.

Table 1. Predicted tide heights for King Bay during the pilot study period (May, 2009). Tide height (Ht) are in metres above Prediction Datum and times are Australian Western Standard Time (+8hrs UTC). Data from the Bureau of Meteorology, Australian Government.

Mon 11		Tues 12		Wed 13		Thurs 14		Fri 15	
time	Ht	time	Ht	time	Ht	time	Ht	time	Ht
0544	1.40	0016	4.06	0045	3.96	0114	3.84	0145	3.69
1139	4.51	0612	1.45	1639	1.54	0706	1.67	0735	1.82
1820	0.81	1210	4.43	1241	4.31	1313	4.15	1347	3.95
		1850	0.90	1919	1.05	1949	1.24	2020	1.46

Table 2. Satellite imagery used for this project including the sensor and data specifications.

Sensor	Resolution	Bands	Band Widths (µm)	Data Type	Frequency	Sensor Type	Data Source
ALOS ANVIR-2	10m	1 2 3 4	0.42 - 0.50 0.52 - 0.60 0.61 - 0.69 0.76 - 0.89	8bit Unsigned Integer	46 days	Multi spectral Satellite	Geoscience Australia
QB2	2.5m resampled to 0.6m with Pan band	1 2 3 4 Panchromatic	0.45 - 0.52 0.52 - 0.6 0.63 - 0.69 0.76 - 0.9 0.45 - 0.9	16bit Unsigned Integer	1- 3.5 days	Multi spectral Satellite	DigitalGlobe, (GeoImage)
Specterra DMSI	0.5m	1 2 3 4	0.44 -0.46 0.54 – 0.56 0.665 – 0.685 0.77 – 0.790	16bit Unsigned Integer	On demand	Multi spectral airborne	Specterra
Aerial Photography (scanned, Ortho-rectified)	0.5m	Red Green Blue		8bit Unsigned Integer	10 years	Photogrammetric camera airborne	Landgate, Western Australian Land Information Authority (WALIA)

2.1.3 Imagery

This project was able to test the suitability of satellite and airborne captured imagery from different sensors to facilitate mangrove monitoring. Three satellite images were available for analysis prior to the field trip, Advanced Land Observing Satellite (ALOS) contains the instrument Advanced Visible and Near Infrared Radiometer type 2 (AVNIR-2) (captured 10 May 2007; Geoscience Australia) and QuickBird 2 (QB2) (captured 6 Nov 2006; DigitalGlobe). Aerial photography (captured 02 August 2004; Landgate) was also available as a high resolution digital ortho-photography of the region. Less than a month after the field trip, Specterra Digital Multi Spectral Imagery (DMSI) data was captured over the study sites (10 Jun 2009). The sensor specifications for all images used are listed in Table 2.

2.1.4 Study site locations

Narrow belts of fringing mangroves line the rocky shores and short tidal creeks of the Dampier Archipelago (Paling *et al*., 1989; and Pedretti & Paling, 2000), including the Burrup Peninsula. Four study sites were selected on the Burrup Peninsula. For the purposes of this pilot study, the sites were *a priori* categorised into "impacted" and "non-impacted" sites, based on the study sites proximity to existing industry.

Those study sites that were *a priori* assigned as impacted were King Bay and Withnell Bay. King Bay (Fig. 2) has a westerly aspect on the Burrup Peninsula, a seasonal creek in the southwest of the bay, and has industry situated immediately adjacent to the mangrove habitat. North of King Bay, Withnell Bay (Fig. 3) also has a westerly aspect, a seasonal creek in the northeast of the bay, and has an industrial site at the southern entrance to the bay.

Two study sites were *a priori* classified as unimpacted sites. Cowrie Cove (Fig. 4) has an easterly aspect on the Burrup Peninsula, facing into Nickol Bay. A tidal creek enters the bay from the southwest, and rocky headlands protect both the north and the south of the bay. An extensive mudflat, protected by a rocky headland, extends north from Cowrie Cove to Watering Cove, the second *a priori* unimpacted study site of the pilot study. However, when inspecting these sites, recent heavy rains had degraded the vehicle tracks in the area, and crossing the mudflat to get to Watering Cove was deemed too hazardous. We were also unable to access a boat, and therefore could not access Watering Cove.

Prior to visiting the study sites the AVNIR-2 and the QB2 images were stratified to only display data from the mangrove extent. To do this, a vegetation index of Band 4/Band 3 and a Normalised Differential Variance Index (NDVI), composed of (Band 4 - Band 3)/ (Band 4 + Band 3), (Jensen, 1996) were applied to the images. Both of the indices were used to determine the most appropriate threshold of mangrove extent for each image.

Figure 2. Image of King Bay, classified a *priori* as an impacted site. Note the seasonal creek in the southwest of the bay, and industrial site to the north.

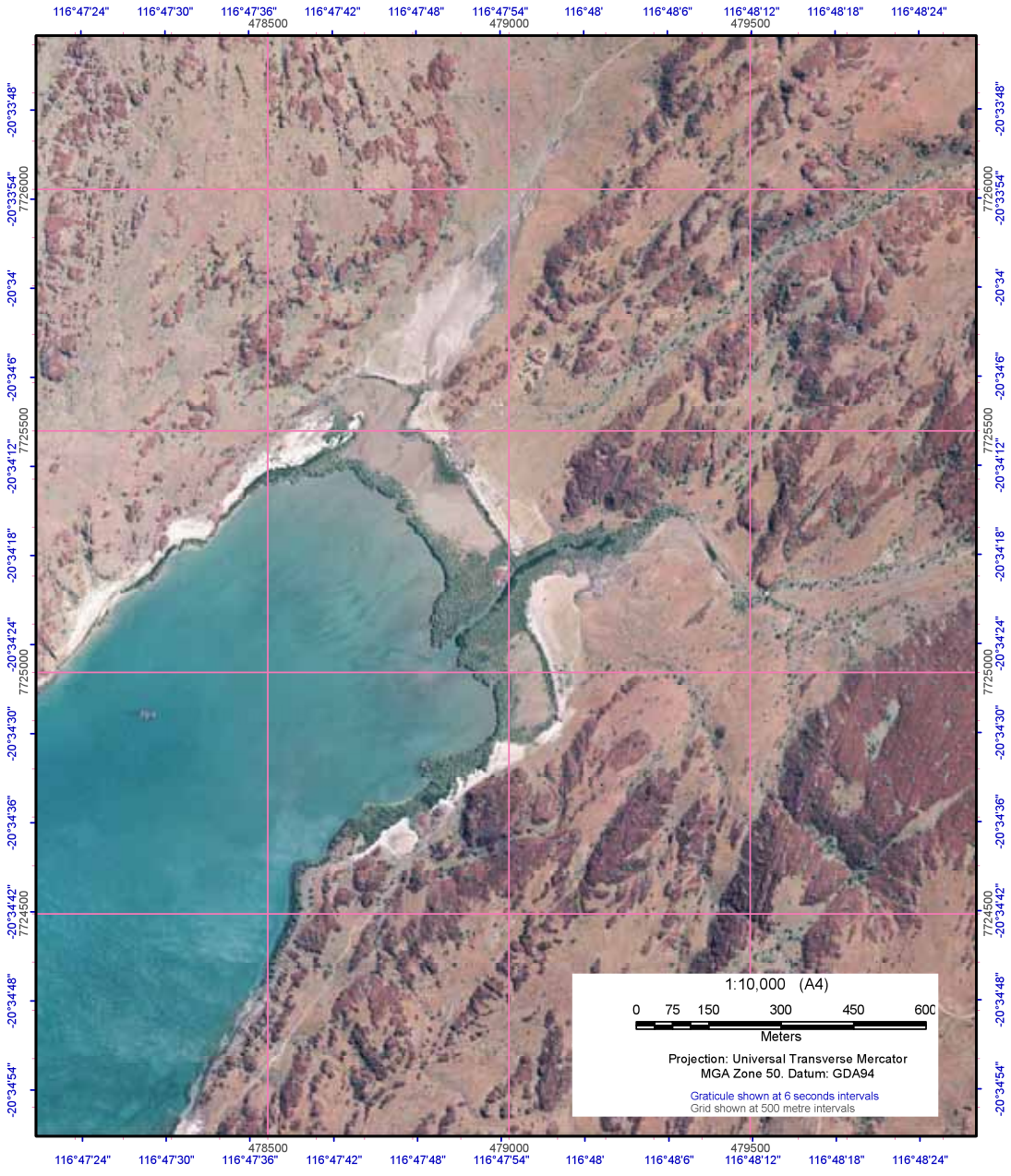

Figure 3. Image of Withnell Bay, classified *a priori* as an impacted site. There is a seasonal creek in the north east of the bay, and a large industrial site in the south.

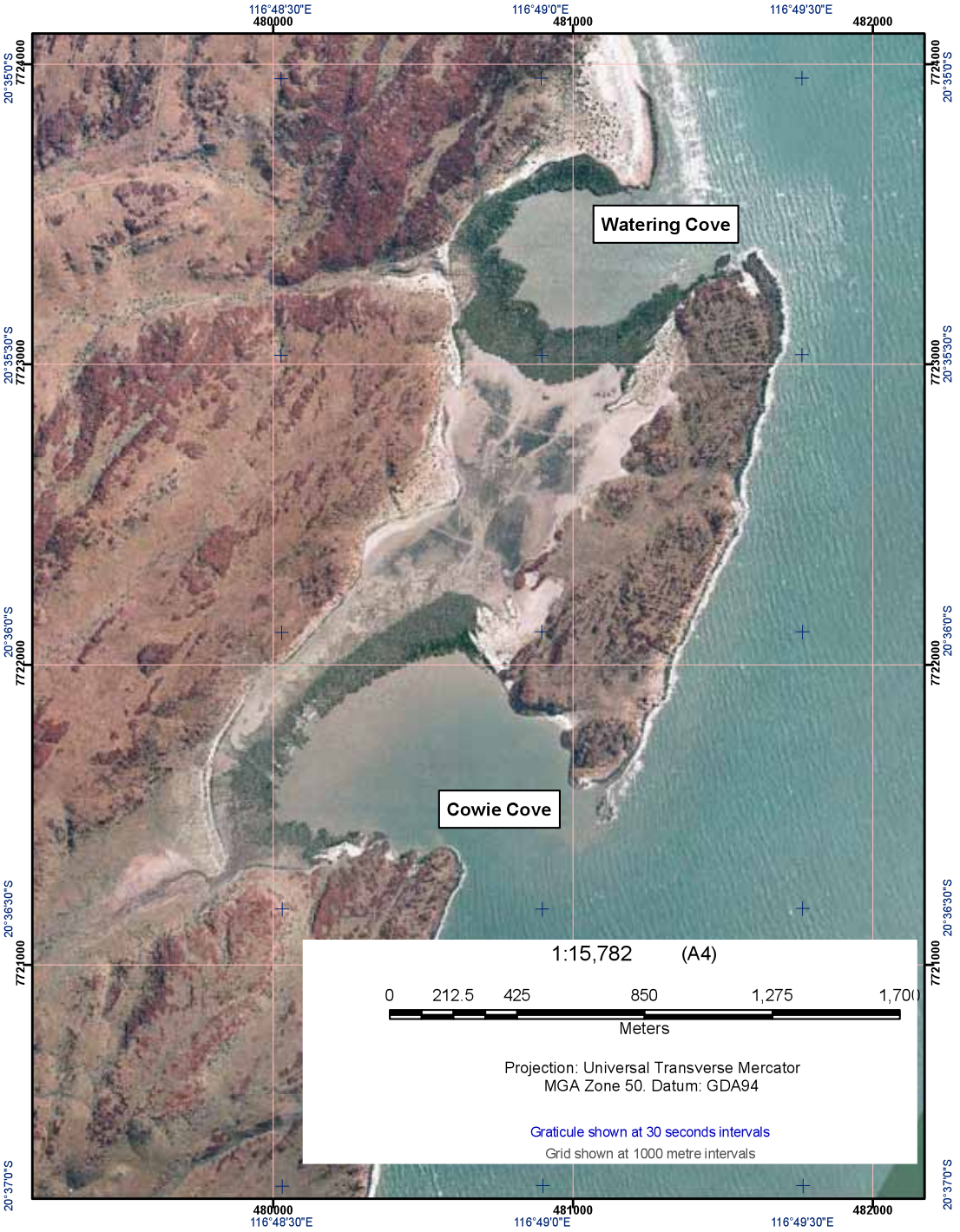

Figure 4. Image of Cowrie Cove and Watering Cove. Both sites were classified a *priori* as unimpacted. An extensive mudflat protected by a rocky headland connects the two coves.

The AVNIR-2 image identified the mangrove extent with the following vegetation index and thresholds:

$$\text{Band 4 / Band 3} > 0.60396 \text{ and Band 4 / Band 3} < 0.1.48$$

The QB2 image identified the mangrove extent with NDVI and the following thresholds:

$$(\text{Band 4 - Band 3})/ (\text{Band 4 + Band 3}) \geq 0.17 \text{ and } (\text{Band 4 - Band 3})/(\text{Band 4 + Band 3}) < 0.61$$

Both indices describe the mangrove front accurately, but other terrestrial vegetation was identified further inland. To overcome this issue, a vector boundary of the high tide mark (the upper mangrove habitat range) was manually digitised and used to exclude terrestrial vegetation. The AVNIR-2 and QB2 images were then clipped to the mangrove extent to isolate the spectral range of the mangrove habitat. The variation within the extracted mangrove extents in the AVNIR-2 and QB2 images was examined using the vegetation index of Band 4 - Band 3. This index describes the variation of vegetation vigour within the mangrove canopy. Local enhancements (interpretive image displays) of the derived index were created for each sensor (see Appendix 1) to illustrate the variation within each study site. An overall enhancement was made to compare between study sites.

The extent of intertidal mud was determined using the 6 Nov 2006 QB2 image, (resampled to 8bit data from 16bit data). This area appeared to vary in spectral values from light mud (possibly dry or drier) to dark mud (possibly wet) and even greenish mud (possibly blue green algal mats) in some places. The mud extent may be confused with other land types such as bare areas, rock, and foredune sand. This approach aimed to map intertidal mud consistently adjacent to the mangroves. Therefore the extent of intertidal mud across the Burrup Peninsular was extracted with two categories, light mud and dark mud. Different thresholds of the developed mud index Band 1/Band 4 were used to create the two classes.

Light mud could be identified with the index and thresholds:

$$\text{Band 4 / Band 1} \geq 1.35 \text{ and Band 4 / Band 1} < 1.45$$

Dark mud could be identified with the index and thresholds:

$$\text{Band 4 / Band 1} > 1.12 \text{ and Band 4 / Band 1} < 1.35$$

A three by three median filter was then applied to remove single pixels. This layer was required to identify the location of mud in the field; therefore it was not clipped to the digitised high tide mark as the mangrove extent was.

2.1.5 Sample site selection

At least three homogenous mangrove sample sites were identified within each study site using a visual assessment of aerial ortho-photography, and the AVNIR-2 and QB2 images with a vegetation index enhancement of the mangrove extent. Homogenous sites were selected for their spatial and spectrally consistent characteristics representing vegetation density and vigour, which can be an indicator of resource condition. Defining a homogenous site based on these characteristics insures that when taking a field measurement any sample site selected within the homogenous site is consistently representative of the environmental conditions, vegetation type, canopy cover, and community structure; all of which contribute to the vegetation density of a site. Therefore, when averaging and analysing samples (point measurement) from a homogenous site for comparison with satellite image data (pixel data representing an area) the field measurement can be converted to an area.

A homogenous area was preferably defined with a nine pixel AVNIR-2 square (3x3, 30m by 30m), however given the fringing nature and narrow distribution of mangroves this was not always possible. Some homogenous sites were defined by a rectangular area of at least six or eight AVNIR-2 pixels, displaying a spatial pattern of mostly uniform vegetation cover in the aerial photography, and little spectral variation in the vegetation index enhancements.

A spatial density scale (Forestry and Timber Bureau, 1950) was used to estimate the degree of vegetation cover from the aerial ortho-photograph as a percentage. This measurement is referred to as the aerial photo density estimate. The density estimates gave an indication of the range of densities that were to be sampled in the field, with the aim to represent sparse, medium, and dense mangrove vegetation at each study site. Priority was given to the most consistent homogenous sites, and representation of the density variations across the study site. The selected homogenous sites are illustrated below in Figures 5 to 7, with aerial ortho-photography.

An example of a homogenous site identified with the aerial ortho-photography, AVNIR-2 and QB2 can be seen in Figure 8. The consistent colour and pattern of the images shows that the site is likely to be homogenous. The centre point positions, and priority of each homogenous sample site, were recorded in a table (Table 3) as a backup reference of 'go to' waypoints.

2.1.6 Field maps

Navigation maps were made for each study site, displaying aerial ortho-photography, local roads, and homogenous site locations and their centre points. Two additional maps displaying an overlay of the AVNIR-2 and QB2 mangrove extent (enhancing the vegetation index for each site) was also used to assist observations of vegetation canopy variation in the field (Appendix 1). All vector and raster image layers were converted into OziExplorer (Newman, 2008) compatible files for loading onto a Trimble Nomad GPS, aiding navigation to the sample site and staying within its boundaries.

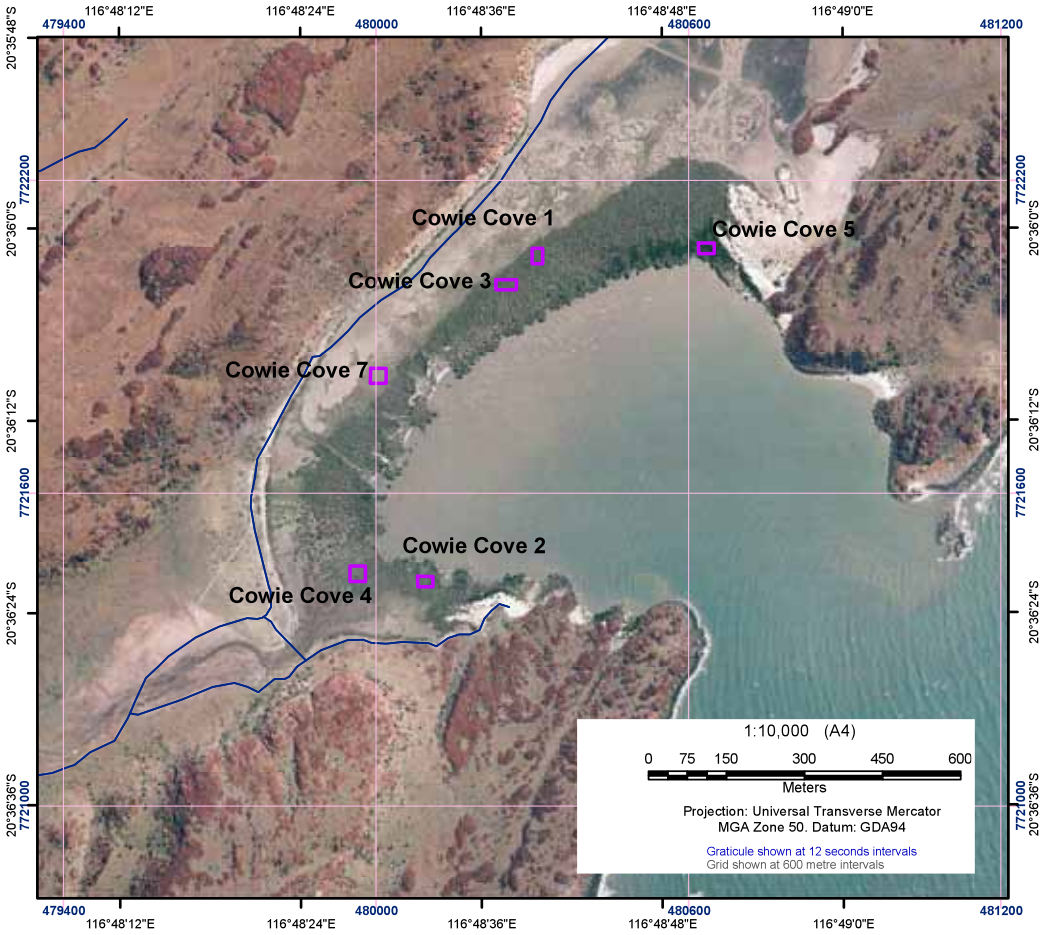

Figure 5. Sample site locations for Cowrie Cove and the 2004 aerial ortho-photograph.

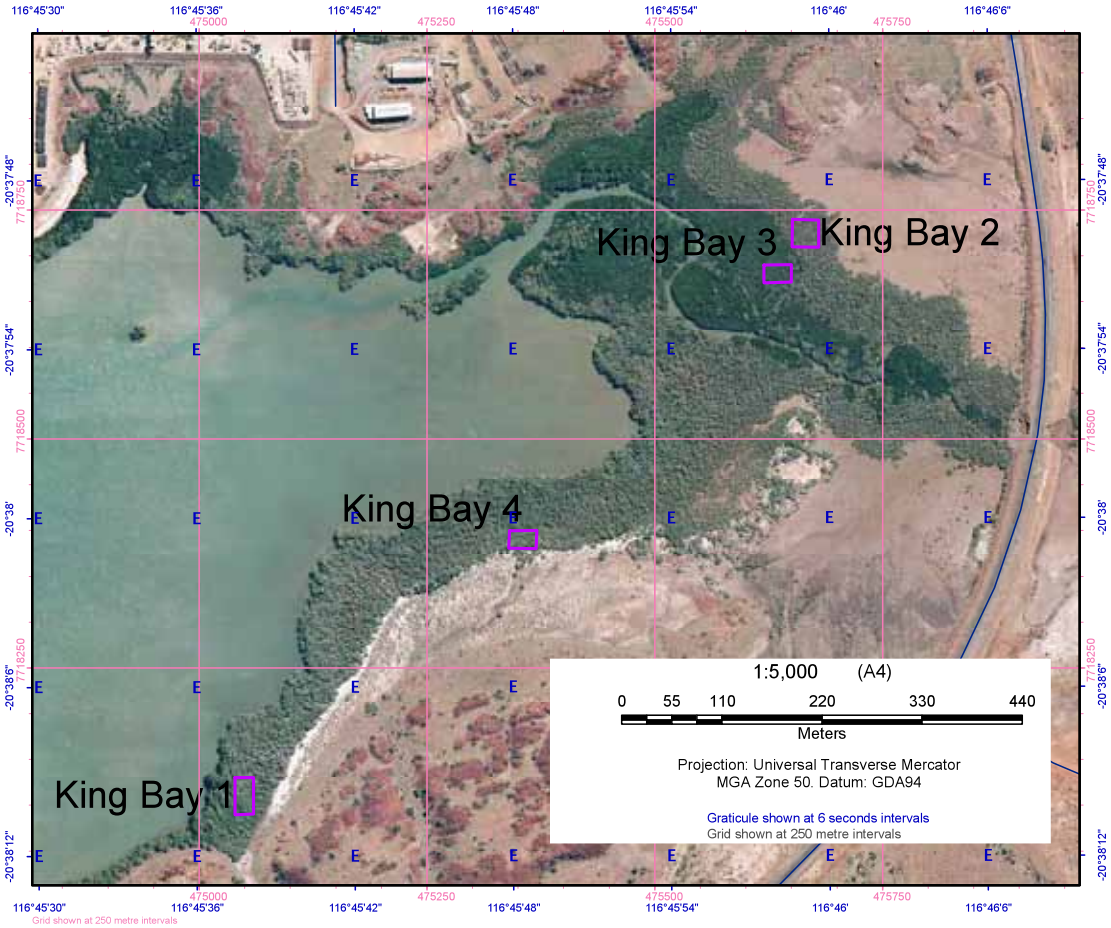

Figure 6. Sample site locations for King Bay over the 2004 aerial ortho-photograph.

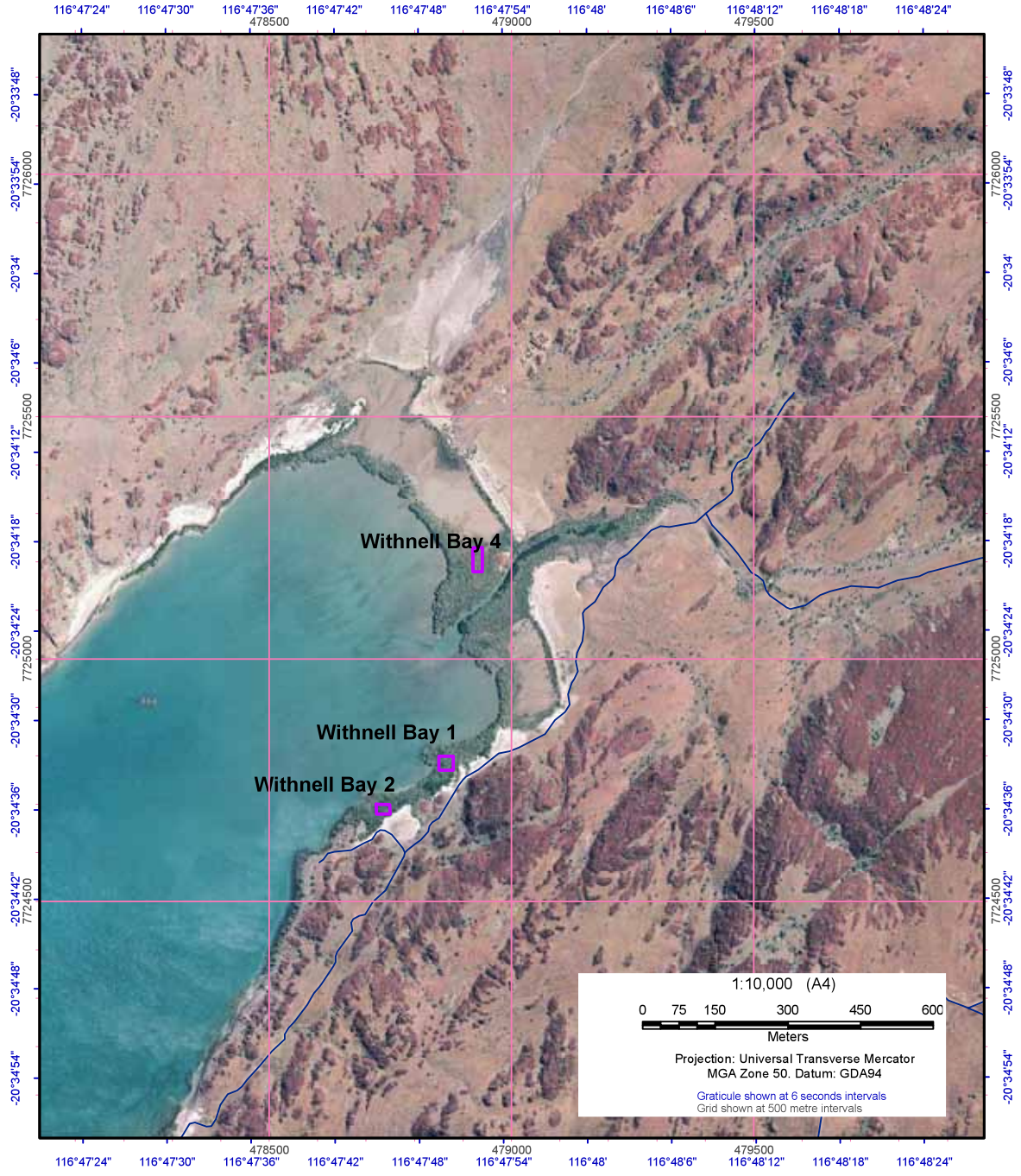

Figure 7. Sample site locations for Withnell Bay over the 2004 aerial ortho-photograph.

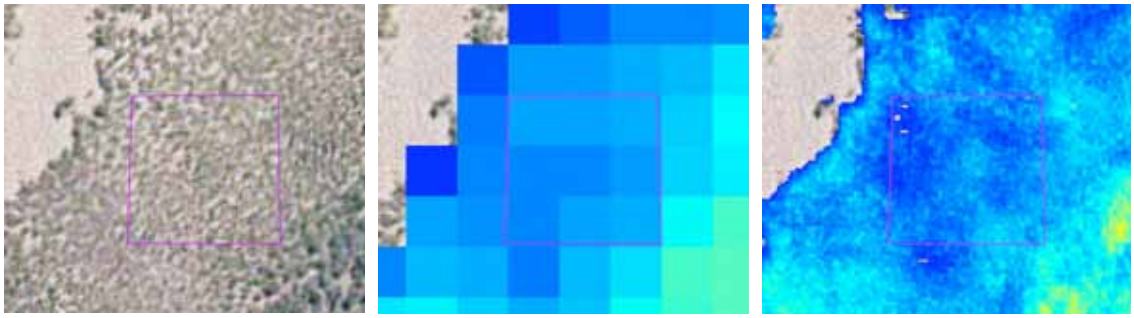

Figure 8. From left to right - aerial ortho-photograph, AVNIR-2, and QB2 images of a homogenous site at Cowrie Cove. These images illustrate homogenous spatial pattern and spectral characteristics for the mangrove vegetation in that location.

Table 3. Homogenous sample site locations used for this study, with the estimated vegetation cover density, the priority ranking for sampling the site, and the centre point positions in Latitude and Longitude, Datum GDA 94, and projected as Eastings and Northings MGA zone 50. These centre points were loaded into the GPS and used as a navigation 'go to' waypoint.

Homogenous Site Name	Estimated Vegetation Cover Density %	Priority	Geodetic coordinates, GDA 94		Projected coordinates GDA 94, MGA Zone 50	
			Latitude	Longitude	Eastings	Northings
Cowrie Cove 1	60	1	116.8110414	-20.6004883	480309.95	7722054.96
Cowrie Cove 2	65	7	116.8089692	-20.6061324	480094.76	7721430.09
Cowrie Cove 4	45	5	116.8077229	-20.6059961	479964.87	7721445.02
Cowrie Cove 5	90	4	116.8141576	-20.6003556	480634.65	7722070.02
Cowrie Cove 6	70	3	116.8104658	-20.6009837	480250.04	7722000.07
Cowrie Cove 7	45	2	116.8081085	-20.6025623	480004.61	7721825.07
Withnell Bay 1	85	2	116.7972068	-20.5758024	478864.94	7724785.16
Withnell Bay 2	85	3	116.7959582	-20.5766605	478734.93	7724690.04
Withnell Bay 4	50	1	116.7978355	-20.5720095	478929.94	7725205.00
King Bay 1	85	1	116.7605029	-20.6360717	475049.47	7718110.07
King Bay 2	55	2	116.7664240	-20.6305277	475665.43	7718724.51
King Bay 3	70	3	116.7661305	-20.6309245	475634.92	7718680.56
King Bay 4	90	4	116.7634434	-20.6335450	475355.39	7718390.14

2.2 Field measurements

Field measurements were recorded at study sites selected for ground truthing, based on the remotely sensed data (see *2.1.6 Site selection*). Homogenous plots of $5m^2$ were marked out with 2x 5m poles, intersecting orthogonally at their mid-lengths, and were temporarily placed on the ground at the site (see *2.2.3 On ground assessments – Remote Sensing*). Potential resource condition indicators were measured, and were also used to compliment the remote sensing findings.

2.2.1 Biological measures – mangroves

Initial attempts to mark transects with chainmen and string were unsuccessful because it was not possible to maintain a straight transect while trying to manoeuvre through the mangroves, whereas the poles could be pushed through the canopy and the understorey with ease. One pole was randomly chosen to conduct the transect for biological measures, with one metre either side of the pole included in the 2m x 5m belt transect. The start and end points of the transect were logged into a handheld GPS, and the following potential resource condition indicators were trialled at each transect: tree height (<1m, 1-2m, >2m); number of healthy, sick, and dead trees in the transect; tree density (obtained by summing the previous three measures); primary mangrove species; secondary mangrove species; and water quality measures of pH, ORP, dissolved oxygen, conductivity, and salinity (measured using a Hanna Instruments HI9828/4 multiparameter water meter).

Multiple digital photographs were taken of the transect area for later reference. Additionally, within the first transect at every site, a mature tree was flagged with fluorescent pink polypropylene tape and its position logged into a handheld GPS, for use in future monitoring studies. The following characteristics of the flagged tree were recorded: greatest trunk diameter at 1m above the ground; percentage of foliage that had suffered from herbivory; number of propagules; and percentage of healthy, sick, and dead leaves. Sediment samples were collected at the first transect at most sites, and were tested for petrochemicals, cadmium, chromium, copper, iron, lead, nickel, and zinc. Sediment samples were analysed by the National Measurement Institute, Australian Government.

2.2.2 Biological measures - Intertidal mud flats

Only one or two transects were conducted for the intertidal mudflats at each of the study sites, given that the mudflats were generally small in area and homogenous. The high tide line was walked along and logged with a hand held Global Positioning System (GPS) for reference to the remotely sensed data, for distances between 100m to 150m. At the beginning of each mudflat transect, sediment and water samples were tested for the quality parameters listed above, and a second sediment sample was processed on site for grain size using 2mm and 1mm Endicotts test sieves, and relative percentages of grain sizes were recorded (large >2mm, medium 1-2mm, small <1mm).

2.2.3 On ground assessments – Remote Sensing

The Field Observation Form (Appendix 2) was completed once at the site. When walking through each homogenous site, a general site description was recorded i.e. location, slope, roads, distance from track / open water, major features, main vegetation type / species, soil colour, shadow, percentage of soil exposed, and general tree height. Representative sample plots (5m x 5m) of the homogenous area were selected, and were marked out in the field with two poles, crossing in the centre, following the protocol provided in Appendix 3. Within each plot the following was estimated or obtained: canopy cover; site vegetation cover; vegetation height; densiometer reading; centre coordinates; canopy photo; and site photo (noting the direction).

Centre coordinates were recorded as a waypoint with a Trimble Nomad GPS, a handheld single GPS. Tracks were continually recorded while in the field and were used as backup for lost waypoints, or were used to determine inaccuracies of the GPS position under different conditions. A differential GPS was originally considered as they are more accurate (sub-metre accuracy) than a handheld single GPS (accuracy of +/- 5-10m) however differential GPS

equipment is more cumbersome and awkward, with a large antenna to manoeuvre, creating logistical problems of carrying it through dense mangrove habitat. The Trimble Nomad GPS was chosen for assisting navigation as it had the advantage of visualising positions and tracks on the aerial ortho-photography in the field, which proved particularly useful when entering the homogenous site and selecting sample plots within the site. Another advantage of using poles to mark the transects is that the GPS unit could be tied to the end of one pole and pushed up through the canopy, increasing the signal strength and improving the accuracy of the GPS.

Three methods were used to estimate canopy cover for the study. These methods include visually estimating the canopy cover percentage with a canopy types key; using a densiometer; and taking a vertical digital photo of the canopy. All three methods were employed at all study sites except for Withnell Bay where densiometer readings were not taken. The crown types key in the Australian Soil and Land Survey Field Handbook (Walker and Hopkins, 1990) was used to visually estimate the percentage canopy cover (with the trunk of a tree behind you). This measure estimates what vegetation cover would be visible from above the canopy (i.e. birds eye view) to simulate what a satellite observes. The site vegetation cover, including the understorey and mid storey was also estimated using this key as an aid.

Densiometers were introduced to the forestry industry in 1957 (Lemmon, 1957) when the methodology was first published for characterising and quantify forest canopy density. The densiometer has been employed to measure mangrove canopy cover in previous studies (Green *et al.*, 1998). A densiometer is a handheld convex mirror marked with a grid of 24 squares, which is held under the canopy to count and record the number of grid quarters not shadowed by canopy. Percentage of canopy openness (Lemmon, 1956) is calculated by multiplying the number of grid quarters by 1.04 (4 quarters x 24 squares = 96, therefore x1.04 to scale up to 100). A reading should be taken from each quarter of the site plot. Although this technique had been successfully used in forest environments replicating the procedure in this mangrove project was less viable and only one reading per site was recorded.

Photographs were taken with a shock- and water-proof compact digital camera with a 35mm equivalent lens. One representative canopy photo was needed per site, but more were taken to ensure that at least one photo was truly representative of the site. A good representative canopy photo captures mostly leaves and little of the trunks. Where the vegetation is sparse the photo captures mostly clear sky. Executing the canopy photo involved pointing the camera skywards in an appropriate position on, and level to, the ground, using a small tripod with a level. The camera timer was used to allow the photographer time to leave the photo space and capture only trees in the photo. Where the canopy was less than 0.5m high, the camera was placed as flat as possible on the ground to take the photo.

Further record keeping instructions for the Observation form can be found in Appendix 3. These field methods have been tried and tested in other studies that have focused on terrestrial vegetation canopy (Behn *et al.*, 2001, 2003; and Zdunic and Behn, 2009).

2.2.4 *Validation sites*

Additional canopy cover estimates were also sampled to test and verify the accuracy of the relationship between ground truth estimates and the image index (see 2.3.4 Remote sensing and ground data relationships**).** The field validation sites (5m x 5m) were selected randomly ad hoc when the opportunity arose, within the mangrove extent but outside the areas preselected as homogenous sites. At each plot the site description (species composition), GPS location, shadow percentage (%), soil colour, canopy cover (%), site vegetation canopy cover,

densiometer reading, and canopy photo were recorded. These validation sites can be used in future mangrove monitoring.

2.3 Field data processing

2.3.1 Biological measurements

Access to all preselected sites prevented the collection of a sample size large enough to conduct a statistical analysis on the biological measures recorded (see *3.1 Biological measures*), therefore the dataset is treated as descriptive.

2.3.2 Mangrove extent and classification

When answering the question of mangrove extent, although AVNIR-2 imagery has a 10m pixel resolution, when comparing this to the aerial photography, it was thought to be too coarse to detect changes in mangrove extent less than a width of 10m. Therefore QB2 and Specterra DMSI image data were used to create the final mangrove extent map.

Post field trip, the method for determining the mangrove extent was refined so that the process of digitising the high water mark could be avoided. A classification technique was used to separate mangrove from other land cover types. A Digital Elevation Model (DEM) with a 30m pixel resolution derived from SPOT imagery (SPOT Image, 2007) assisted this process. The DEM was used to stratify each image by masking the majority of the land and leaving the intertidal and coastal fringe below 10m. This mask was applied to the QB2 and Specterra DMSI images.

The classification of the mangrove extent was determined using the thresholds derived from the scatter plots (see *3.3 Mangrove extent classification*). The average band values for each training site were extracted and compared in a scatter plot to show the spectral variation between the training sites. All bands were investigated and, in addition, vegetation indices NDVI and band 4-band 3, including using a variance index and a NDVI. For both QB2 and Specterra DMSI band 3 and band 4 illustrated the best separation of mangrove reflectance values from other classes. Classification of mangroves could now be carried out using a threshold equation where band 3 and band 4 values only represent mangroves (see *3.3 Mangrove extent classification*). Areas where other classes overlap with mangroves were dealt with using a membership function. A membership function equation was determined using the range of uncertain mangrove extent (where other classes overlapped) (Bonham-Carter and Graeme, 1994). This gave the uncertainty range of 0 to 1, where values from 0.5 to 1 are most likely mangroves. A non vegetation mask, which excluded rock and shadow from the extent, was created by applying thresholds to an NDVI image.

2.3.3 Remote sensing and ground data relationships, and canopy cover estimation

The field data was entered into a personal geodatabase in ArcGIS, containing the GPS sample site locations and the polygon boundaries of the 30m x 30m homogeneous site. This data was then exported into Microsoft Excel, where the sample site estimations of vegetation canopy, densiometer reading, and digital photo cover percentage were averaged for each homogeneous site and compared (see *3.4 Comparison of field methods to remote sensing imagery*). The densiometer canopy openness was calculated and converted to a canopy cover percentage (100 – % canopy openness = % canopy cover).

Of the different canopy estimates collected in the field, the canopy cover and site vegetation canopy cover estimates, determined using the key and photo canopy cover, were converted to Projected Foliage Cover (PFC). Specht *et al*. (1974) defined Projected Foliage Cover (PFC) as "*the percentage of the sample site occupied by the vertical projection of foliage only*". PFC was estimated for each homogeneous site by averaging the field canopy estimates, estimated with the key (%), multiplying the estimate by the aerial photo density estimate (%, spatial density), and then dividing by 100. This widely accepted method is illustrated in Figure 9, with an example from Behn *et al* (2001).

To calculate the canopy percentage cover for the site canopy photos, each digital photo was processed using ER Mapper 7.1 (ERDAS, 2006). Shading analysis of images classified dark vegetation (representing the canopy) from light sky. Statistics were then calculated to determine the area of canopy verses non-canopy (i.e. sky). Different threshold values were determined to classify the light and dark parts of each photo due to differences in environmental conditions such as: the position of the sun, cloud cover, shadow, and mangrove species (Fuentes *et al*., 2008).

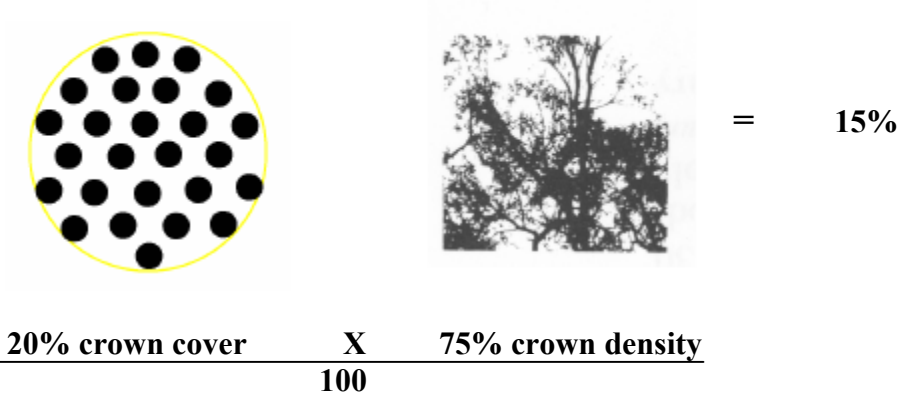

Figure 9. An example of how to determine projected foliage cover. The example was derived from Behn *et al* (2001).

The combinations of different PFC methods are compared in Table 4. PFC values are referred to as PFC(f) where 'f' defines derivation from field observations. Specific field methods were abbreviated as follows:

PFC(vc) is the percentage product of the **aerial photo density estimate** for the site, and represents the average site vegetation canopy estimate;

PFC(cc) is the percentage product of the **aerial photo density estimate** for the site, and represents canopy cover estimate;

PFC(p) is the percentage product of the **aerial photo density estimate** for the site, and represents average photo canopy estimate;

PFC(pvc) is the percentage product of the **average photo canopy percentage** for the site, and represents average photo estimate with average site vegetation cover.

The other ground field methods, photo canopy cover and densiometer readings, were also used to calibrate imagery and were included in table 4. See *2.2.3 On ground assessments – Remote Sensing*, for densiometer estimate calculations.

2.3.4 Image pixel values

To calibrate and test each sensor's imagery (ANVIR-2, QB2 and DMSI) with the field canopy estimates or PFC(f), pixel values were extracted from each image using ER Mapper 7.1 for each 30m x 30m aerial photo (homogenous) site. The mean and standard deviation summary statistic reports were generated for all bands of each image. These statistics were then imported into Microsoft Excel to be compared with the aerial photo density estimate, field observations, and PFC(f) values (Appendix 5, which also includes the raw field observations for homogenous sites and for each waypoint sample).

Table 4. Methods used for estimating field canopy cover (%) and deriving Projected Foliage Cover (PFC). Specific field methods were abbreviated as follows (vc) represents vegetation canopy estimate; (cc) represents canopy cover estimate; (p) represents average photo canopy estimate; (pcv) represents average photo estimate with average site vegetation cover.

Field canopy measure estimates used in linear analysis	Abbreviation PFC(f) f = field observation method
PFC = Aerial photo density estimate x site average vegetation cover / 100	PFC(vc)
PFC = Aerial photo density estimate x average canopy cover / 100	PFC(cc)
PFC = Aerial photo density estimate x average photo canopy percentage / 100	PFC(p)
PFC = Average photo canopy estimate x site average vegetation cover / 100	PFC(pvc)
Site average densiometer converted to canopy cover	-
Site average canopy photo estimate	Photo %

The standard deviations determined from the imagery data assisted in identifying if the site was heterogeneous and should be excluded. The high spatial resolution of the DMSI data (0.5 metres) and larger dynamic range (16bit data compared to 8bit) resulted that some sites, otherwise classified as homogenous, were being identified as heterogeneous. Therefore the boundary of the homogenous area was edited for DMSI image data only. The other satellite imagery used in this study have smaller ranges of reflectance values and coarser resolutions, which causes an averaging effect of an area. For these reasons the pixel value statistics of each aerial photo site extracted from the other sensors were still interpreted as homogenous and not altered.

The sites Cowrie Cove 2 and Cowrie Cove 6, were found to be consistently heterogeneous from field observations, image statistics, and all methods of canopy readings and regression results. Once available, the DMSI data (the closest imagery data captured to the field trip date) enhanced for greenness (Red Green Blue in Bands 3, 4, 2) and false (red image) colour (Red Green Blue in Bands 4, 3, 1) illustrated that Cowrie Cove 2 and Cowrie Cove 6 were obviously heterogeneous. When comparing the aerial photo with the DMSI in Figure 10, visual differences can be seen within the site for Cowrie Cove 2. Including the omitted sites with edited homogenous boundaries did not inform the regression results, and therefore both sites were removed from further regression analyses.

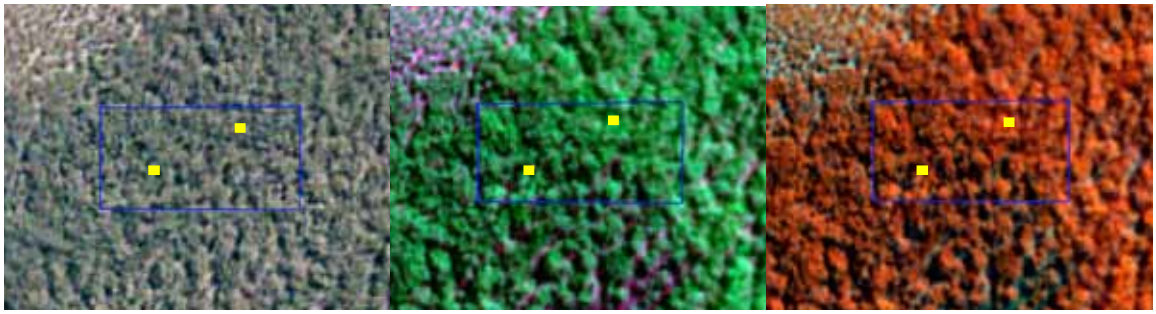

Figure 10. Comparison of DMSI imagery and aerial photography (left) where the DMSI (middle image - greenness enhancement and right image- false colour enhancement) visually prove that Cowrie Cover 2 was a heterogenous site unlike the aerial photograph which lead this site to be interpreted and preselected as a homogenous site. The yellow points represent sample sites within the preselected area.

2.3.5 *Remote sensing and ground data calibration*

PFC(f) values and raw field estimates were orthogonally plotted against different image band or band combinations (indices) to determine if a linear relationship was present. The bands and indices tested were NDVI, band 4 - band 3, band 3 and band 4. These specific band combinations are all known to expose differences in vegetation cover for each of the sensors (AVNIR-2, QB2 and DMSI). The linear regression equation ($y = m.x + b$) can be applied to the image data index to create an image. The values produced from these images are referred to as PFC(i) values, where 'i' indicates the resulting image index as opposed to the field value, PFC(f).

A linear relationship was considered strong if the correlation coefficient of best fit was greater than 0.7. However, if a sensor did not achieve this limit in any of the combinations, the combination with the highest correlation coefficient was selected for application to the

image data. The following field data and image index combinations have very strong linear relationships, and were applied to all sensor data; PFC(vc) and NDVI; PFC(cc) and NDVI; PFC(p) and NDVI; PFC(pvc) and NDVI; and densiometer and NDVI.

There were some exceptions in the application. The following Specterra DMSI combinations had strong linear relationships and thus were applied to the image data: Photo% and NDVI; Photo% and band 3; densiometer and band 3; and PFC(p) and band 3.

The final developed images were clipped with the DMSI mangrove extent classification when testing the applied field method regressions. This ensured that comparison of each mangrove condition index range was consistent.

2.3.6 *Validation assessment of images*

Validation assessment of each resulting image was essential to assess the accuracy and suitability of each method and the sensor used. The field ground validation point locations were used to extract the pixel values from each PFC image (PFC(i)) created and compared on an orthogonal plot with the field derived PFC(f). The centre of the sample plot point was used to extract the image value to compare the QB2, and AVNIR-2 data. The resolution of Specterra DMSI imagery is 0.5m, which is a much finer resolution than the accuracy of the handheld GPS, and the field variables are observed on a 5m x 5m quadrant. To mitigate these effects the pixels values where extracted over a 5m x 5m area and averaged.

A visual assessment was carried out on each resultant image. This included noting the range of PFC(i) values produced, then three different transects per study location were used to assess if the PFC(i) values returned were keeping with the field observations and image interpretation. Hnatiuk *et al.'s* (2009) definition of canopy cover classes was referred to as a guide to the percentages expected for dense, medium, and sparse foliage crown cover. When interrogating the image transect, the following questions were asked: Are the PFC(i) values representative in the sparse, medium, and dense ranges? Do bare areas and water have values? Do shadows have values? Is the range too high or too low?

An assessment scheme was devised to rate the image at each transect. When the response to the questions were negative, 0 was assigned, 1 represented a satisfactory response, and 2 was a representative response. In addition to the subjective transect test, a second validation comparison was undertaken. All validation and ground observations, or PFC(f) values, were plotted across the sites in ascending order of ground value. Also graphed at each site were the corresponding PFC(i) values. These graphs show how each sensor's image index or PFC(i) compared to the ground observations for each method (Figs. 29, 33, 38, 43, and 46).

3.0 Results

3.1 Biological measures

Data were collected for various potential RCI's at 17 sites (see *2.1.6 Site selection*) in a total of 27 transects for both mangroves (14 sites, 23 transects; Appendix 6) and intertidal mudflats (4 sites, 4 transects; Appendix 6).

At most mangrove sites, *Avicennia marina* was the dominant mangrove tree (20 sites) with *Rhizophora stylosa* present as a significant secondary species at 3 of those sites. *Rhizophora stylosa* dominated at 3 sites, with 2 of those sites having *A. marina* as a significant secondary species. A total of 13 trees were flagged (11 *A. marina*; 2 *R. stylosa*; Appendix 6) and studied in relative detail.

Given the time constraints and the primary objective of this pilot study (to ground truth remotely sensed data and test the validity of potential RCI's), it was not possible to conduct many replicates at each site. These sites proved highly variable (an artefact of the non-random sampling design to ground truth sites exhibiting various characteristics), and replicates were too low in number to perform tests of statistical significance, including water quality and soil sediment analyses data. It was therefore not possible to test for differences between sites, or to test the *a priori* hypotheses of "impacted" and "unimpacted" sites.

However, it is possible to comment on the practicality and validity of the RCI's trialled here, which are presented in Table 5. Remote sensing indicators are also included in Table 5. Many of the RCI's trialled here are subjective and are impractical to implement in the field. For example, apparent tree health is a highly subjective measure, and near impossible to assess visually, as trees that have been classified dead in the first instance have been found to be alive and healthy on subsequent surveys, in other studies (Paling *et al.*, 2003). It is also worth noting that although physico-chemical water measurements are nearly ubiquitously used as water quality indicators in marine and aquatic environments, they are so highly variable in intertidal habitats, such as those studied here, that their use becomes dependant on automated continuous sampling to be able to account for that variability, and considerable resources need to be assigned to firstly collect the data, and secondly, to analyse the data.

It is evident from Table 5 that few of the potential RCI's trialled here are practical, truly indicative of resource condition, and are actually valid as RCI's (50% of potential RCI's trialled here). In general, valid RCI's tend to be complex to measure and/or analyse, however, this is to be expected when trying to monitor ecological processes in highly dynamic and complex systems such as coastal and marine environments.

Table 5. Pro's and con's for the use of various potential RCI's, and validity of use as an RCI, in mangrove and inter-tidal mudflat habitats.

Mangrove Transect			
Potential RCI	**Pro's**	**Con's**	**Use as a valid RCI**
Tree height	1. Easily measured	1. Tree height does not reflect the health of the system. A sick tree will not shrink before dying	**NO**
Tree health (healthy/sick/ dead)		1. Highly subjective 2. Apparently dead trees can be alive and therefore lead to false negative results	**NO**
Tree Density		1. Difficult to count accurately when mangroves are dense 2. Difficult to count accurately when transect is dominated by multi-trunked species (eg. Rhizophora) 2. Trees remain in the count long after mortality	**NO**
Primary and Secondary species	1. Indicator of regime shift 2. Easily measured (with the assistance of an identification guide) 3. Low cost	1. By the time this indicator changes, the regime shift has already occurred 2. Interpretation of data requires expert analyses	**YES**
Water quality	1. Ubiquitous use of water quality measures in numerous studies	1. Water quality measures vary greatly throughout a 24hr cycle (tide, evaporation, etc) 2. Would only be useful if monitored continuously with an automated station to account for short term variance 3. High cost - automated station 4. Expert analyses required for automated stations 5. Given the above, this RCI is impractical	**NO**

Table 5. Cont.

Mangrove Transect cont.			
Potential RCI	**Pro's**	**Con's**	**Use as a valid RCI**
Sediment quality (petrochemicals/ heavy metals)	1. Indicator of anthropological impact 2. Easily analysed by well equipped analytical laboratory services 3. Ubiquitous use of sediment quality measures in numerous studies	1. Difficult to transport samples 2. Requires analyses to be performed soon after sample collection 3. High cost when multiple samples analysed	**YES**
Remotely sensed canopy cover	1. Whole of ecosystem or environment perspective can be gained 2. Good for assessing catastrophic events (eg. cyclones) 3. Can be used as a trigger indicator to warrant further investigation if a change is detected 4. Pinpoints where changes have occurred and where to focus further investigation 5. Cost effective for large geographic areas 6. Cost effective when monitoring remote locations	1. Variably sensitive to different impacts 2. May not be able to determine cause if change detected 3. Image acquisition/capture confounds calculating exact timing of impact events 4. Spatial resolution needs to be critically assessed prior to the commencement of monitoring, subject to the objectives of the program 5. Expert analyses required 6. Specialised hardware and software expenses	**YES**
Remotely sensed habitat extent	1. Detects change in spatial distribution of the habitat 2. Reliable desktop production of extent (any type of extent change may warrant further investigation) 3. Cost effective for large geographic areas 4. Cost effective when monitoring remote locations	1. Spatial scale is inversely proportional to sensitivity to change 2. Does not indicate condition within habitat extent 3. Expert analyses required 4. Requires ground truthing	**YES**

Table 5. Cont.

Flagged Mangrove Tree			
Potential RCI	**Pro's**	**Con's**	**Use as a valid RCI**
Greatest trunk diameter @ 1m		1. Branching nature of mangrove tree trunks can make choice of trunk difficult (particularly with R. stylosa) 2. Does not necessarily indicate current health of tree	**NO**
% herbivory	1. Indicator of stress through immune response (ie immunosuppression and increased herbivory through increased environmental stress)	1. Difficult to accurately count number of leaves and associate leaves with a specific tree (high tree densities and branch interlocking) 2. May be necessary to take serum samples for immunochemical analyses 2. Immunochemical analyses expensive and requires experts	**YES**
# of propagules	1. Indicates tree fecundity (high fecundity assumed for healthy trees) 2. Easily measured	1. Seasonally dependant 2. Relatively brief event for some species 3. Requires advanced planning for field work	**YES**
Leaf health (healthy/sick/ dead)		1. Highly subjective 2. Difficult to accurately count number of leaves and associate leaves with a specific tree (high tree densities and branch interlocking) 3. Leaf distribution on a given tree can be highly heterogeneous	**NO**

Table 5. Cont.

Intertidal Mud Flats			
Potential RCI	**Pro's**	**Con's**	**Use as a valid RCI**
Grain size		1. Would require a number of mesh sizes to accurately measure small changes (more than the number of meshes used here)	**YES**
Water quality	1. as for Mangrove Transect	1. as for Mangrove Transect	**NO**
Sediment quality (petrochemicals/ heavy metals)	1. as for Mangrove Transect	1. as for Mangrove Transect	**YES**
Remotely sensed habitat extent	1. Moisture indicates tidal range 2. Tide lines can be used to monitor changing coastlines (i.e. changes in sedimentation rates) 3. Cost effective for large geographic areas 4. Cost effective when monitoring remote locations	1. Different soil types and algal mats produce heterogeneous reflectance values, therefore difficult to map 2. High water mark needs to be accurately interpreted from image 3. Expert analyses required	**YES**

3.2 On ground assessment - remote sensing

Uninterrupted on ground observations can be found in Appendices 4 and 5. The applied results of these observations and field measurements can be found in the following sections.

3.2.1 Comparison of canopy field measurements per site

Variation in canopy cover estimates measured in the field can be seen in Figure 11. The homogenous site density estimate from aerial photos has also been added, to illustrate the differences and similarities between human interpretation (in the field and from the aerial photo) and photo calculations. The results show some consistency in the range of canopy cover estimates, as most of the values are within 20% of each other. Those methods estimated with human interpretation, such as the average canopy cover and site vegetation cover, resulted in lower canopy cover estimates, whereas densiometer readings, another human interpretation method, almost always had the highest canopy cover. The photo estimates displayed in Figure 11 are within the mid to upper range of other canopy cover estimates.

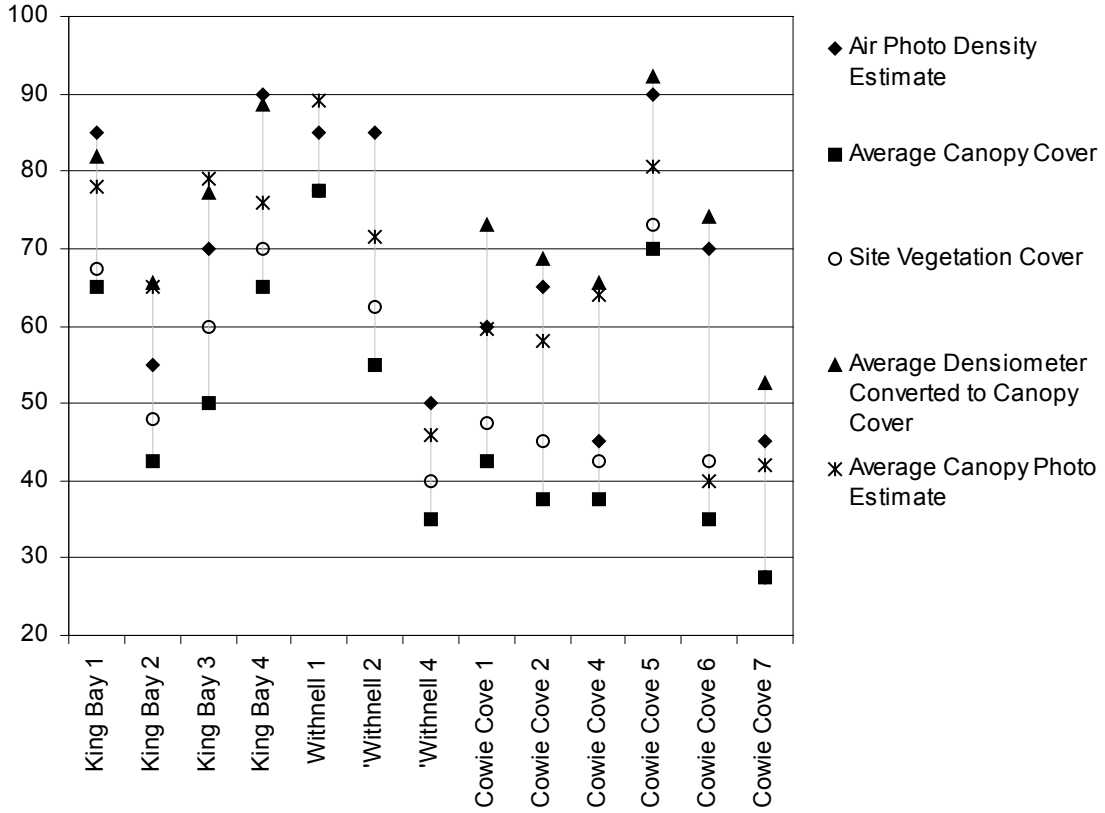

Figure 11. Comparison of the canopy cover derived from different field methods and canopy densities from the ortho-photography of homogenous site estimated by one person.

Assuming that the photos taken are representative, they may be closer to the real canopy cover estimate, but if the photo is taken in the wrong place the site could also be misinterpreted. Human interpretation methods that use a key or densiometer can be inconsistent, even if the same person is interpreting all measurements. It is known that adjusting perceptions to accurately interpret the canopy cover percentage from a key, or count the gaps in the case of the densiometer, requires training with the vegetation type beforehand (Lemmon, 1957). For this pilot study, the time spent in the field was limited by the tide, budget, and time frame of

the project, which precluded practice of field measurements prior to actual data collection and prohibited sufficient collection of replica measurements.

The canopy photo method was quick and consistent, even though the average canopy cover and the site vegetation canopy cover estimates were low. The key method was also consistently low.

3.3 Mangrove extent classification

The results of the classification of the mangrove extent were determined using the thresholds derived from the scatter plots of band 3 and band 4 (inputs into NDVI) in Figures 12 and 13. These plots show the clustering of different land cover types and the variation within each cover type. The 'mangrove' class shows separation from other classes, however some overlap with 'other vegetation' is present in both the DMSI (Fig. 12) and QB2 (Fig. 13) images. 'Shadow' also overlaps with 'mangroves' and 'other vegetation' in the QB2 plot (Fig. 13).

The classification thresholds selected for the uncertain mangrove class were determined by observing the commission and omission errors in the extreme mangrove densities i.e. very sparse or very dark mangrove in the shadows. The limits chosen, and set to define the mangrove extent for each class (mangrove, not mangrove and uncertain mangroves), were derived from the plots. Where upper or lower limits were not sampled with the training sites, the thresholds were adjusted manually to find the balance between including mangrove and excluding other land cover.

Class thresholds applied to QB2 were:

QB2: Mangrove if Band 3 ≤300 and (Band 4 > 400 and Band 4 <1200), then 1 else null

Not mangrove if ((Band 4 - Band 3) / (Band 4 - Band 3)) <0.085, then 2 else null

Uncertain if (if Band 4 >200 and Band 4 <400, then (0.005*i1-1) else null)>0.5, then else null

Uncertain if (if Band 3 >300 and Band 3 <430 and Band 4 >450 then (-0.0077* Band 3 +3.307) else null)>0.05, then 1 else null

Class thresholds applied to DMSI were:

DMSI: Mangrove if Band 3 ≤450 and (Band 4 ≥500 and Band 4 ≤1600), then 1 else null

Not mangrove if ((Band 4 - Band 3) / (Band 4 + Band 3)) <0.11, then 1 else null

Uncertain if (Band 3 >450 and Band 3 <800) and (i2 >300 and Band 4 <2050), then 1 else null

Uncertain if (Band 3 >0 and Band 3 <800) and (Band 4 >300 and Band 4 <500), then 1 else null

Uncertain if (Band 3 >0 and Band 3 <800) and (Band 4 >1600 and Band 4 <2050), then 1 else null

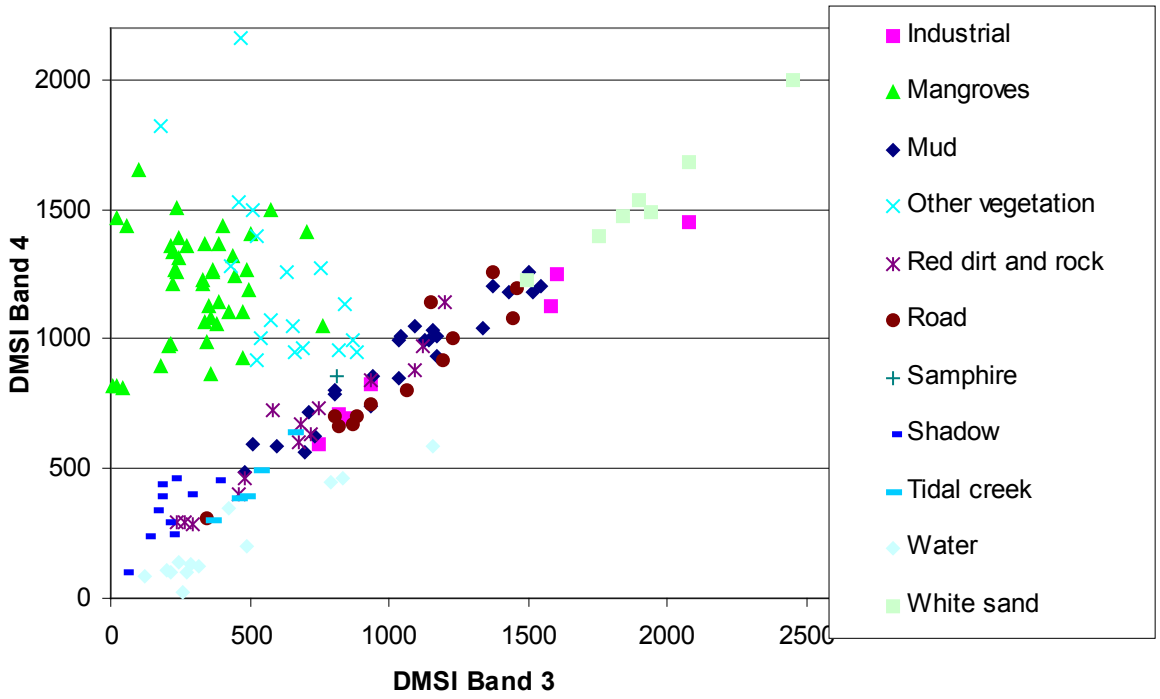

Figure 12. This scatter plot of the average training site values for band 4 and band 3 illustrates the separation found in training site classes with DMSI imagery.

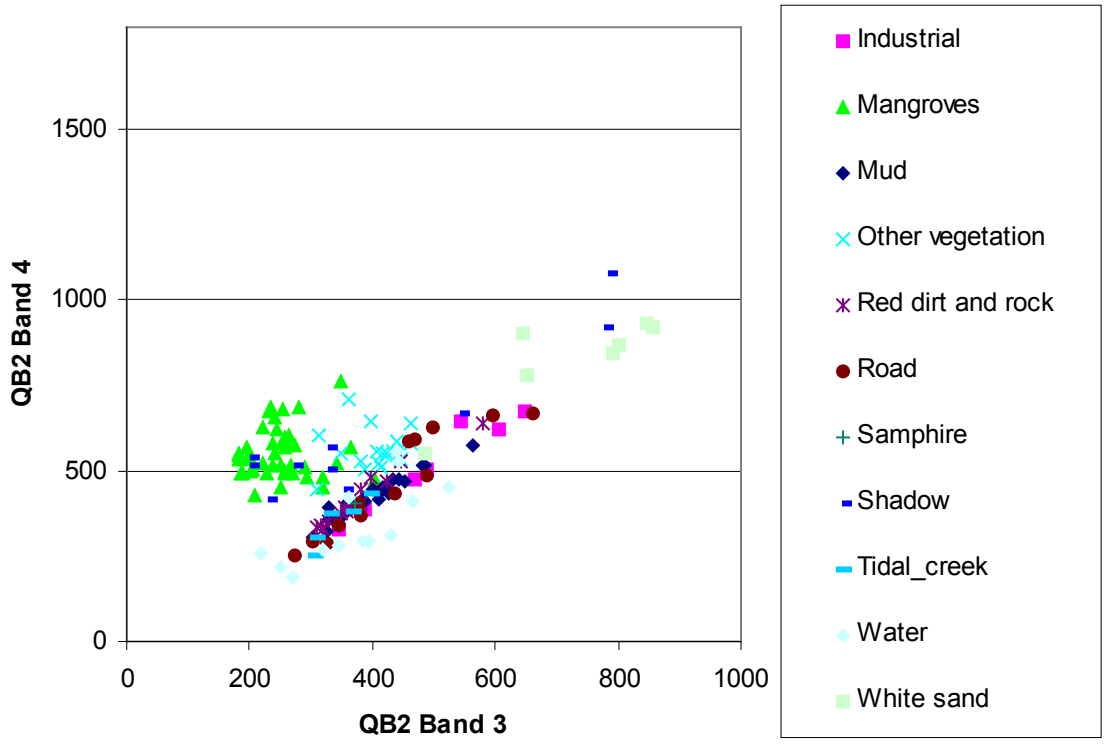

Figure 13. This scatter plot of the average training site values for band 4 and band 3 illustrates the separation found in training site classes with QB2 imagery.

Any nulls or gaps in the classification (i.e. where the image was not classified as mangrove or 'Not mangrove') were classified as 'Not mangrove'. One mangrove mask was made by reclassifying the uncertain mangrove class to mangrove, leaving only two classes, mangrove and non mangrove.

The DEM used to mask the inland cover of the images was not effective enough to eliminate other vegetation from the coastal area. To further refine the classification and remove other vegetation from the mangrove class, the digitised high water mark was applied to clip any data higher than the high water mark in both the QB2 and DMSI classifications. Once thresholds were set and classes 'certain mangrove', 'not mangrove', and the probability scale for 'uncertain mangrove' had been applied to DMSI and QB2 images, each classification was assessed to determine which image had the better mangrove extent.

The classified images defined 'certain' mangroves in brown, areas that are not mangrove (mud /water/ other vegetation) are in white in each classification image. The bright colours represent 'uncertain' mangroves in each classification. Cool colours (blue, green, cyan) of the 'uncertain' mangroves have a smaller chance of being classed as a mangrove; where as warm colours, (red, orange and yellow) were more likely to be classed as mangrove. The key below assists interpretation of the 'uncertain mangrove' and the 'certain mangrove' classification for each image of mangrove extent (Fig. 14).

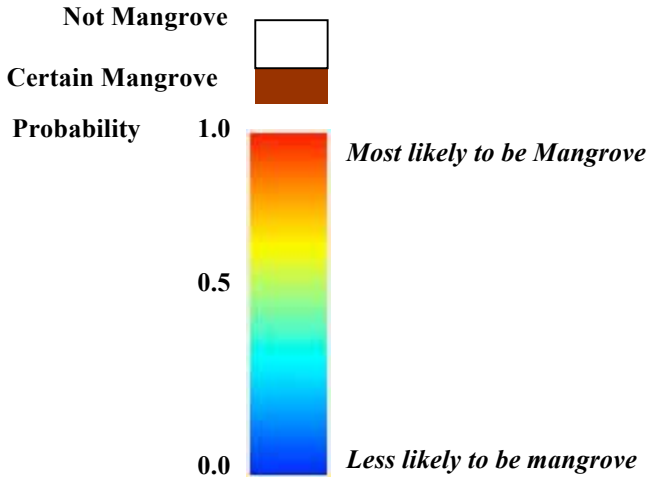

Figure 14. Mangrove extent classification key.

Figures 15 to 26 illustrate an example, per study site, of the derived QB2 and DMSI classifications. These figures illustrate the performance of each sensor's classification, particularly for the uncertain mangrove class. Example images of the aerial photo, and a natural colour enhancement of the DMSI image, were used as an uninterpreted land cover reference to compare with the QB2 and DMSI classifications (Figures 15 to 18 for Cowrie Cove; Figures 19 to 22 for King Bay; and Figures 23 to 26 for Withnell Bay).

Cowrie Cove

Figure 15. Aerial photography of Cowrie Cove captured in August 2004 RGB, displayed in bands 3, 2 and 1. Used as a visual reference.

Figure 16. Specterra DMSI imagery of Cowrie Cove captured in June 2009 displayed in RGB, bands 3, 2 and 1.

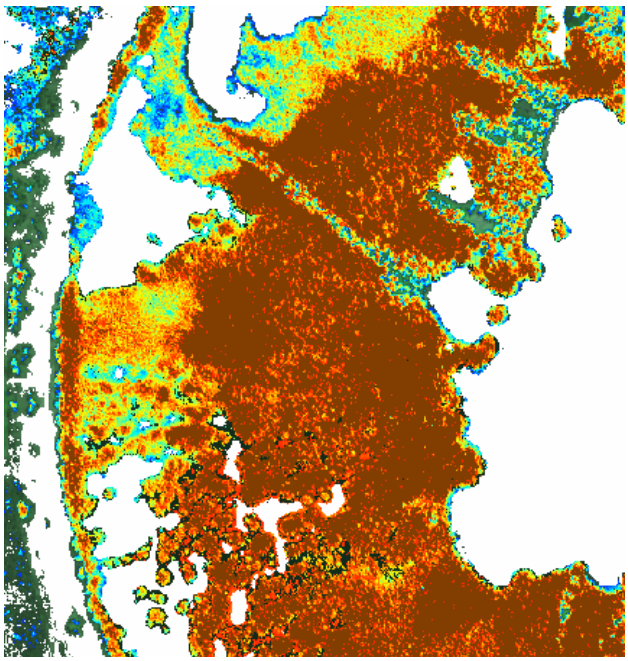

Figure 17. QB2 image classification of Cowrie Cove, captured in November 2006.

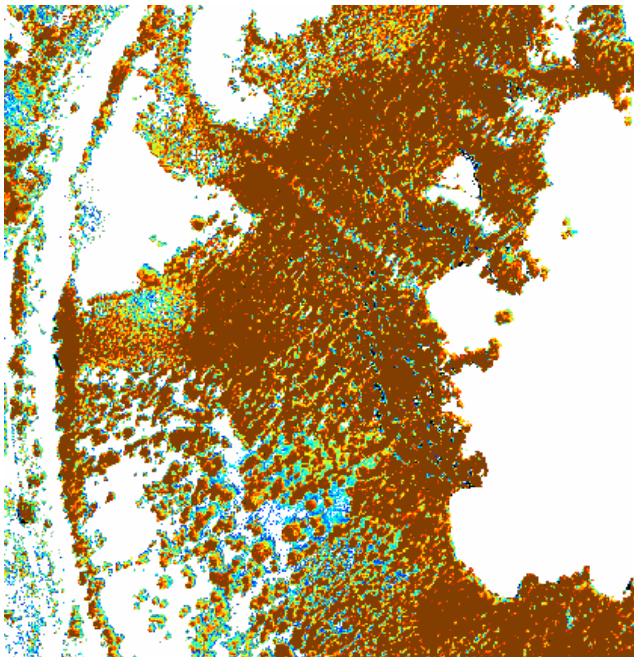

Figure 18. Specterra DMSI image classification of Cowrie Cove, captured in June 2009.

King Bay

Figure 19. Aerial photography of King Bay captured in August 2004 RGB, displayed in bands 3, 2 and 1. Used as a visual reference.

Figure 20. Specterra DMSI imagery of King Bay captured in June 2009 displayed in RGB, bands 3, 2 and 1.

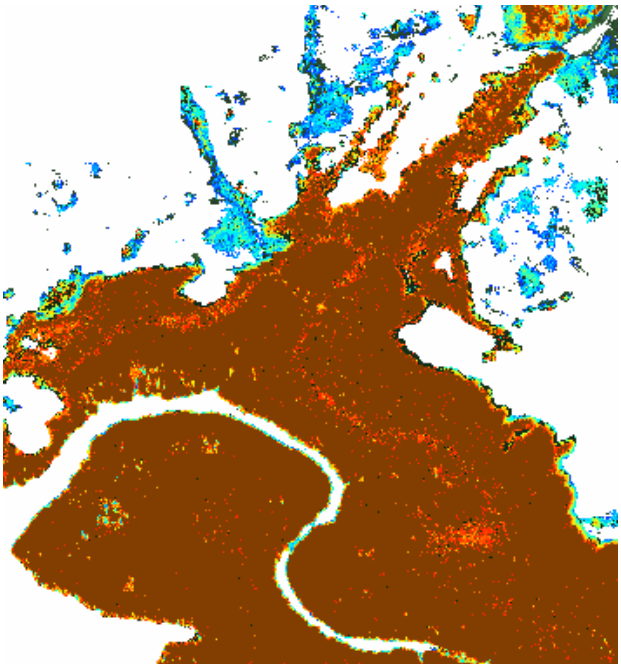

Figure 21. QB2 image classification of King Bay captured in November 2006.

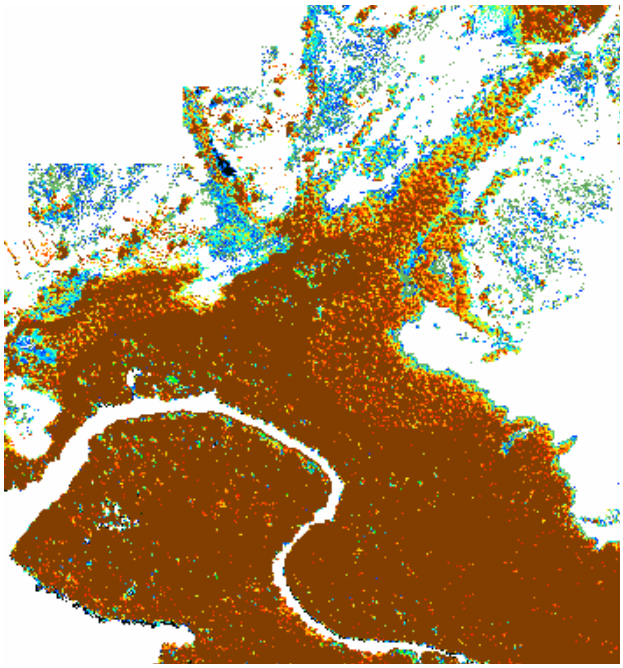

Figure 22. Specterra DMSI image classification of King Bay captured in June 2009.

Withnell Bay

Figure 23. Aerial photography of Withnell Bay captured in August 2004 RGB, displayed in bands 3, 2 and 1. Used as a visual reference.

Figure 24. Specterra DMSI imagery of Withnell Bay captured in June 2009 displayed in RGB, bands 3, 2 and 1.

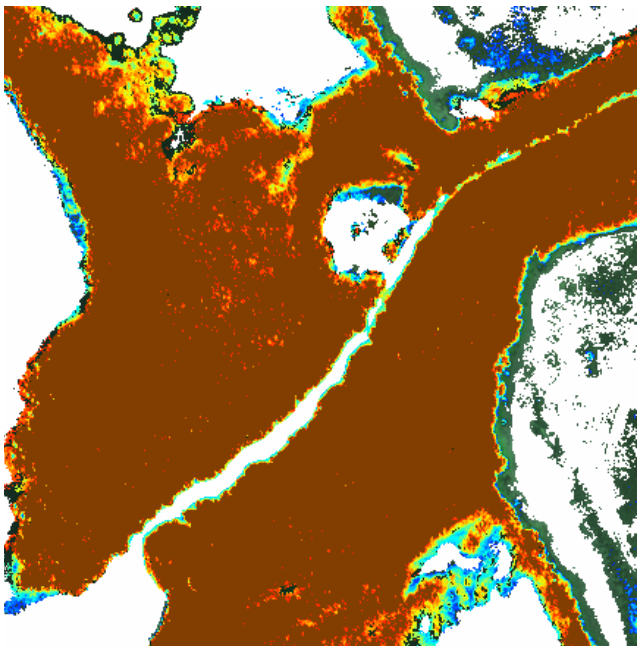

Figure 25. QB2 image classification of Withnell Bay, captured in November 2006.

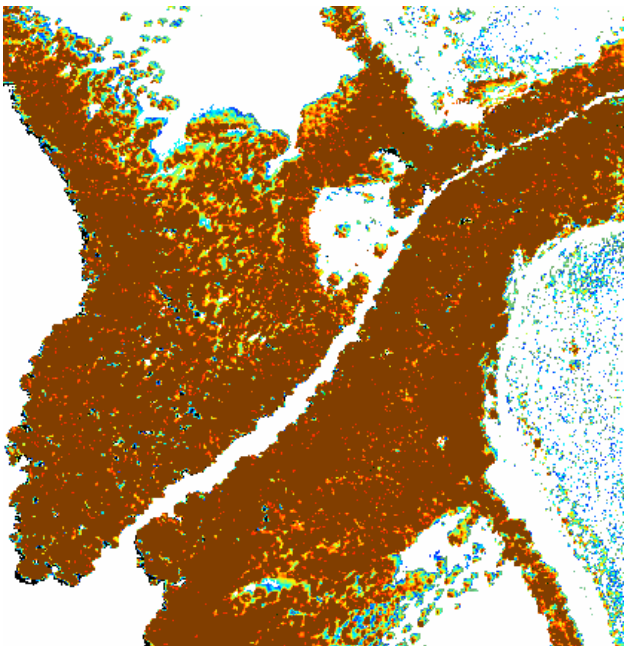

Figure 26. Specterra DMSI image classification of Withnell Bay, captured in June 2009.

Final mangrove extent classification images were created once the most appropriate probability for the 'uncertain mangrove' class was determined. The results were two classification images, one derived from QB2, the other from DMSI, illustrating 'mangrove' and 'non mangrove'.

When both mangrove extents were compared to the aerial photography the following differences were noticed:

With more time, an omission and commission validation test for classification error should be conducted to fully test the mangrove extent determined from each sensor. A quick comparison of the QB2 and DMSI mangrove masks against the aerial photography highlighted some omission and commission errors, described below. These observations were used in determining which sensor better defined the mangrove extent.

Both classifications did not pick up very sparse mangroves at Cowrie Cove, but in the rest of the mangrove extent they were very similar. QB2 appeared to show more omission errors, as a result of a slightly larger pixel size, that the image was captured from a satellite and the atmospheric interference blurs and dulls the spectral response, and the image has been resampled from 2.5 m to 0.6m with the panchromatic band. DMSI has a smaller pixel size (0.5m), and this characteristic may be the reason why in sparse areas of the mangrove extent, for the extent to be broader in the QB2 image compared to the DMSI image. The DMSI tends to more discretely capture the same area, by not including the surrounding mud. Other effects of the classification applied to QB2 were that areas of sand/mud and shadow have also been included in the uncertain mangrove class. Shadow was also included in some places. Further manipulation of the uncertain mangrove class boundaries or applying a ratio to eliminate shadow may improve these errors of omission.

The clipping of imagery from each sensor, with the coastal SPOT DEM, reduced commission errors in other vegetation. However, the coarser spatial resolution of the coastal DEM did not eliminate all terrestrial vegetation. In minor cases, the DEM mask excluded mangrove extent (omission errors) in areas where the mangrove extent was narrow and terrain was steep. A more refined DEM would negate these errors and should even improve the in classification of the mangrove extent by excluding more areas above the high water mark.

Both QB2 and DMSI classifications classify dense stands of mangrove forest as certain mangrove. Whereas sparse mangroves and those located in the narrow or edge intertidal areas were only partially classified as certain mangrove, but often classed as uncertain mangrove.

Commission errors could be seen in QB2 mangrove classification where the atmospheric affect of industrial dust or smoke plume over the port, and a berthing ship, was classified as mangroves.

As both images were also clipped to the digitised high water mark, this was also another source of commission and omission, as the technique relied on human interpretation of the high tide mark and the estimated mangrove/ other vegetation boundary. This could be improved with ground truthing, or replaced as a method by using a DEM of a higher resolution.

3.4 Comparison of field methods to remote sensing imagery

3.4.1 AVNIR-2

Comparisons of the linear analysis of the vegetation indices of the AVNIR-2 satellite sensor and the different field derived PFC or canopy cover estimates are recorded in Table 6. The square of the Pearson product moment correlation coefficient (r^2) is used to assess the strength of the linear relationship between the imagery and field data. The r^2 values for almost all of the regressions, for both NDVI and Band 4-3 vegetation indices, were very high, representing a strong relationship (>0.75). However, the r^2 regressions with the photo canopy percentage were not as strong (<0.75), as were most of the r^2 values for all of the regressions tested with band 3 and band 4. The values highlighted with red in Table 6 were chosen to apply the corresponding regression equations to the AVNIR-2 imagery to test for suitability and representation of mangrove density.

3.4.2 Quick bird -2

The results of the linear analysis of the vegetation indices of the QB2 satellite sensor and the different field derived PFC or canopy cover estimates are shown in Table 7. The r^2 values for the regressions between the NDVI vegetation index and PFC(c), and PFC(vc) and the densiometer, were greater then 0.75, representing a strong relationship. PFC(vc) was very close to 0.75 and was also considered a strong relationship. The r^2 regressions with the photo canopy percentage was not as strong (<0.75), as were most of the r^2 values for all of the regressions tested with band 3 and band 4. The values highlighted with red in Table 7 were chosen to apply the corresponding regression equation to the QB2 imagery to test its suitability as an index of mangrove density.

3.4.3 DMSI

The results of the regression between the vegetation indices of DMSI airborne sensor and the different field derived PFC or canopy cover estimates are shown in Table 8. The r^2 values for all of the regressions were less than 0.75. However, those considered strong enough to apply the corresponding regression equation to the DMSI imagery, are highlighted with red in Table 8, and were chosen to test their suitability as an index of mangrove density. This included: PFC(vc) with NDVI; and PFC(p), densiometer and photo canopy percentage with the NDVI index and band 3.

Where low r^2 were found, particularly for the DMSI sensor, it could be that there were not adequate sample sites to determine the relationship. The strong regression results for both the QB2 and AVNIR-2 would also benefit from further analysis with more sample sites to avoid the risk that the correlation coefficients of the regressions are misleadingly high.

3.5 Validation assessment of mangrove density indices

Initial assessment of the applied regression images examined the range of values and the general representation of the mangrove canopy habitat. Each PFC(i) or applied field index were visually assessed to find out if the resulting index range was reasonable, initial observations from the image, and transect test observations.

Validation sites that were collected in the field were also used to compare the regression between the validation site and the image to see if a strong relationship could still be found. However, only 8 validation sites (only 5 for the densiometer) were available to test. These

Table 6. Regression results comparing field methods and AVNIR-2 imagery.

ALOS AVNIR 10 May 2007		Canopy estimate method					
		PFC Visual field estimate		PFC Photo canopy estimate		Densiometer	Photo Canopy %
Index		PFC(cc)	PFC(vc)	PFC(p)	PFC(pvc)	Densiometer corrected for canopy cover	Photo Canopy %
NDVI	Linear Regression	y = 122.72x + 30.777	y = 126.11x + 33.616	y = 127.55x + 41.488	y = 105.53x + 33.841	y = 76.909x + 71.451	y = 78.161x + 63.511
	r^2	0.8693	0.888	0.8636	0.8088	0.9007	0.6718
Band 4-3	Linear Regression	y = 0.9718x + 32.429	y = 0.8126x + 26.372	y = 1.0015x + 35.296	y = 0.8481x + 35.188	y = 0.6244x + 72.71	y = 0.6361x + 64.462
	r^2	0.8451	0.8261	0.8683	0.8098	0.9086	0.6899
Band 3	Linear Regression	y = -0.9515x + 91.112	y = -1.0234x + 98.156	y = -1.0669x + 108.53	y = -0.9187x + 91.315	y = -0.634x + 110.57	y = -0.75x + 109.95
	r^2	0.5334	0.5969	0.6167	0.6257	0.7585	0.6314
Band 4	Linear Regression	y = 1.7181x - 67.563	y = 1.6304x - 59.124	y = 1.5528x - 46.385	y = 1.2098x - 34.254	y = 0.7303x + 30.934	y = 0.708x + 24.649
	r^2	0.531	0.4626	0.3989	0.3313	0.1889	0.1718

Table 7. Regression results comparing field methods and QB2 imagery.

Quickbird- 2, 6 November 2006		Canopy estimate method					
		PFC Visual field estimate		PFC Photo canopy estimate		Densiometer	Photo Canopy %
Index		PFC(cc)	PFC(vc)	PFC(p)	PFC(pvc)	Densiometer corrected for canopy cover	Photo Canopy %
NDVI	Linear Regression	y = 197.32x - 31.68	y = 200.7x - 29.835	y = 198.53x - 21.106	y = 163.3x - 17.611	y = 124.67x + 32.16	y = 118.08x + 26.419
	r^2	0.7973	0.7607	0.7423	0.6872	0.8428	0.544
Band 4-3	Linear Regression	y = 0.204x - 19.88	y = 0.2037x - 16.737	y = 0.1969x - 6.8446	y = 0.1595x - 5.1807	y = 0.131x + 39.658	y = 0.1081x + 37.472
	r^2	0.678	0.6543	0.5813	0.5219	0.6164	0.3628
Band 3	Linear Regression	y = -0.3131x + 119.35	y = -0.3347x + 128.01	y = -0.3509x + 140.16	y = -0.3047x + 119.2	y = -0.2095x + 129.12	y = -0.2526x + 133.73
	r^2	0.5268	0.5825	0.6087	0.6278	0.7712	0.6536
Band 4	Linear Regression	y = 0.1441x - 40.187	y = 0.1334x - 31.324	y = 0.1161x - 13.941	y = 0.0844x - 5.6997	y = 0.0408x + 53.109	y = 0.0354x + 48.955
	r^2	0.2369	0.1964	0.1414	0.1023	0.0417	0.0273

Table 8. Regression results comparing field methods and DMSI imagery.

Specterra DMSI 10 June 2009		Canopy estimate method					
		PFC Visual field estimate		PFC Photo canopy estimate		Densiometer	Photo Canopy %
Index		PFC(cc)	PFC(vc)	PFC(p)	PFC(pvc)	Densiometer corrected for canopy cover	Photo Canopy %
NDVI	Linear Regression	y = 118.03x - 20.846	y = 128.84x - 23.206	y = 135.93x - 18.791	y = 117.18x - 18.393	y = 84.064x + 32.456	y = 100.36x + 18.037
	r^2	0.4559	0.5255	0.5561	0.5654	0.7196	0.628
Band 4-3	Linear Regression	y = 0.0819x - 17.845	y = 0.0896x - 20.047	y = 0.0954x - 16.028	y = 0.0836x - 16.988	y = 0.0645x + 29.235	y = 0.0746x + 17.24
	r^2	0.3337	0.3861	0.4158	0.4376	0.6433	0.5266
Band 3	Linear Regression	y = -0.1337x + 84.839	y = -0.1463x + 92.262	y = -0.1536x + 102.78	y = -0.1325x + 86.422	y = -0.0964x + 109.07	y = -0.1117x + 107.21
	r^2	0.4566	0.5285	0.5542	0.5636	0.7042	0.6072
Band 4	Linear Regression	y = 0.0443x - 7.5871	y = 0.0484x - 8.7669	y = 0.0551x - 7.6891	y = 0.0522x - 13.72	y = 0.0923x - 23.357	y = 0.0575x + 8.8906
	r^2	0.0292	0.0337	0.0415	0.051	0.2457	0.0935

sites were also captured opportunistically from non homogenous sites which were often on the edge of the mangrove extent. These sites were not ideal but the time constrains of the project, restricted the replicaiton and quality of validation sites. This factor should therefore be considered when interpreting this validation assessment, and determining the suitability of the field method and sensor index.

All field samples were used to compare each sensor's response to the PFC(i) or applied field index with the corresponding ground truth value. This is shown as a graph for each PFC (i) or applied field index. Again, in an ideal situation, more field validation sites with preselected locations and variation in range, should be used for validation assessments.

3.5.1 NDVI images transformed to PFC(cc)

When applying the developed transform of the PFC(cc) to the NDVI of AVNIR-2 and QB2, the range of PFC values for both images were very similar, 1 to 79 and 1 to 80, respectively. For both images, initial observations indicated that the values in the image may be too low, and very sparse mangroves were not included in the QB2 image.

When the transformed image values were extracted at validation sites and examined against the field observation (PFC(cc)), the results for AVNIR-2 had a very strong relationship of $r^2 = 0.88$, and QB2 had a strong relationship of $r^2 = 0.64$ (Figures 27 and 28). However this test only had 8 validation points available.

A transect test was conducted to assess the suitability of the canopy density method to the sensor. Both AVNIR-2 and QB2 appeared to have lower than expected densities across most transects especially where the mangroves were expected to be very dense. The QB2 was the better performer of the two sensors. Appendix 7 contains tables of observations from each transect tested across each study area and provides an overall ranking for the image index.

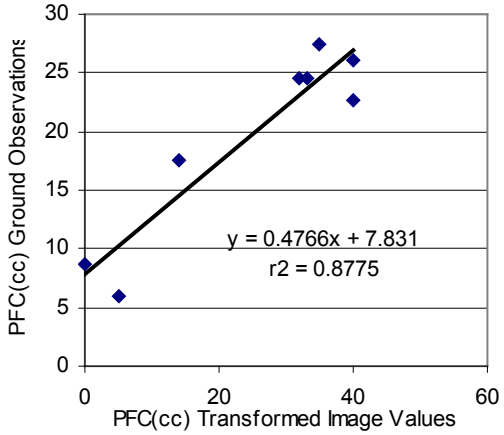

Figure 27. Regression between the ground truth validation site values and the extracted AVNIR-2 NDVI converted to PFC(cc).

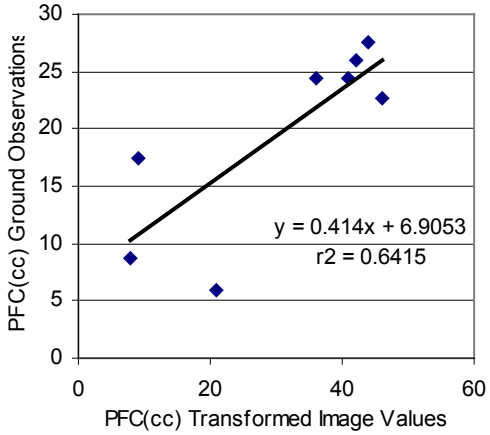

Figure 28. Regression between the ground truth validation site values and the extracted QB2 NDVI converted to PFC(cc).

A comparison of all ground data sites, including the field validation with the corresponding PFC(cc) values for each image, illustrates how both QB2 and AVNIR-2 images values generally fall within 5 to 10% of the ground truth PFC(cc) at the high and low density ranges, but are generally 10 to 20% higher in the middle range (Figure 29).

Despite the higher density values in the mid range, the relationship is approximately linear, and shows density variation across all sites. Therefore, NDVI and the field method PFC(cc), was found to be suitable to both sensors but particularly to AVNIR-2, which provided consistent results. AVNIR-2 may have provided a more consistent linear relationship because of the larger pixel size (10m by 10m). This characteristic of AVNIR-2 averages out the variation in the canopy density in that area and is similar to the PFC field methods, which averages an area by multiplying the aerial photo estimate for the homogenous site with the canopy cover estimate of the sample site.

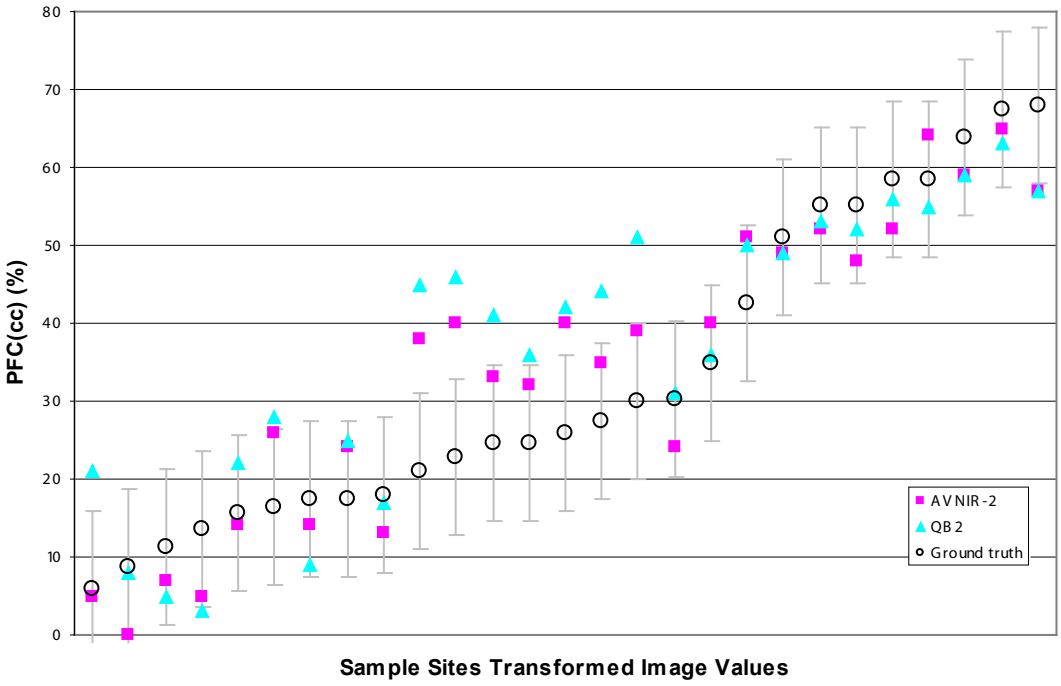

Figure 29. All ground truth values for PFC(cc) compared to extracted image NDVI values of QB2 and AVNIR-2. The data has been sorted into ascending order by ground data PFC values to visualise the results over different density ranges: low, mid, and high. An error bar (±10%) has been added to each ground data site.

3.5.2 NDVI images transformed to PFC(vc)

When applying the transformation of the PFC(vc) to the NDVI of AVNIR-2 and QB2, the PFC(vc) values range for both images were again very similar, with 1 to 79 and 1 to 80, respectively. When applied to DMSI, the range extended from 1 to 105. For both of the AVNIR-2 and QB2 images, initial observations indicated that the density values in the image were too low, and in the QB2 image, very sparse mangroves were not included. The PFC(vc) transformation appeared to be representative when applied to the DMSI image, but in some places displayed lower than expected densities in known higher density areas.

When transformed image values were extracted at validation sites and examined against the field observation PFC(vc) values, the results for all sensors had very strong relationships with an $r^2 = 0.88$ for DMSI, $r^2 = 0.85$ for QB2, and $r^2 = 0.80$ for AVNIR-2 (Figures 30, 31, and 32, respectively). However only eight validation points were available to test.

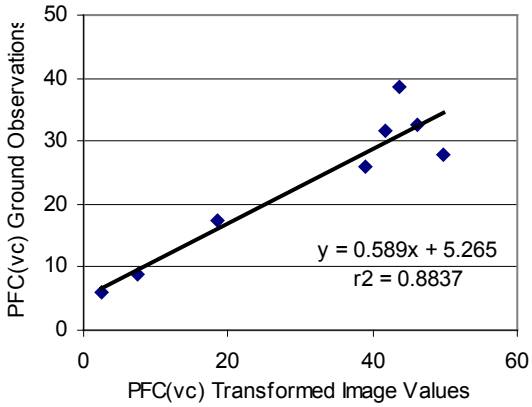

Figure 30. Regression between the ground truth validation site values and the extracted DMSI NDVI transformed to PFC(vc).

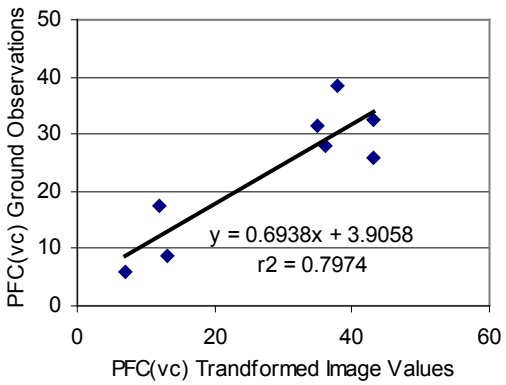

Figure 31. Regression between the ground truth validation site values and the extracted QB2 NDVI transformed to PFC(vc).

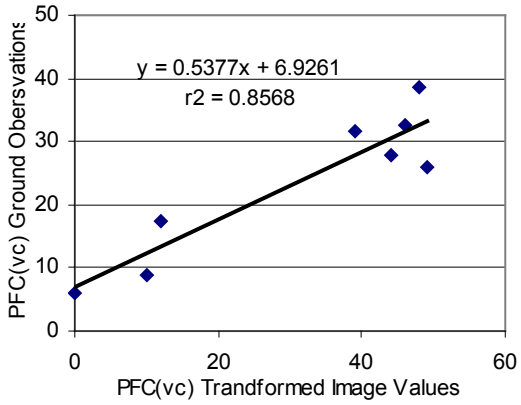

Figure 32. Regression between the ground truth validation site values and the extracted ALOS NDVI transformed to PFC(vc).

A transect test was conducted to assess the suitability of the mangrove PFC(vc) method and NDVI to each sensor. Both AVNIR-2 and QB2 appeared to have lower than expected densities across most transects particularly in the high density areas, with the exception of AVNIR-2 in two transects in Whitnell Bay and King Bay. Transect observations from DMSI generally illustrated that the image density values were not large enough in high density areas, but representative on low cover values, with the exception of Cowrie Cove where two transects returned lower than expected values. The transect test found that the DMSI was the better performer of the sensors when applying the PFC(vc) field method. Appendix 7 tables observations from each transect tested across each study area and provides an overall ranking for the image NDVI transformed to PFC(vc).

A comparison of all ground truth sites, including the field validation, with the corresponding projected canopy cover values for QB2, AVNIR-2, and DMSI are illustrated in Figure 33. DMSI, QB2, and AVNIR-2 images fall within 5 to 10% of the ground truth PFC(vc) values at low and high density cover ranges. In the mid range densities, QB2 and AVNIR-2 were generally 5 to 30% higher, whereas DMSI performed better with 5 to 20% deviations from the ground truth value. Although the initial validation regression implies a strong relationship, the comparison of all sites implies that the variation in the mid to high range is poor and the PFC(vc) field method is not suitable to QB2, AVNIR-2, and DMSI with NDVI.

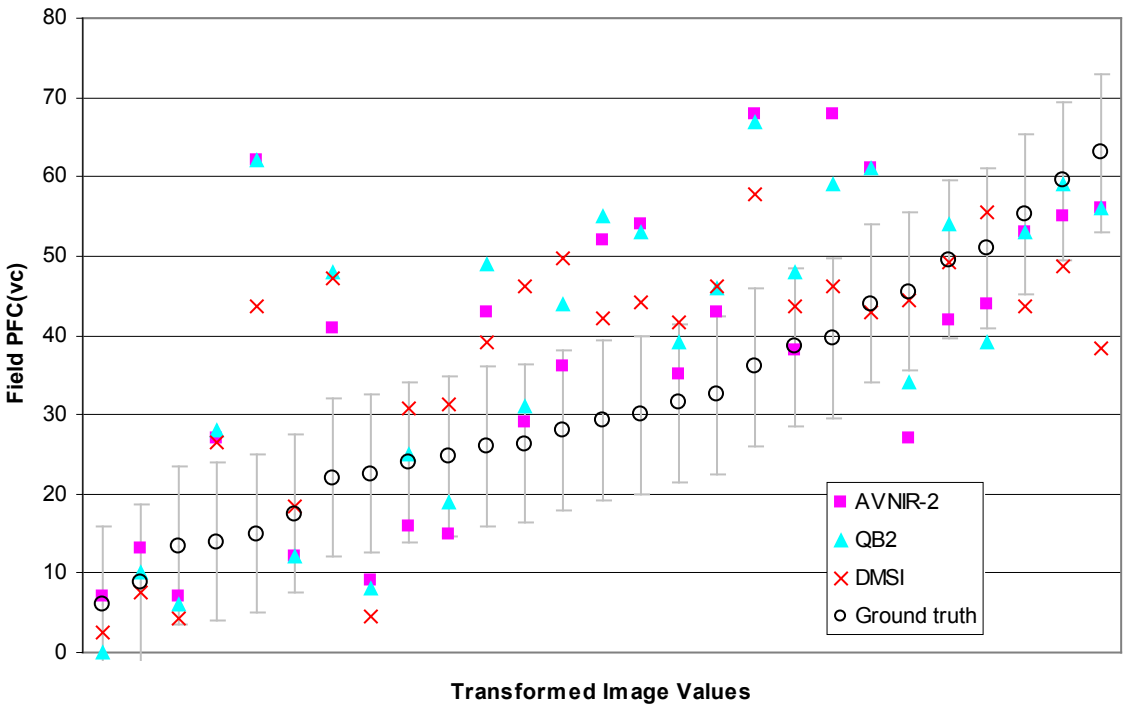

Figure 33 All ground truth values for PFC(vc) compared to extracted image densities derived from NDVI, AVNIR-2, QB2, and DMSI. The data has been sorted into ascending order by ground data PFC values to visualise the results over different density ranges: low, mid, and high. An error bar (±10%) has been added to each ground data site.

3.5.3 NDVI and Band 3 images transformed to PFC(p)

For the PFC(p) transformation applied to the NDVI for AVNIR-2 and QB2, the range of PFC(p) values for both images was 1 to 92. When applying the transformation to the DMSI NDVI image, the range extended from 1 to 117. Whereas the range of PFC(p) values for PFC(p) transformation applied to DMSI with the index of band 3 was 1 to 103. For both of the AVNIR-2 and QB2 images, initial observations indicated that the values in the image were representative, except where values were lower in the sparser cover. The DMSI NDVI transformed to PFC(p) appeared to display higher than expected densities, whereas the DMSI Band 3 transformed image possibly had values that were higher in the middle density range.

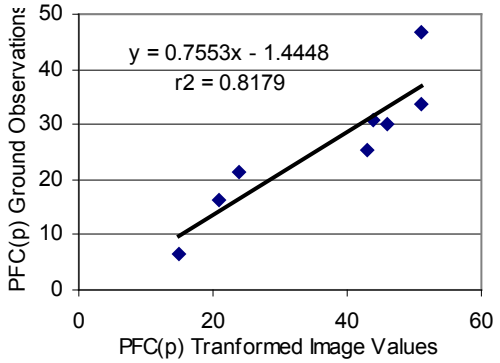

Figure 34. Regression between the ground truth validation site values and the extracted AVNIR-2 NDVI transformed to PFC(p).

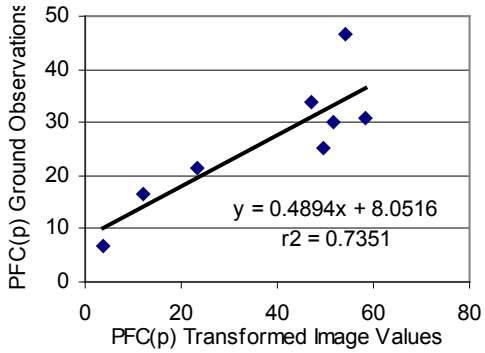

Figure 35. Regression between the ground truth validation site values and the extracted DMSI NDVI transformed to PFC(p).

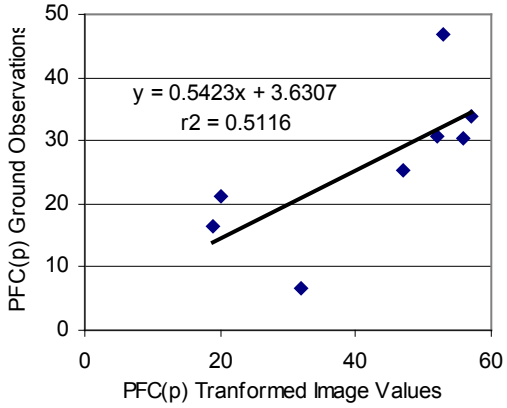

Figure 36. Regression between the ground truth validation site values and the extracted QB2 NDVI transformed to PFC(p).

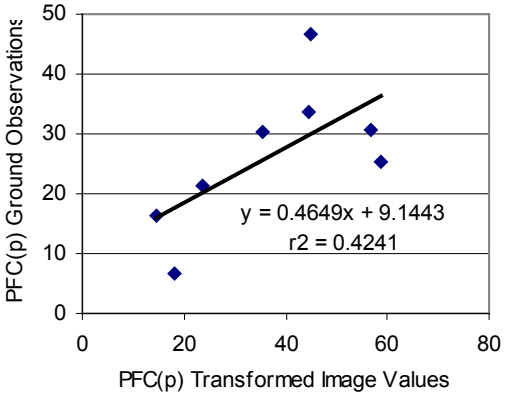

Figure 37. Regression between the ground truth validation site values and the extracted DMSI Band 3 transformed to PFC(p).

The transformed image values were extracted at the validation sites and examined against the PFC(p) field observations. The sensors with the strongest relationship were AVNIR-2 NDVI transformed to PFC(p) with an $r^2 = 0.82$, and DMSI NDVI, $r^2 = 0.74$. QB2 NDVI and DMSI Band 3 transformed images illustrated weak regression relationships with $r^2 = 0.51$ and $r^2 = 0.42$, respectively (Figures 34 to 37). However only eight validation points were available to test.

A transect test was conducted to assess the PFC(p) suitability of the canopy density field method and NDVI and Band 3 vegetation indices for each sensor. Both AVNIR-2 and QB2 appeared to be the most representative across most transects, with the following exceptions. Values intercepted for AVNIR-2 were lower than expected in the area of higher density for two transects in Withnell Bay, and for one transect in Cowrie Cove. QB2 values were higher in the very dense, and lower in the sparser vegetation in one transect of Withnell Bay, and another transect in Withnell Bay had values that were generally too low. Transect observations from DMSI NDVI transformed image generally illustrated that across all transects the projected density values were too low in the high density vegetation, and in one transect of Cowrie Cove, very sparse mangrove had a zero value. The DMSI Band 3 also generally returned lower than expected values across all sites, but also assigned higher values to shadow. Appendix 7 tables observations from each transect tested across each study area and provides an overall ranking for each of the image indices

A comparison of all ground truth PFC(p) values, including the field validation, with the corresponding PFC(p) image values for AVNIR-2, QB2, DMSI NDVI, and DMSI Band 3 are illustrated in Figure 38. DMSI, QB2, and AVNIR-2 images generally fall within 5 to 10% of the ground truth PFC(p) in the low cover density. In the mid cover densities, all sensors were generally 5 to 30% higher than the PFC(p) ground truth value. In the higher density range, QB2 and AVNIR-2 were generally 10 to 15% greater than the ground truth values, whereas DMSI for both NDVI and Band 3 had a 0 to 10% deviation from the ground truth value.

Overall DMSI NDVI transformed image followed by AVNIR-2 NDVI transformed image was more closely calibrated to PFC(p) ground truth results; however both results had high mid range cover values, indicating more sampling needs to be conducted. QB2 NDVI consistently had higher cover values, often over 10%. This may imply that the photographs of the mid range cover density mangroves were not representative of the vegetation cover.

3.5.4 NDVI images transformed to Densiometer values

When applying densiometer transformations to the AVNIR-2 NDVI and QB2 NDVI images, the projected canopy cover ranges were similar, with ranges of 8 to 101 and 1 to 101, respectively. Initial observations of these images indicated that the values in the image were representative, with the exception that values of ~ 34% assigned to bare ground, and canopy cover starting at ~ 37%.

When applying the transformation of DMSI NDVI, the densiometer range extended from 28 to 116. DMSI NDVI transformed image included bare ground and appeared to overestimate cover values by 15 to 20%. The densiometer transformation to DMSI Band 3 had a range of densiometer values between 7 to 109, which appeared to be representative in the higher density vegetation range, but too low in the sparse vegetation.

Validation site regressions for each sensor provided very low r^2 results (< 0.21 or less for all sensors; Figures 39 to 42). This implied that the relationships between the densiometer field readings and the sensor indices were very weak. However, only 5 validation sites were

available to test, and therefore this should be considered when determining the suitability of the field method and sensor index.

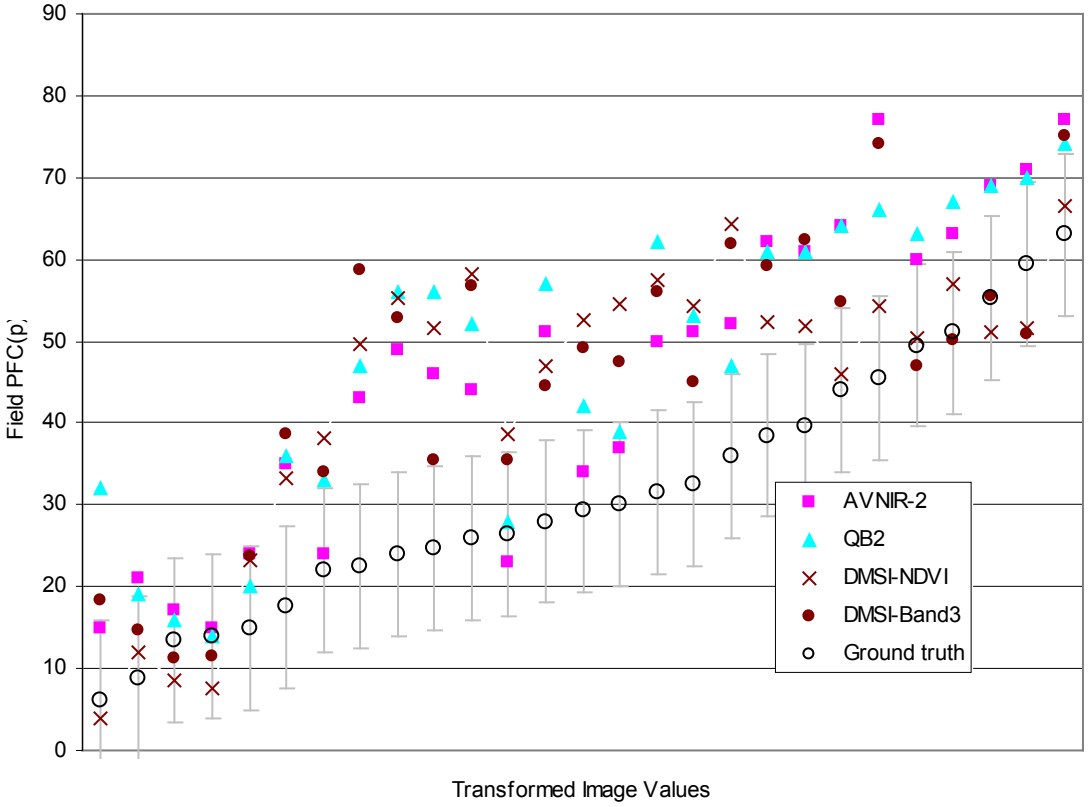

Figure 38. All ground truth site field values for PFC(p) compared to extracted image NDVI index values of AVNIR-2, QB2, and DMSI. Additionally the DMSI extracted image Band 3 index values have also been compared to the ground truth site field values PFC(p). The data has been sorted into ascending order by ground data PFC values to visualise the results over different density ranges low, mid, and high. An error bar (±10%) has been added to each ground data site.

A transect test was conducted to assess the suitability of the densiometer method and index to each sensor. Using the vegetation index NDVI for AVNIR-2, QB2, and DMSI, the transformed densitometer images provide somewhat satisfactory value ranges, where in most cases the sparse vegetation had values that were too high, and bare areas had been assigned values. Transect observations of DMSI Band 3 transformed image illustrated that across most transects the projected densiometer values were too high in the sparse vegetation, except at Cowrie Cove, where the sparse vegetation appeared representative. The DMSI Band 3 also generally assigned high densiometer values to shadow. Appendix 7 tables observations from each transect tested across each study area and provide an overall ranking for the image indices.

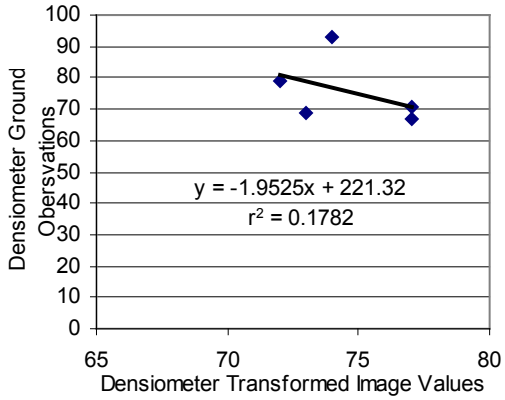

Figure 39. Regression between the ground truth validation site values and the extracted AVNIR-2 NDVI transformed to densiometer.

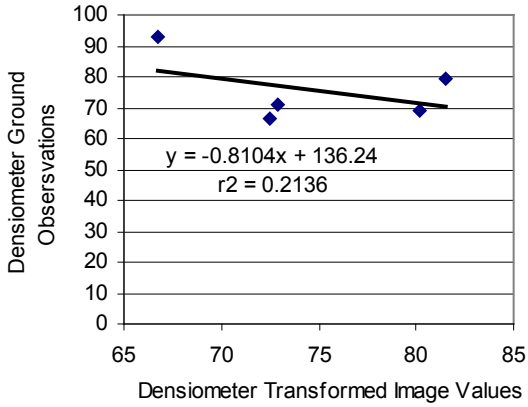

Figure 40. Regression between the ground truth validation site values and the extracted DMSI Band 3 transformed to densiometer.

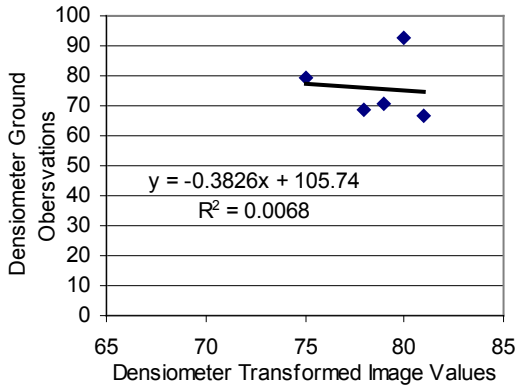

Figure 41. Regression between the ground truth validation site values and the extracted QB2 NDVI transformed to densiometer.

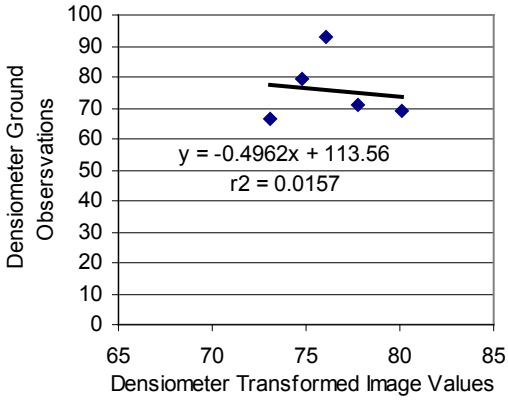

Figure 42. Regression between the ground truth validation site values and the extracted DMSI NDVI transformed to densiometer.

A comparison of all ground truth densiometer values, including the field sites validation, with the corresponding projected densiometer values for AVNIR-2 NDVI, QB2, DMSI NDVI, and DMSI Band 3, are illustrated in Figure 43. This method of measuring canopy density had a higher percentage range than previous methods, starting from ~50 to 95. With the exception of a few outliers, QB2 and AVNIR-2 transformed images quite accurately and generally projected values within 0 to 10% of the ground truth densiometer values. Excluding outliers, DMSI for both NDVI and Band 3, transformed images had a 5 to 10% deviation from the ground truth value, except in the upper density range where the image values were often ~15% lower. All sensor images generally appeared to predict values that were above the ground truth data in the mid range densiometer values.

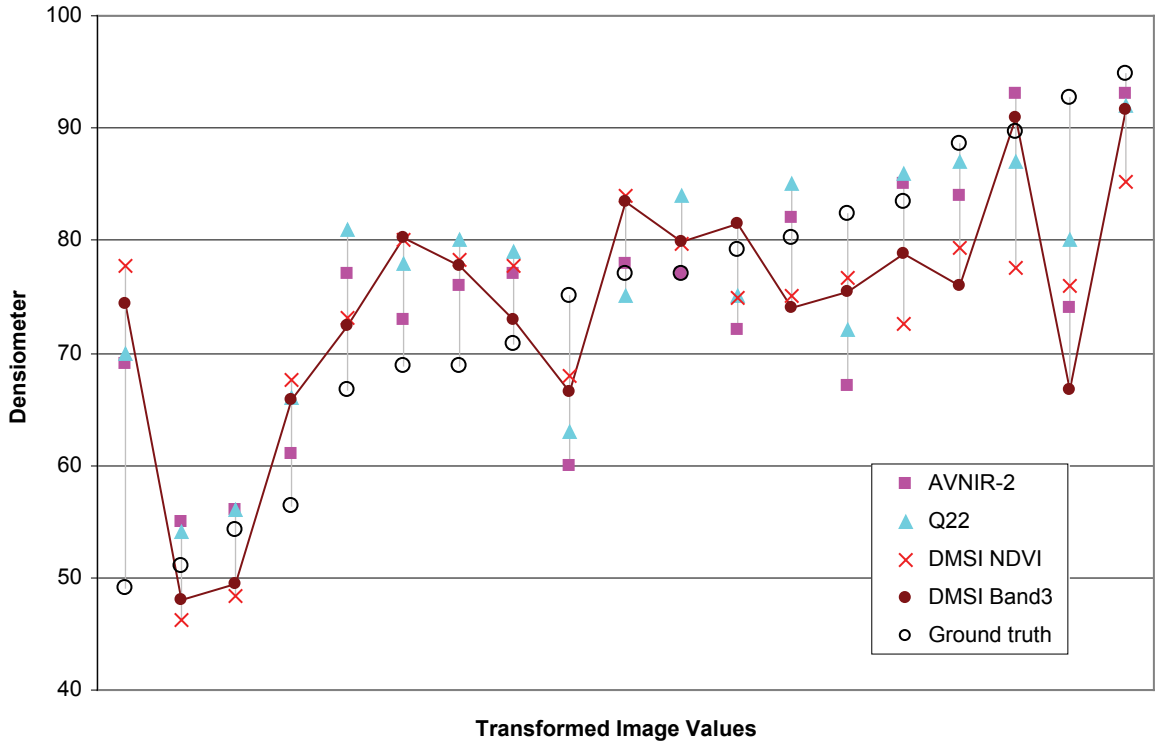

Figure 43. All ground truth site field values for the densiometer compared to extracted image NDVI index values of AVNIR-2, QB2, and DMSI. Additionally the DMSI Band 3 index values have also been compared to the densiometer ground truth field values for the densiometer. The data has been sorted into ascending order by ground data PFC values to visualise the results over different density ranges low, mid, and high. An error bar (±10%) has been added to each ground data site.

All sensor transformed images returned the majority of values between 75 to 85 in the medium to dense range, and dense vegetation image values were lower than the ground truth values. This implies that there is no variation in the upper range, probably due to the combination of the field method using the densiometer and the sensor indices tested.

3.5.5 NDVI and Band 3 transformed to Photo Canopy Percentage

When applying photo canopy percentage transformations to the DMSI NDVI image, the resultant image range of values was 1 to 117, which appeared to be representative. However, areas of bare ground had low values and many of the very dense vegetation exceeded 100%. These areas of greater than 100% had not been sampled for canopy cover, and may be another species (*Ceria australis*) that was observed in the field.

Other areas with greater than 100% canopy cover in the derived image match the habitat description for *C. australis*, which is a denser species of mangrove, occurring in narrow edges along the inner mangrove forest (Duke, 2006). This species was identified a few times in the field, in such habitats, and the coordinates were noted. These areas require further field sampling to capture the full variation in mangrove canopy cover for the region.

Initial observations of the DMSI Band 3 transformed image appeared to have a good range of values (18 to 107) across sparse, medium, and dense canopy cover. Validation of the photo

canopy cover field readings and DMSI sensor, with both NDVI and Band 3 indices, were weak with low r^2 values for the Band 3 index (Figures 44 and 45).

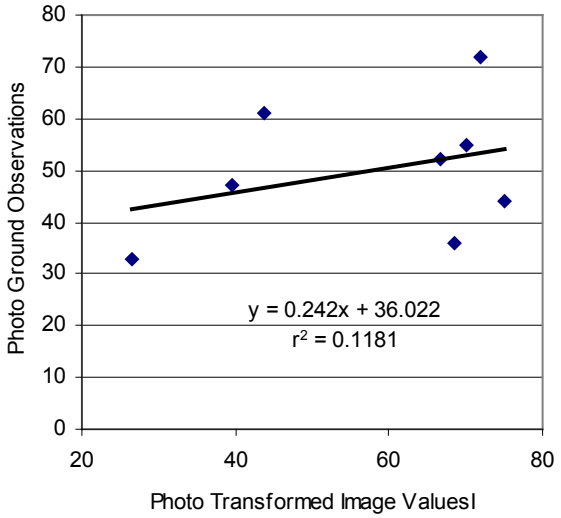

Figure 44. Regression between the ground truth validation site values and the extracted DMSI NDVI transformed to photo canopy percentage.

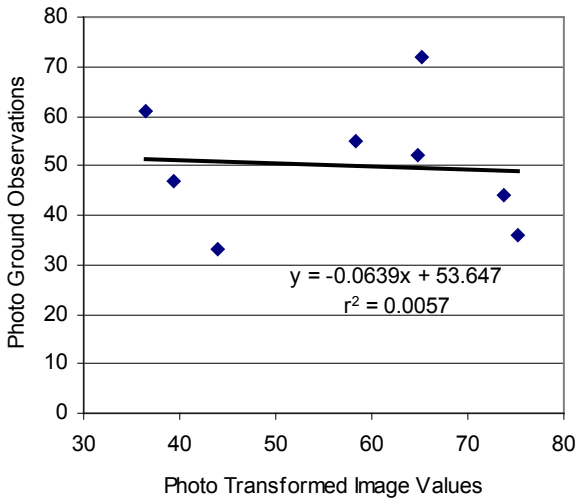

Figure 45. Regression between the ground truth validation site values and the extracted DMSI Band 3 transformed to photo canopy percentage.

A transect test was conducted to assess the suitability of the canopy density method, and both indices derived from the DMSI sensor. Values were found to be too high in sparse vegetation for the indices NDVI and Band 3 in Withnell Bay, and only Band 3 in King Bay. At King Bay and Cowrie Cove, the NDVI of the transformed image values assigned bare ground low values. In the Band 3 derived image, some higher values included shadow rather than vegetation. Appendix 7 tables observations from each transect tested across each study area and provides an overall ranking for the image indices.

The comparison of all ground truth photo canopy cover percentage sites, including the field validation, with the corresponding projected photo canopy cover percentage values for DMSI NDVI and DMSI Band 3, are illustrated in Figure 46. Excluding outliers, the DMSI for both NDVI and Band 3 had a 0 to 10% deviation from the ground truth value, in the mid to upper vegetation density range. However, in both the highest density reading and the low density range, fall out of the 10% error margin. With these indices and the photo canopy field methods, the DMSI sensor images seem to return similar densities (65 to 80%) across the mid to high range, and therefore indicate that there was no variation in the mid to upper range of image densities. This inference supported the validation regression results, which implied that there was no linear relationship established. The likely reason for this was that the photo density did not represent a pixel, and had not been projected to the pixel size or the homogenous area size, to give the context of the surrounding vegetation like the PFC method does.

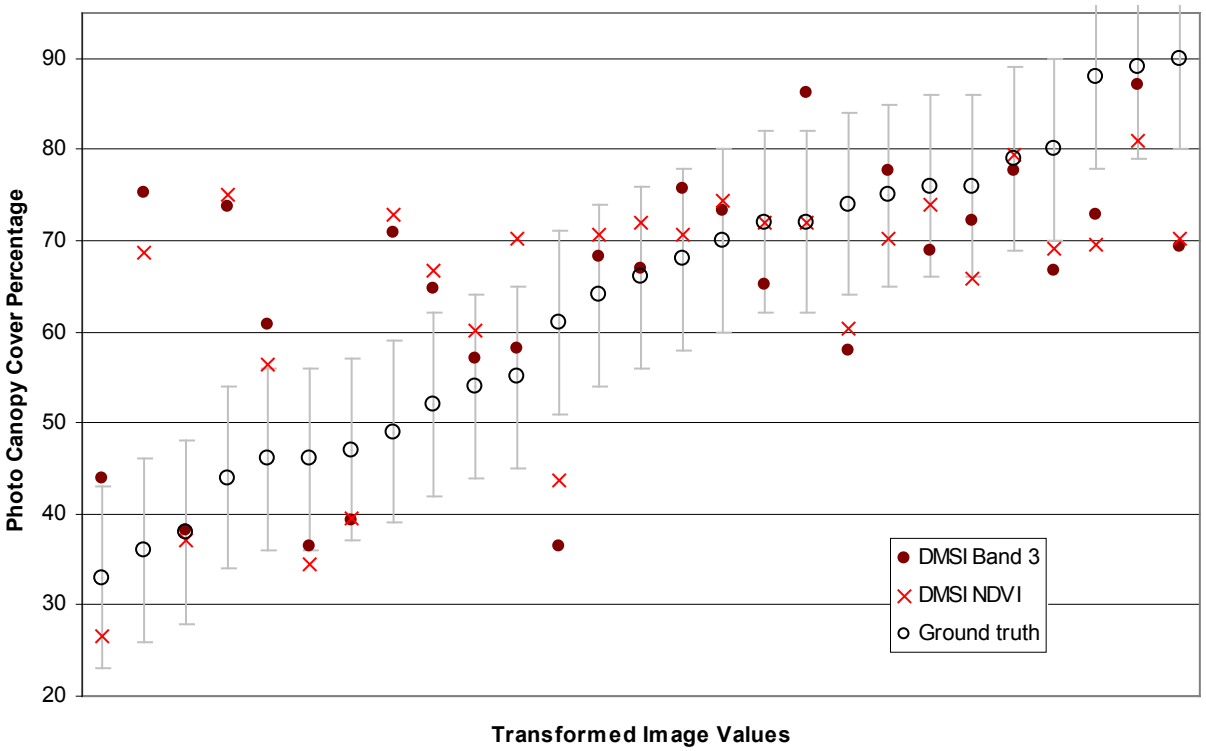

Figure 46. All ground truth site field values for the canopy cover photo estimate compared to the extracted NDVI and Band 3 image values of DMSI. The data has been sorted into ascending order by ground data PFC values to visualise the results over different density ranges low, mid, and high. An error bar (±10%) has been added to each ground data site.

4.0 Discussion

4.1 Considerations for collecting ground data

4.1.1 Field logistics

The most restrictive factor for collecting field data in this study was the tide. The Pilbara and Kimberley are recognised as having some of the greatest tidal ranges in the world (DEWHA, 2008). The limited time frame for conducting this pilot study unfortunately coincided with king tides. In an intertidal environment where a small change in vertical tide height translates to large horizontal movements of water, the timing of field studies to coincide with neap tides is imperative. This study was restricted to data collection only during early morning hours, which in turn affected the canopy cover estimations (see below). Also, the minimal field time prevented the collection of a suitable number of validation sites, homogenous sites for statistical analyses of 'impacted' versus 'unimpacted', and it may be necessary to complete more validation sites in the study area in order to conduct future monitoring there.

Measuring of canopy cover estimates began at first light, resulting in long shadows and/or poor lighting, affecting shadow estimations and also the amount of light that could penetrate the canopy. Poor lighting also affects colour perception of the vegetation and soil, particularly when taking photographs, which can result in large differences compared to when the sun is bright and directly overhead. This further complicates calibrations and comparisons between on ground photographs and remote imagery.

The canopy cover key should be used to record the canopy cover percentage as a way of assisting the field officer to select a representative place to photograph the canopy, and to train their eye in canopy cover interpretation. Replica photographs from different quarters of the site should be taken where possible.

This pilot study highlighted the utility of the site selection methodology employed to select homogenous sites for ground truthing. Also highlighted, was the need to use imagery of the appropriate resolution to identify truly homogenous sites. Despite potential resolution issues, the use of QuickBird imagery proved very successful here.

The use of the Nomad GPS, with the capacity to display the orthorectified aerial photograph as a moving map, proved to be a great advantage. The ability to visualise the terrain on-site allowed navigation to the target sites, while avoiding the densest patches of mangrove. Other studies that did not use this technology were less successful in reaching their target sites (Alan Kendrick, pers. comm.). This technology would be indispensable in navigating denser mangrove areas, such as those found in the Kimberley, and could even be used to plan a navigable route to the target site.

However, the dense canopy often obstructed the GPS signal, compromising the position and track accuracy. Also affected by the canopy was the GPS compass bearing. A possible solution would be to attach a Bluetooth GPS receiver (cost approx. $150) to a pole and push this through the canopy to increase the GPS signal reception. Despite these accuracy issues, tracks recorded by the GPS can be linked to photos taken on site, for further ground truthing, and opportunities were also taken to record the most inland extent of the mangroves (tidal creek), to assist discrimination between mangroves and non mangroves.

The use of poles to mark out transects was the preferred method compared to using a chainman and string. Having smaller poles that could be quickly and easily fited together to achieve the desired length, could be pushed through dense vegetation with relative ease. This allowed transects to be placed in areas that could not be walked through, in some instances, making transect positioning more accurate when using pre-selected sites. Other advantages of the use of poles is that they were of a known length, therefore could be used as a rough guide for measuring things such as tree height; and could also be used to strap the GPS to and push through the canopy to obtain higher accuracy position data. Carrying the poles by hand did not compromise travel time between transects, and could be used to push branches aside when trying to access a transect site.

Travel time between transects was underestimated in this study. In planning the field sampling, 15 minutes was allocated for travelling between transects. However, we rarely were able to travel between transects in 15 minutes, and 30 - 60 minutes is a more realistic travel time. The difficulties of navigating through dense vegetation, even with the use of the Nomad GPS to plan routes, should not be underestimated.

In the original strategy for field sampling, one person was allocated to each transect, and that person was to collect all of the data for that transect by themselves. However, we found that working as a team was the better option. Ideally, the team would consist of 2 or 3 people collecting biological and ground truth data, with a further 1 or 2 people acting as scribes. The use of scribes is essential because in collecting data, one is completely occupied with that activity, and would result in repeatedly having to stop measurements in order to record the data on the data sheet, markedly increasing the time spent at each transect. Furthermore, the muddy environment is not compatible with paper data collection sheets and pens. Working as a team also increases the safety factor when working in remote and harsh environments, and particularly in mangroves in the Kimberley, crocodiles are a consideration to be taken seriously.

A final consideration for field logistics is that the data collection team be rehearsed in the data collection they will be undertaking. For example, the key for estimating canopy cover was at first difficult to use, but became routine once familiar with the key and the prevailing conditions. When collecting data unfamiliar to the data collection team, it is highly recommended that the team engage in practice data collection missions to ensure that data is collected efficiently, and accurately, when collecting data of importance.

4.1.2 Densiometer readings

The densiometer results from this study imply that it is difficult to establish a linear relationship with the field densiometer values and sensor indices applied. However, the densiometer method has been used successfully in other studies, and it is likely that the limited number of replica readings that represent all quarter of the sample site and replica ground sites have influenced these results (see *4.4 Considerations for remote sensing imagery*). Green and Clark (2000) successfully used a densiometer to estimate canopy density, but averaged 80 readings per site, of which there were 29 sites. Although producing very good relationships with the imagery used (CASI, Landsat, and SPOT SX), the number of replica sites took 33 person days to complete. With more field observations a stronger relationship with the image data may be possible to establish, but a balance must be met between time spent in the field obtaining replica site readings and the associated costs. The success of the densiometer use in mangroves and other vegetation environment implies this instrument should be tested again, with more replica measurement, in a situation where time is not a limiting factor.

4.1.3 Site selection considerations

The pre-site selection and identification of homogenous sites proportionally selected the visually dominate species *Avicenna marina* and *Rhizophora stylosa*. A range of different homogenous sites were selected to represent these species proportionally. However, when post processing the larger range of values in the DMSI derived PFC(p) image highlighted the high canopy densities greater than 100% where the mangrove species *C. australis* had been observed (*3.5.5 NDVI and Band 3 transformed to Photo Canopy Percentage*). *Ceriops australis* was described by Duke (2006) as preferring a sheltered habitat at the landward side of the mangrove extent. The areas observed to have a higher than normal density range in the DMSI derived images were located in areas matching the preferred habitat of *C. australis*. These areas were much denser than where other mangrove species occurred. The reason this species was highlighted in the data was because it was only observed in the field, and not field sampled, therefore was omitted from the regression analyses. Hence the density range was not a true representation of the mangrove community at the study sites. Given that areas occupied by *C. australis* are now known in the study sites, this information can be used to preselect homogenous sites for future field visits.

4.2 Considerations for remote sensing imagery

4.2.1 Imagery resolution, spatial scale, and trigger values

As described above (*1.3.3 Landsat imagery as a monitoring tool* and *1.3.4 Spatial resolution*), the Landsat imagery lacked the resolution needed to accurately determine habitat extent due to the fringing nature of these habitats at the location of the study sites. However, this does not necessarily preclude the use of lower resolution imagery from monitoring.

It is essential to define in a monitoring program what is considered to be a trigger value, warranting further investigation, from each particular measurement being used as a resource condition indicator. For instance, in relation to monitoring mangrove habitat, it must be decided during the planning phase of the program, how much change is needed to trigger further investigation? If the mangrove extent moved 5m over the duration of one year, is this enough to trigger further investigation? If the answer is no, then there is no need to use imagery with a resolution finer than 5m.

Therefore, in deciding what resolution of imagery to use in a monitoring, one must first decide the amount of spatial change that is considered to indicate change in that habitat. For example, Paling *et al.* (2003) determined that creek erosion varied from 0 to 2.8m.yr^{-1} in Port Dampier (northeast of the current study sites), which did not constitute a significant change to the habitat. Therefore, one could conclude that the use of imagery with a resolution less than 3m is appropriate. This also illustrates the importance of having baseline data to which the magnitude of change values can be set against.

4.2.2 Coincident timing of image acquisition and field data capture

An issue in determining the correct calibration of the field data with the imagery can be when the date of imagery does not coincide with the field data capture. The QB2 and AVNIR-2 images were both captured in different years and seasons to the field data. While it is possible

that mangrove condition has not changed greatly, in an ideal situation imagery utilised should be captured closest to the field visit date. Imagery captured within a month of the field visit should be representative of the of mangrove condition, depending on the localised occurrence of events such as fire, storms, cyclone, or the change of season. The ideal season for capturing field data, and the imagery, to carry out mangrove monitoring is the middle of the dry season, when there is more likelihood of capturing cloud free imagery, climatic and tidal conditions are suitable for field work, and grasses are dry. To compare results reliably between years, the date of imagery capture should be similar.

Airborne capture of DMSI imagery has the advantage of being able to plan the imagery capture to coincide with the field visit, and will capture only the areas needed. Satellite imagery, unless tasked to capture at a certain date, is dependant on the sensor orbit frequency and the climatic conditions at the time. The orbit frequency for the satellite sensors used in this study varies, however capture dates within a month of field visits should be possible.

This study shows that even if the initial survey does not coincide well with the capture date of the imagery used, it none the less provides baseline data relevant to the target area. The reality of monitoring programs, and the limited time spans of funding that are provided for pilot studies, usually means that the baseline data collection will not coincide with image capture. However, once the baseline data is collected, and the long term monitoring program has been given approval, funding time frames become less of an issue, and more time can be spent planning field trips to coincide with image acquisition, within ideal seasonal conditions, or perhaps to compare seasonal differences.

4.2.3 Imagery calibration

Calibration of imagery must also be considered if the imagery is to be used in a monitoring sense. If the NDVI is calculated from calibrated data, then it is repeatable between times of measurement. However, if NDVI is calculated from raw counts without calibration to reflectance values of the image, then NDVI will vary and will only create a meaningful image for that particular data capture. Therefore when an area is acquired at a later date, without calibration, the next set of NDVI values will not be comparable. The DCC Landsat dataset is calibrated (Wu *et al.*, 2004), however cross calibration to a base year will need to be undertaken to calibrate QB2, ALOS, and DMSI. Investigating an atmospheric correction for ALOS similar to the technique used for the DCC Landsat dataset may be possible with funding to employ the services of the CSIRO Centre for Mathematics, Information and Sciences team.

4.2.4 Ground truthing

This study shows that sufficient replication of sites, across the greatest range of homogenous sites possible, are needed in order to obtain regressions that are representative of the target area. Pilot studies, such as this one, are necessary to establish data baselines, and also identify weaknesses in monitoring designs. This was indeed the case in this study, as a mangrove species with relatively low abundance, but with apparently restricted and specialised habitat preference, was most likely the cause of over estimating canopy cover at some of the study sites used here. This highlights that seemingly trivial details of an environment can have unforseen and significant impacts on the interpretation of remote sensing imagery. This is yet another example from this study highlighting the importance of having baseline data and the need for rigorous on-ground validation prior to commencing a monitoring program.

4.3 Choice of resource condition indicator

This pilot study has shown that the number of measures that can be used as true indicators of resource condition in these habitats are limited. The choice of measures is further limited by practicality, and financial and personnel investment costs. The result is that there are very few resource condition indicators that are usable in a long term resource condition monitoring program, given the financial and time constraints for data collection and analyse that are typically associated with such programs.

Potential resource condition indicators field trialled here for mangrove and intertidal mudflats were compiled from previous studies. However, only a relatively small number of these indicators were chosen for the field trial, and were chosen based on two criteria: that the indicator was suitable for the scale of the area to be monitored, and that the indicator was readily and easily measured. This is a current trend in promoting long-term monitoring programs. Another current trend to implement long term monitoring is to use a community based approach. This further highlights the need to select indicators that do not require specialists to measure them. In this instance, the indicators chosen should allow any person with a moderate to low level of scientific and/or field training or expertise to measure the indicators.

The reality of such an approach may be less than desirable however, as this study has shown that indicators that truly reflect the condition of a resource tend to require expert analyses, and in some instances, expert data collection. This is because of the complexity of the habitat and the processes driving the environment (multiple species, highly dynamic physical variables, etc…).

4.3.1 Baseline data

As alluded to above (*4.2.1 Imagery resolution, spatial scale, and trigger values*), baseline data is essential in setting trigger values for resource condition indicators. For any particular resource condition indicator, the trigger value should signal that a change has occurred as a result of something significantly impacting the habitat. One needs to understand the magnitude of impact needed to significantly impact a habitat, and therefore set an appropriate trigger value. This task is considerably simplified if one has baseline data for the area targeted for monitoring.

A pilot study, such as this, is a cost-effective means of collecting baseline data for a monitoring program. Although the data may be preliminary, it is derived from the monitoring site and is therefore ideal data to begin with. A pilot study will also help identify unexpected problems in the survey design (see *4.2.4 Ground truthing*).

If baseline data is not available, and a pilot study is not possible, then it could be possible to use data from studies published for similar habitats from different areas, although less than ideal. In such a strategy, an assumption is made that the ecological processes occurring in both systems are identical, however, this is not always the case. For example, different localised factors can fundamentally alter the life history traits of species living within apparently identical environments (Reznick, 1997; and Walker, 2007), and these different life history traits can reverberate through trophic webs, and other ecological processes, that ultimate lead to apparently similar habitats or environments having different suites of ecological drivers. If a monitoring program must base trigger values on studies outside of the target region for monitoring, then it is essential that an adaptive management model is utilised, and that monitoring in the early stages of the program is more vigilant, to validate the use of the adopted trigger values, or change them if necessary.

Similarly, if an environment to be monitored is completely devoid of data to set trigger values, then conservative, scientifically based judgement is needed. Again, this approach would need an adaptive management plan that is able to change trigger values, if needed, and maintain vigilance in the initial phases of the program to ensure that the current trigger values are appropriate. Trigger values could be made less conservative over time, if no significant impacts have been detected.

4.4 Mangroves

4.4.1 Mangrove extent

When determining mangrove forest extent DMSI was more representative than QB2. DMSI imagery has a multispectral pixel size of 0.5m, unlike QB2 which has a 2.5m multispectral pixel resampled to 0.6m with a panchromatic band, which blurs the mangrove edge with shadow and water.

Although both sensors produced similar results, the higher resolution of DMSI captured the mangrove extent more discretely. The DMSI mangrove classification more accurately defined the mangrove edge and therefore it would be a good sensor to monitor changes in mangrove extent greater than 0.5m.

Considering the cost of this imagery, a baseline mangrove extent should be established at the earliest possible date and then imagery recaptured every 3 to 5 years, depending on the rate of detectable change expected on the mangrove edges. A consistent imagery source, processing method, and repeated image capture of the mangrove area of interest, will allow change analysis between dates. This will provide a reliable and measurable area of extent that can be used to assess the state of the environment.

One satellite dataset currently available that fits the requirements of consistent imagery processed to a standard is the Department of Climate Change (DCC) annual continental coverage of Australia. As previously mentioned Landsat has successfully been used to detect mangrove extent across the North West of Australia (Manson *et al,* 2001*;* Behn, 1999) however the 25m by 25m pixel size of the dataset preclude it from being an effective indicator of mangrove extent change in areas where the width of the mangrove stand is less than 50m i.e. narrow fringing mangrove stands (Manson *et al.*, 2001) and where the threshold of acceptable change is less than 25m. Where large stands of mangroves exist and major impacts (anthropogenic or natural) influence mangrove distribution, Landsat is considered more appropriate for broad scale mangrove extent change detection and monitoring (Behn, 1999; Manson *et al.*, 2001; and Paling *et al.*, 2008).

4.4.2 Mangrove vegetation condition index

For determining the density of mangroves as an indicator of vegetation condition, this study found that using the vegetation index NDVI with the AVNIR–2, was the most representative when converted to PFC(cc) and PFC(p). PFC(p) was consistently linear with the validation results for AVNIR-2 with NDVI. The larger pixel in this case is an advantage, as the 10 m pixel averages the density of many trees that may be growing in the same conditions and with the same habit. For this reason it is most applicable when describing a homogenous area. Another advantage of using AVNIR-2 image data is that it is relative cheap to purchase, process, and has a swath width of 70km, so a large area can be captured and processed for any given image.

The PFC(cc) method applied to the AVNIR-2 and QB2 found the range of mangroves was between 1 to 80 % PFC. This is similar to the PFC range described by Hnatiuk *et al.* (2009), which stated that the canopy cover range for most Australian woody vegetation is 40 to 70%. The PFC(cc) transformed QB2 NDVI was fairly representative, as it also has a larger pixel size, which is resampled, and averages the area to a lesser extent. However, there is no control over calibration of QB2 imagery, and it is expensive data to purchase, therefore this sensor would not be the preferred option for long term monitoring programs.

The DMSI NDVI transform of the PFC(p) field method yielded a strong relationship, but needs more field sites and validation points to determine if it would be a useful indicator of mangrove condition. Being airborne imagery, the spectral range is larger, and being captured just after the field visit, the DMSI sensor provided the most representative imagery of the mangroves forest and surrounding area. DMSI data also has the advantage of greater resolution (0.5m) compared to QB2 imagery (2.4m, panchromatic sharpened to 0.6m). Furthermore, being collected at a lower altitude, the DMSI imagery has less atmospheric related distortions and/or obstructions (particularly cloud) compared to satellite imagery, and versus original data.

It is recommended that the PFC(cc) and the PFC(p) field methods be used for mangroves. However more field sites and validation sites should also be selected and visited to improve the regression and the application to remote sensing data. Despite the strong regression and r^2 values found when comparing the imagery indices with the field data, many of the strongest regressions applied to the sensor images and tested for validation failed to show the full variation in the vegetation density range. This was the case for the densiometer, PFC(vc), the photo estimates field methods, and to a lesser extent the transformation of the PFC(p). This can be attributed to the regression model having misleadingly high fits to the data, indicating that more homogenous sample sites were needed.

Another factor that could assist the development of PFC images is more replica readings at each sample site. These replica readings would be averaged to ensure the observation is representative of the sample plot. For example, four replica photos captured from each quarter of the sample plot would not take up much more time; however some consideration should be put into the composition and position of the photo. Replica densiometer readings would take longer, and in an intertidal mangrove environment, time may not always be available.

Although Landsat has not been tested in this study, the DCC has the largest, most consistent, and reliable Landsat dataset for Australia. Despite the larger pixel size, Landsat imagery has been successfully used to monitor the density of riparian vegetation in the Pilbara (Behn, 2001), and mangroves in the northwest of Western Australia and Queensland. However, these studies often have investigated mangroves occupying larger spatial stands when establishing a relationship with ground measurement. If sample sites can be selected on a regional scale, more homogenous sites (75m by 75m) may be found and used to calibrate the imagery. Further work to investigate a robust Landsat index that determines mangrove density should be undertaken. The benefit of this would be an annual snapshot of the general vegetation condition of mangrove across the state, which although would not give detailed information such as individual tree deaths, or show sensitivity to changes in mangrove extent under 25m, would act as a detector for change for larger events.

4.5 Conclusions

This pilot study has shown some of the potential problems that may be encountered in resource condition monitoring, if remote sensing is to be the primary monitoring tool and baseline data of the target site is absent. The use of pilot studies for collection of baseline data, prior to the commencement of a monitoring program, is reinforced here.

There are logistical problems associated with on-ground data collection that do not become apparent until in the field. These problems can fundamentally influence the ability of the program to properly monitor a site, ie. low sample size not allowing for statistical comparisons. In such instances, the ability of the monitoring program to detect change, and respond appropriately to that change, will almost certainly be compromised. Again, a pilot study highlights such issues prior to the commencement of the monitoring program, proper.

To monitor a site a baseline dataset is essential for setting trigger values, if those trigger values are to be dependable from the outset of the monitoring program. Surrogate trigger values are less dependable, and will reduce the effectiveness of the monitoring program in the early phases, whilst appropriate trigger values are being determined. Intricately associated with the setting of trigger values is determining the appropriate spatial scale (and hence imagery resolution) needed to detect change that is considered to be significant to the habitat/ environment being monitored.

The choice of resource condition indicators that will be used to monitor a particular habitat/ environment is fundamental to the success of a monitoring program. Using inappropriate or misleading indicators will almost certainly result in the failure of the monitoring program, either detecting and recognising insignificant change as a trigger, or not detecting significant change. A suite of indicators is needed in such complex and dynamic environments as those investigated here. Due to the environmental complexity, complex resource condition indicators are often needed to accurately portray the condition of these environments. This increases the complexity of the monitoring program by increasing the sophistication of the data collection and analyses. However, if more simplistic resource condition indicators are chosen that are less effective, then the chances of failure of the monitoring program will increase, resulting in higher costs, both in terms of the costs associated with a failed program, but also in the costs associated with rehabilitating the environment.

This study has shown that remote sensing can be employed as a tool for monitoring mangrove and intertidal mudflat habitats in the Pilbara, which can be used as a baseline for extension into monitoring those habitats in the Kimberley. These habitats are often remote and difficult to access, therefore remote sensing provides a cost effective solution. Remote sensing does not eliminate the need for on ground measurements however, and ground truthing is essential for calibrating remotely sensed data with on ground data. These data and calibrations ensure that the remote sensing data is being used effectively and efficiently, to the satisfaction of the monitoring programs objectives and ability to detect trigger changes.

5.0 Acknowledgements

A strong collaboration between DoF and DEC was established in order to standardise the indicators and methods used in this study, and promote a standardised methodology for long term resource condition monitoring. To this end, Kim Friedman and Thomas Holmes (Marine Monitoring Unit, DEC) contributed greatly to compiling a total list of indicators, choosing indicators suitable for this type of study, and developing a field sampling strategy.

Mike Dunne, Keith Saunders, and Terry Molloy of the Karratha regional DoF office, and Cath Samson of the Karratha regional DEC office, provided invaluable local knowledge of the Burrup Peninsula. Cath Samson also assisted in the field for a day at Cowrie Cove.

Thanks are also due to Carly Bruce and John Eyres (DoF, WAFMRL) for their valuable assistance and hard work in the field.

This study was funded by the WA State NRM Office as part of the Coastal and Marine Resource Condition Monitoring - Scoping Project (073007). It is with regret that this funding acknowledgement was overlooked in a previous report (Human & McDonald, 2009).

6.0 References

Anderson, T.W. 1958. An Introduction to Multivariate Statistical Analysis. Wiley, New York.

Behn, G., Muller, C., and Stovold, R. 1990. Vegetation Monitoring, Karijini National Park. Department of Environment and Conservation, DEC internal report, Kensington, Western Australia.

Behn, G. 1999. Mangrove and Mud Flat Mapping, WA, (from Northern Territory to Shark Bay). Department of Environment and Conservation, DEC internal report, Kensington, Western Australia.

Behn, G., Brandon, M., Raudino, A., and Stoneman, G.L. 2003. Mapping Forest Cover in the Midwest, Goldfields and South Coast Regions of Western Australia. Department of Conservation and Land Management.

Behn, G., McKinnell, F.H., Caccetta, P.A., and Vernes, T. 2001. Mapping Forest Cover, Kimberly Region of Western Australia. Australian Forestry 64(2):80-87.

Behn, G., Kendrick, P., and Bowman, M. 2004. Monitoring Riparian vegetation within Millstream - Chichester National Park. Department of Environment and Conservation, 12th Australian Remote Sensing and Photogrammetry Conference, Fremantle, Western Australia.

Bellairs, S.M., Turner, N.C., Hick, P.T., and Smith, R.C.G. 1994. Plant and soil influences on estimating biomass of wheat in plant breeding plots using field spectral radiometer. Australian Journal of Agricultural Research 47(7):1017-1034.

Bonham-Carter, G.F. 1994. Geographic Information Systems for Geoscientists, Modelling with GIS. Pergamon Press, Tarrytown, N.Y. pp. 291-302.

Caccetta, P.A., Bryant, G., Campbell, N.A., Chia, J., Furby, S.L., Kiiveri, H.T., Richards, G., Wallace, J.F., and Wu, X. 2003. Notes on Mapping and Monitoring Forest Change in Australia Using Remote Sensing and Other Data. 30th International Symposium on Remote Sensing of Environment, Honolulu, Hawaii, November 10-14.

Campbell, N.A., and Atchley, W.R. 1981. The geometry of canonical variate analysis. Systematic Zoology 30:268-280.

Chia, J., Caccetta, P.A., Furby, S.L., and Wallace J.F. 2006. Derivation of Plantation Type Maps. 13th Australasian Remote Sensing and Photogrammetry Conference, Canberra.

Curry, P., Zdunic, K., Wallace, J., Law, J. 2008. Landsat Monitoring of Woodland Regeneration in Degraded Mulga Rangelands: Implications for Arid Landscapes Managed for Carbon Sequestration. 14th Australian Remote Sensing Photogrammetry Conference, Darwin.

Department of the Environment, Water, Heritage, and the Arts. 2008. The North-West Marine Bioregional Plan. Bioregional Profile. A description of the ecosystems, conservation values and uses of the North-West marine region. Commonwealth of Australia, Canberra. 170pp + CD-ROM.

Department of the Environment and Heritage. 2008. Estuarine, Coastal and Marine Habitat Integrity. Indicator Guideline: Extent and distribution of key habitat types. National Land & Water Resources Audit. Department of the Environment and Heritage. 8pp.

Duke, N. 2006. Australia's Mangroves. The Authoritative Guide to Australia's Mangrove Plants. University of Queensland, Brisbane. 200pp.

ERDAS (2008) ERDAS ER Mapper Professional, version 7.2, ERDAS Inc, United States of America

ESRI, (1999-2006) ARCGIS 9.2 Build 1500, Patent No. 5 710 835, ESRI Inc, United States of America.

Fuentes, S., Palmer, A.R., Taylor, D., Zeppel, M., Whitley, R., and Eamusd, D. 2008. An automated procedure for estimating the leaf area index (LAI) of woodland ecosystems using digital imagery, MATLAB programming and its application to an examination of the relationship between remotely sensed and field measurements of LAI. Functional Plant Biology 35:1070–1079.

Green E.P., Mumby, P.J., Edwards, A.J., and Clark, C.D. 2000. Assessing Mangrove Leaf Area Index and Canopy Closure. In Remote Sensing Handbook for Tropical Coastal Management. Edwards, A.J. (Ed.). Coastal Management Sourcebooks series, UNESCO Publishing.

Green E.P., Mumby, P.J., Edwards, A.J., and Clark, C.D. 2000. Guidelines for Busy Decision Makers. In Remote Sensing Handbook for Tropical Coastal Management. Edwards, A.J. (Ed.). Coastal Management Sourcebooks series, UNESCO Publishing.

Green, E.P., Mumby, P.J, Edwards, A.J., Clark, C.D., and Ellis, A.C. 1998. The Assessment of Mangrove Areas Using High Resolution Multispectral Airborne Imagery. Journal of Coastal Research 14(2):433-443.

Giri, C., Pengra, B., Zhu, A., Singh, A., and Tieszen, L.L. 2007 Monitoring mangrove forest dynamics of the Sundarbans in Bangladesh and India using multi- temporal satellite data from 1973 to 2000. Estuarine, Coastal and Shelf Science 73:91-100.

Hnatiuk, R.J., Thackway, R., and Walker, J. 2009. Vegetation. In Australian Soil and Land Survey Field Handbook. 3rd Edition, CSIRO Publishing, Collingwood Victoria, pp.73- 125.

Human, BA and JI McDonald. 2009. Knowledge review and gap analysis: Resource condition monitoring in the Pilbara and Kimberley regions of Western Australia. Coastal and Marine Resource Condition Monitoring - Scoping Project. Final NRM Report, Project 073007 - Part 1. Department of Fisheries, Government of Western Australia. Fisheries Research Report No. 197, 192pp.

Husch, B., Miller C.I., and Beers T.W. 1982. Forest Mensuration. Third edition. John Wiley and Sons, United States of America. pp203.

Jensen, J.R. 1996. Digital Image Processing – A Remote Sensing Perspective. 2nd Edition, Prentice Hall, Upper Saddle River, New Jersey.

Kay, R.J., Hick, P.T., and Houghton, H.J. 1991. Remote sensing of Kimberley rainforests. In Kimberly Rainforests of Australia. McKenzie, N.L., Johnston, R.B., and Kendrick, P.G. (Eds.). Surrey Beatty and Sons. Department of Conservation and Land Management, Western Australia; and Department of Arts, Heritage and the Environment, Canberra, pp41-52

Kimber, P.C., Forster, J.E., and Behn, G.A. 1991. Mapping Western Australian rainforests- an overview. In Kimberly Rainforests of Australia. McKenzie, N.L., Johnston, R.B., and Kendrick, P.G. (Eds.). Surrey Beatty and Sons. Department of Conservation and Land Management, Western Australia; and Department of Arts, Heritage and the Environment, Canberra, pp37-40.

Kuhnell, C.A., Goulevitch, B.M., Danaher, T.J., and Harris, D.P. 1998. Mapping woody vegetation cover over the state of Queensland using Landsat TM imagery. Proceedings for the Ninth Australasian Remote Sensing and Photogrammetry Conference, Sydney, July 1998.

Lemmon, P.E. 1956. A Spherical Densiometer for Estimating Forest Overstory Density. Forest Science 2(4):314-320.

Lemmon, P.E. 1957. A New Instrument for Measuring Forest Overstory Density. Journal of Forestry 55(9):667-668.

Lyne, V., Fuller, M., Last, P.R., Butler, A., Martin, M., and Scott, R. 2006. Ecosystem Characterisation of Australia's North West Shelf. North West Shelf Joint Environmental Management Study. NWSJEMS Technical Report No. 12, 73pp.

Mason F.J., Loneragan, I.M., McLeod, I.M., Kenyon, R.A. 2001 Assessing techniques for estimating the extent of mangroves: topographic maps, aerial photographs and Landsat TM images. Marine and Freshwater Resources 52:787-92.

Newman, D. 2008. OziExplorer. Version 3.95. Brisbane, Australia. (http://www.oziexplorer.com/OziExplorer).

Paling, E.I. 1986. Ecological Significance of Blue-Green Algal Mats in the Dampier Mongrove System. Technical Series 2. Report to the Department of Conservation and Environment, Western Australia. University of Western Australia. Perth. ix + 134pp.

Paling, E.I., McComb, A.J., and Pate, J.S. 1989. Nitrogen fixation (acetylene reduction) in nonheterocystous cyanobacterial mats from the Dampier Archipelago, Western Australia. Australian Journal of Marine and Freshwater Research 40(2):147-153.

Paling, E.I., Humphreys, G., and McCardle, I. 2003. The effect of a harbour development on mangroves in northwestern Australia. Wetlands Ecology and Management 54:281-290.

Pedretti, Y.M., and Paling, E.I. 2000. WA Mangrove Assessment Project 1999-2000. Murdoch University. Perth. 83pp.

Reznick, D.N. 1997. Life history evolution in guppies (Poecilia reticulata): Guppies as a model for studying the evolutionary biology of aging. Experimental Gerontology 32(3):245-258.

Semeniuk, V., Kenneally, K.F., and Wilson, P.G. 1978. Mangroves of Western Australia. Handbook No. 12. Western Australian Naturalists' Club, Perth. 92pp.

Specht, R.L., Roe, E.M., and Boughton, V.H. 1974. EDS Conservation of major plant communities in Australia and Papua New Guinea. Australian Journal of Botany Supplement No. 7.

SPOT Image. 2007. Reference 3D Product Description. Version 5.3. September 19th, 2007.

Tucker, C.J. 1979. Red and photographic infrared combinations for monitoring vegetation. Remote Sensing of the Environment 8:127-150.

Tucker, C.J., and Sellers, P.J. 1986. Satellite remote sensing of primary production. International Journal of Remote Sensing 7:1395-1416.

Walker, J., and Hopkins, M.S. 1990. Vegetation. In Australian soil and land survey handbook: field handbook. 2nd Edition. McDonald, R.C., Isbell, R.F., Speight, J.G., Walker, J., and Hopkins, M.S. (Eds.). Inkata Press. Melbourne. pp56-86.

Walker, T.I. 2007. Spatial and temporal variation in the reproductive biology of gummy shark Mustelus antarcticus (Chondrichthyes : Triakidae) harvested off southern Australia. Chondrichthyan Special Issue. Marine and Freshwater Research 58(1):67-97.

Wallace, J. F., Behn G. and Furby, S. L. 2006, Vegetation condition assessment and monitoring from sequences of satellite imagery. Ecological Management and Restoration, Vol. 7, Sup 1, pp 33-36.

Wu, X., Furby, S. L. and Wallace, J. F. 2004. An Approach for Terrain Illumination Correction, The 12th Australasian Remote Sensing and Photogrammetry Conference Proceedings, Fremantle, Western Australia, 18-22 October

Zdunic, K., and Behn, G., 2009. Exploiting Time Sequences of Satellite Imagery to Monitor Landscape Aspects. Australian Spatial Sciences Conference, Adelaide 2009.

7.0 Appendices

Appendix 1. Navigation maps for each study site

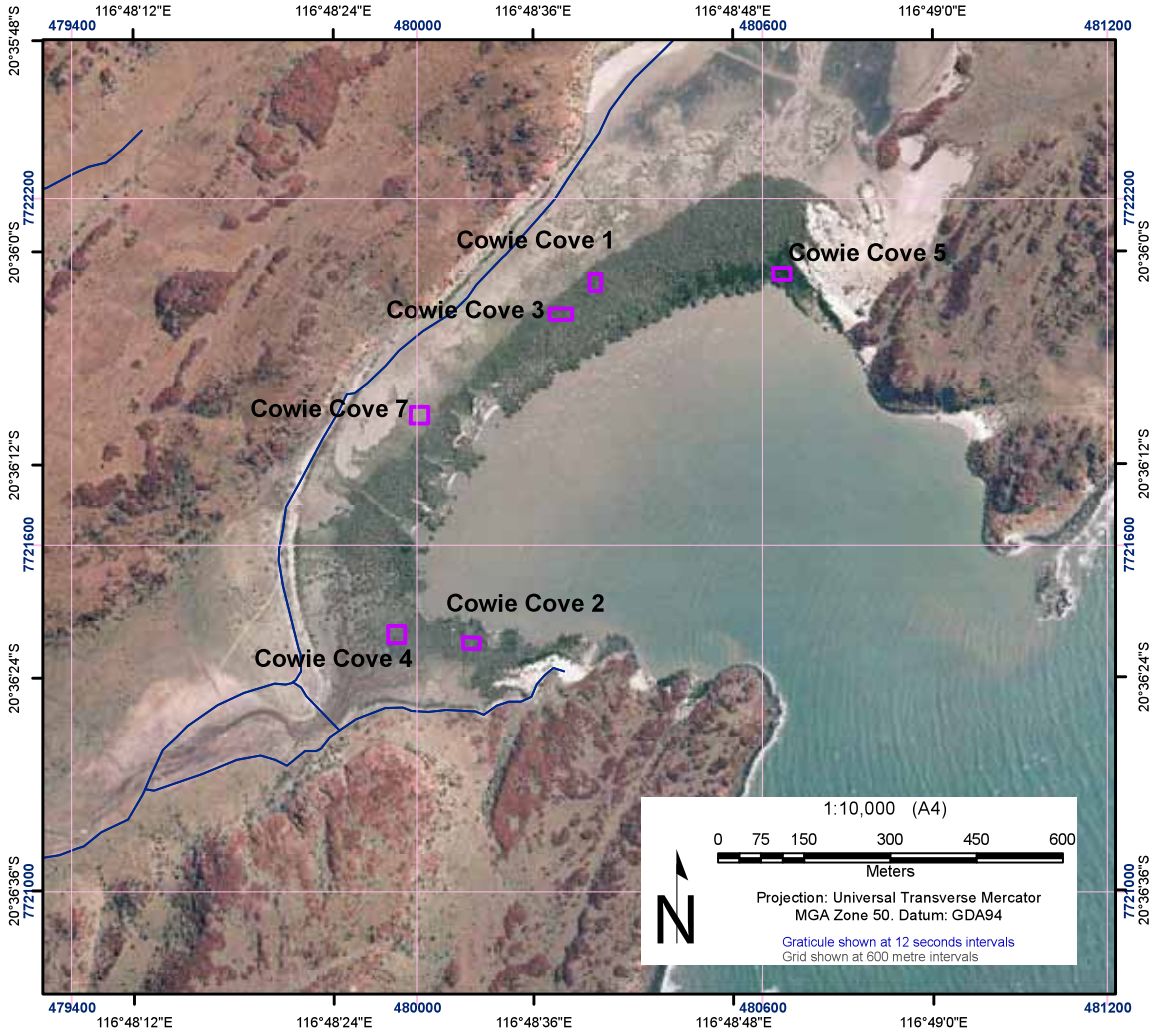

Figure 47. This map was created for navigation of Cowrie Cove highlighting the homogenous site locations and local roads overlaying 2004 aerial ortho-photography from Landgate.

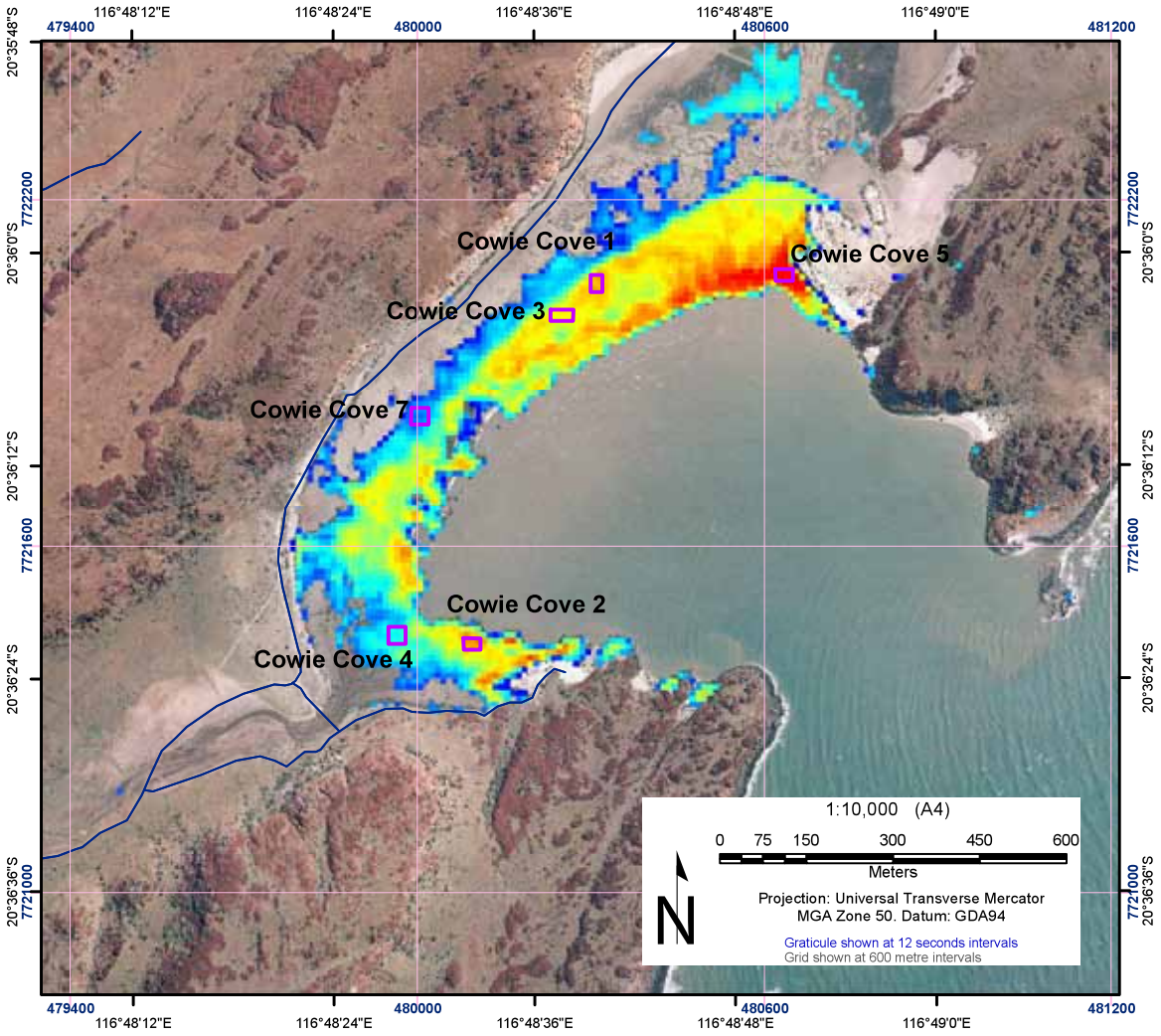

Figure 48. This map was created for navigation of Cowie Cove, highlighting the homogenous site locations, local roads and variations in the greenness of the mangrove canopy with AVNIR-2 NDVI enhancement overlaying 2004 aerial ortho-photography from Landgate.

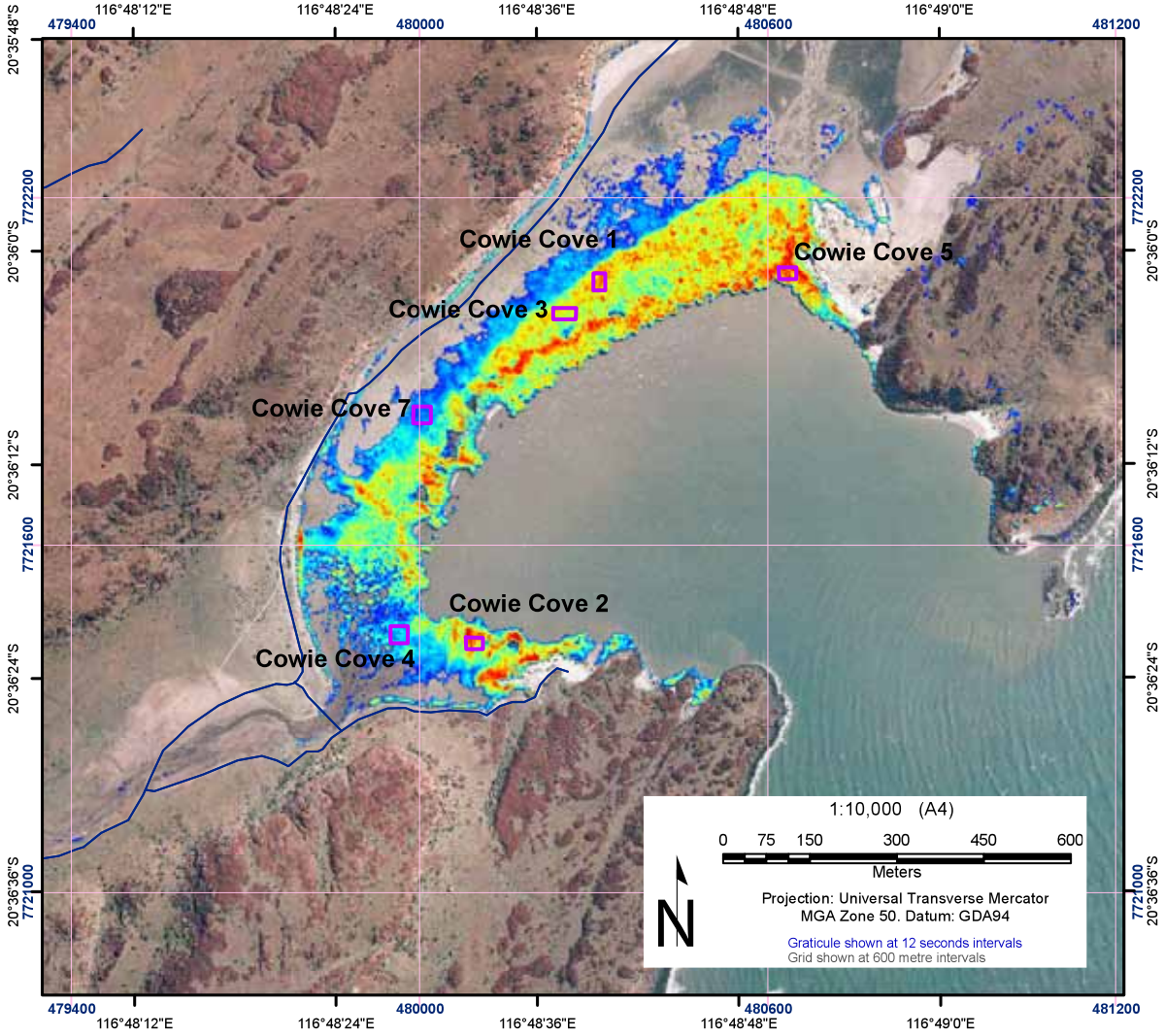

Figure 49. This map was created for navigation of Cowie Cove, highlighting the homogenous site locations, local roads and variations in the greenness of the mangrove canopy with QB2 NDVI enhancement overlaying 2004 aerial ortho-photography from Landgate.

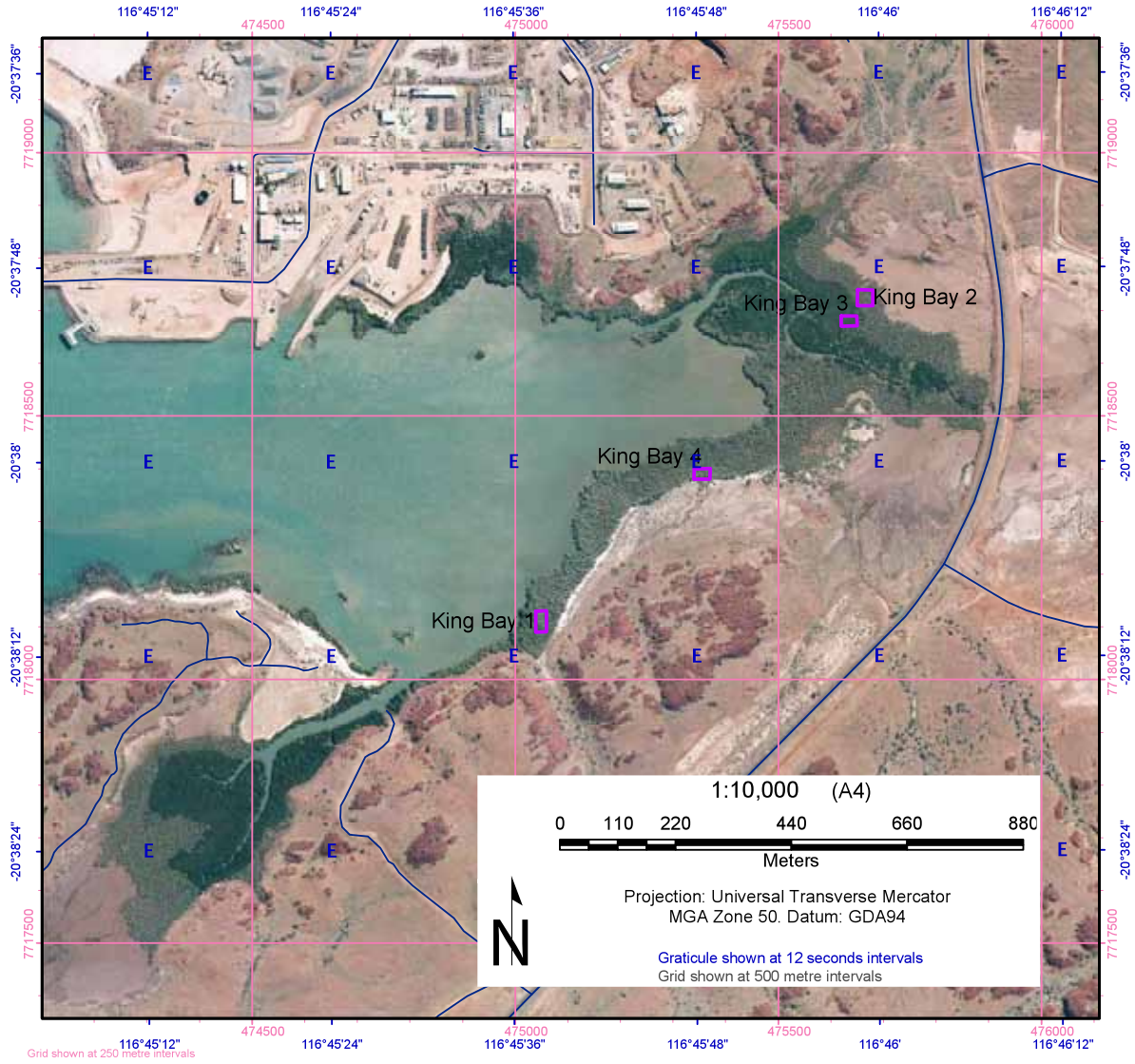

Figure 50. This may was created for navigation of King Bay highlighting the homogenous site locations and local roads overlaying 2004 aerial ortho-photography from Landgate.

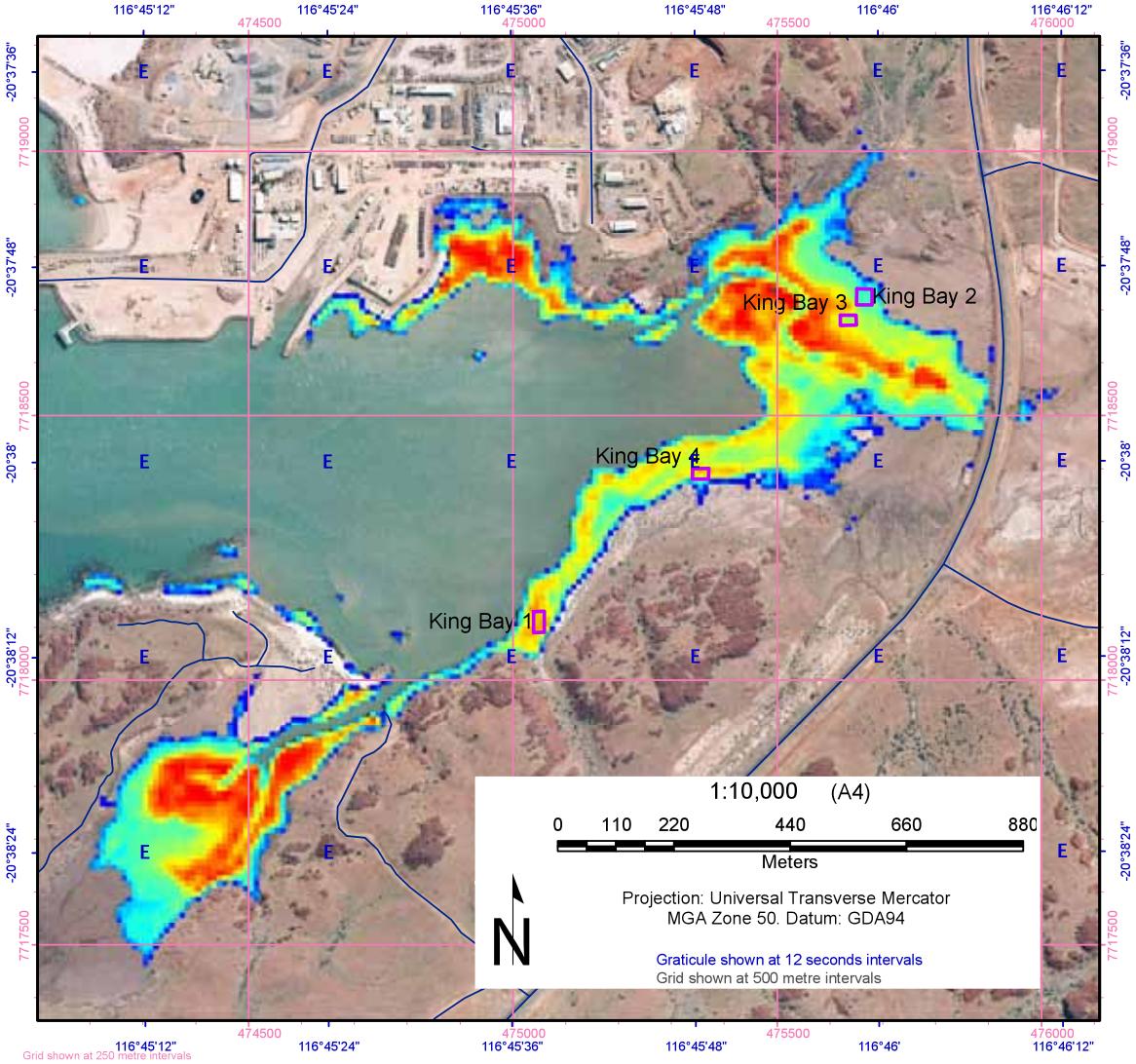

Figure 51. This map was created for navigation of King Bay, highlighting the homogenous site locations, local roads and variations in the greenness of the mangrove canopy with AVNIR-2 NDVI enhancement overlaying 2004 aerial ortho-photography from Landgate.

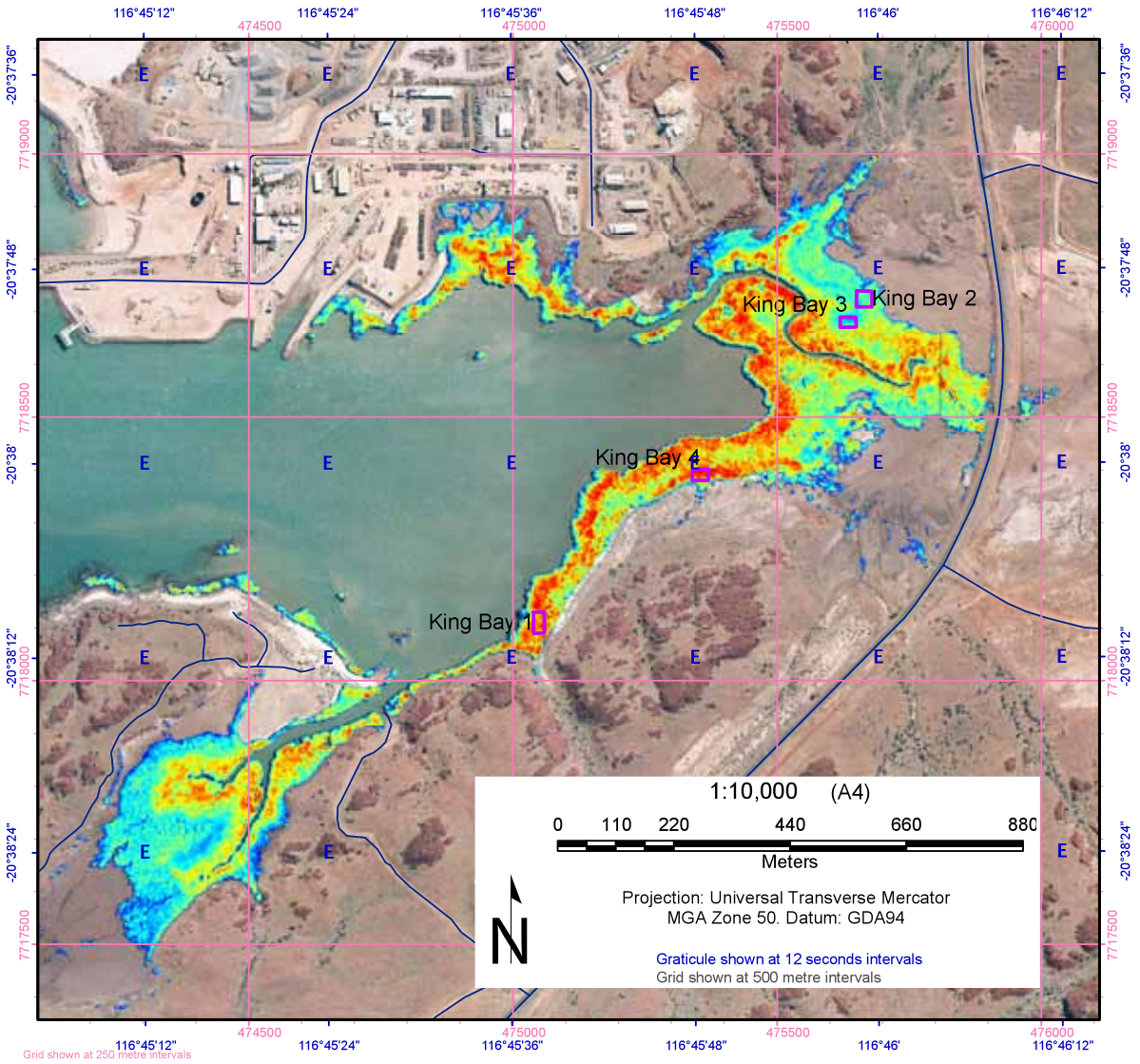

Figure 52. This map was created for navigation of King Bay, highlighting the homogenous site locations, local roads and variations in the greenness of the mangrove canopy with QB2 NDVI enhancement overlaying 2004 aerial ortho-photography from Landgate.

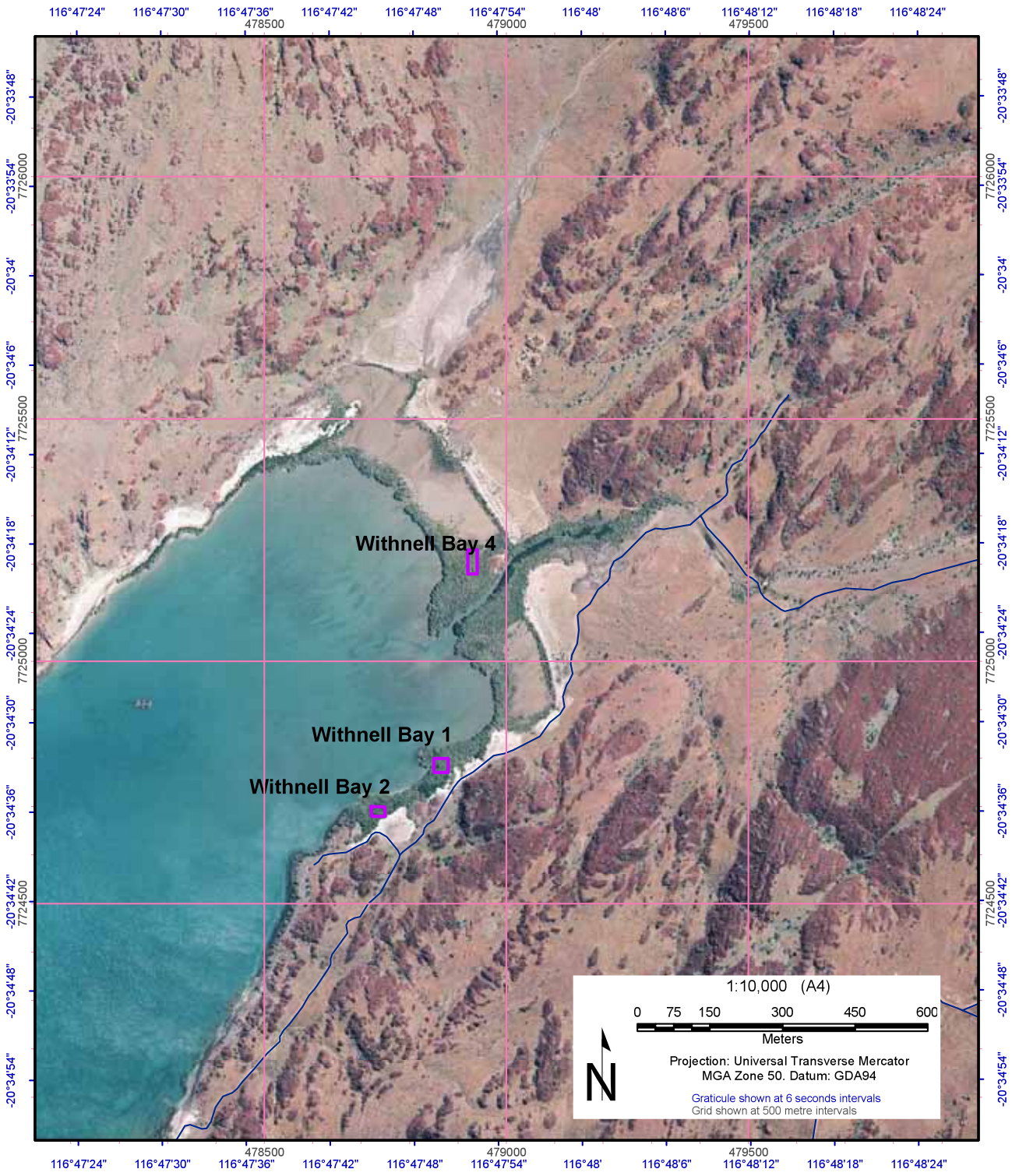

Figure 53. This may was created for navigation of Withnell Bay highlighting the homogenous site locations and local roads overlaying aerial 2004 ortho-photography from Landgate.

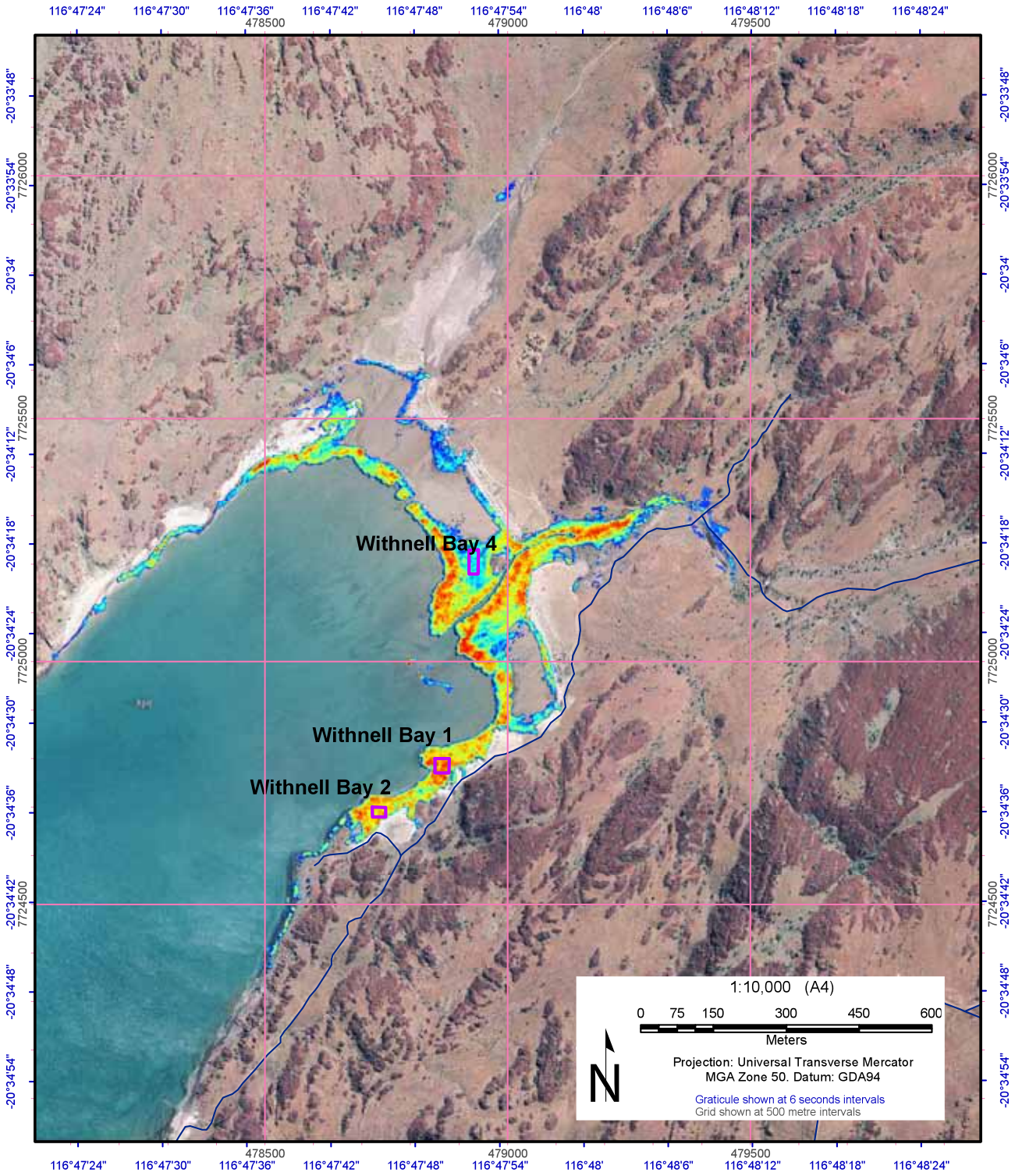

Figure 54. This map was created for navigation of Withnell Bay, highlighting the homogenous site locations, local roads and variations in the greenness of the mangrove canopy with AVNIR-2 NDVI enhancement overlaying 2004 aerial ortho-photography from Landgate.

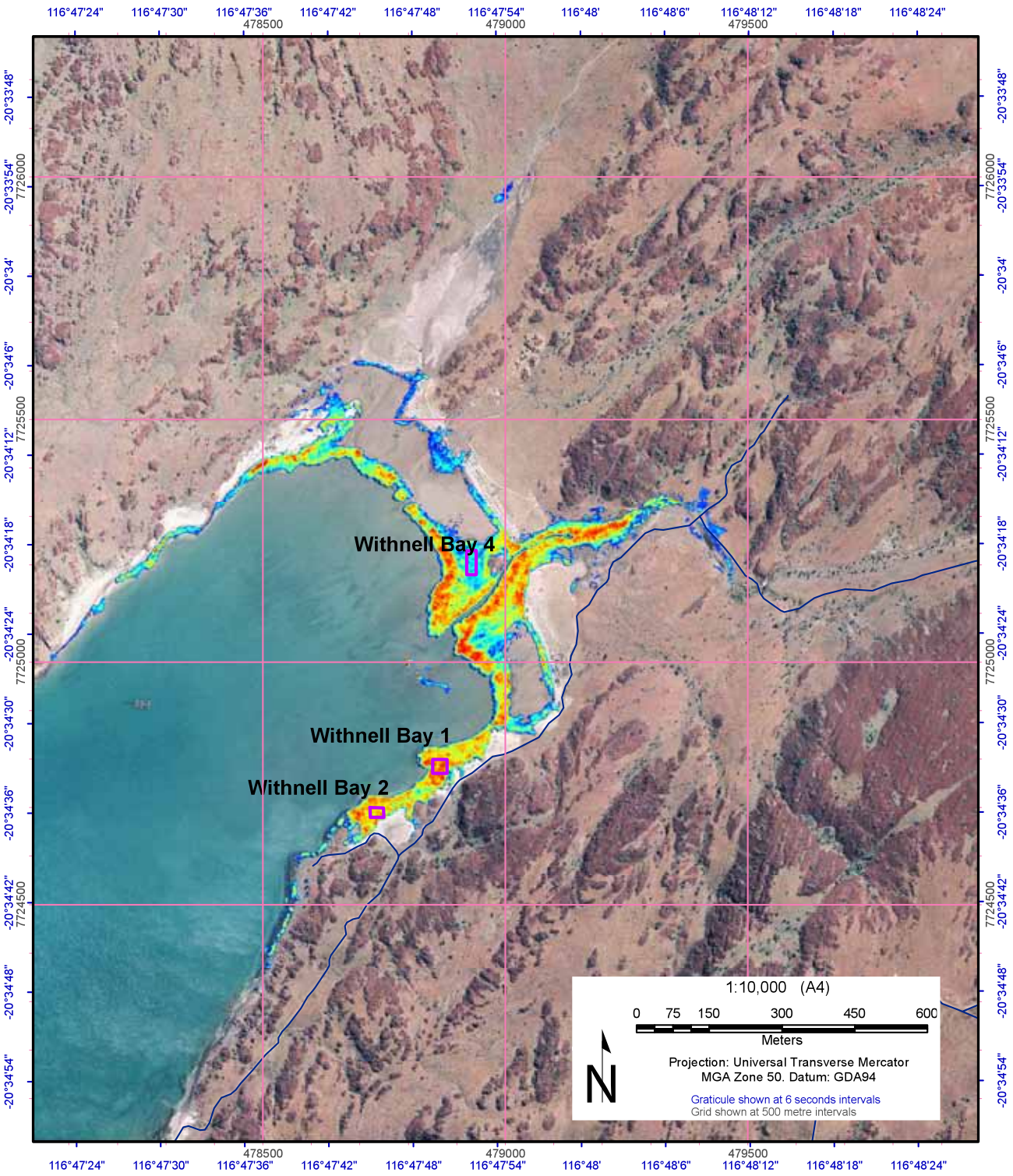

Figure 55. This map was created for navigation of Withnell Bay, highlighting the homogenous site locations, local roads and variations in the greenness of the mangrove canopy with QB2 NDVI enhancement overlaying 2004 aerial ortho-photography from Landgate.

Appendix 2. Field Observation Form for verifying remote sensing data.

Burrup Mangrove Field Observation Form

Site Number _____ Date _____ Recorded By _____

General Site Description
Site Location Description (location eg/ slope, roads, distance from track, major features eg/wetland, main vegetation, landscape type, vegetation height)

Across site estimates

Canopy cover % _____
Mid storey cover % _____
Ground cover % _____
Litter % _____
Exposed Soil % _____
100%

Shadow (% on ground) _____
Soil Colour _____

Site Measurements Choose 3 sites demonstrating the typical structure of the vegetation

Site 1 - Waypoint ID		Densiometer Reading (n/96)	
Latitude/Northing		GPS Quality - PDOP	
Longitude/Easting		Vegetation Height	
Canopy Cover %		Canopy Photo ID	
Site Vegetation Cover%		Photo ID & Direction	
Site 2 - Waypoint ID		Densiometer Reading (n/96)	
Latitude/Northing		GPS Quality - PDOP	
Longitude/Easting		Vegetation Height	
Canopy Cover %		Canopy Photo ID	
Site Vegetation Cover%		Photo ID & Direction	
Site 3 - Waypoint ID		Densiometer Reading (n/96)	
Latitude/Northing		GPS Quality - PDOP	
Longitude/Easting		Vegetation Height	
Canopy Cover %		Canopy Photo ID	
Site Vegetation Cover%		Photo ID & Direction	

Appendix 3. Protocol for canopy cover estimation and methods for completing the Field Observation Form.

Mangrove Vegetation Canopy Cover Estimation Methods for filling out the Field Observation form

Aim: To calibrate the imagery with ground measurements

Three point sites will be captured within the pre-selected homogenous sites. Homogenous sites are delineated by a polygon boundary with location extents.

Record keeping:

Site Number [ ] **Date** _____ **Recorded by**_____

General Site Description
Use the GPS waypoint to guide you into the centre of the homogeneous site, observe the landscape as you walk through the area, and record this in the **General site Description** and **Across site estimates.** *(If there is more than one GPS way point go to all and use these points as your plot sites).*

Site Location Description:

A general site description of each homogenous site should be recorded (location eg: slope (%), aspect, soil type, roads, distance from track, nearby major features eg/ wetland, main vegetation type, condition of vegetation or age of vegetation, landscape type, vegetation height). General tree height – use the poles marked every meter to estimate a range (to the nearest half metre).

Across site estimates:	**All fields should add to 100%**
Canopy cover	x %
Mid storey cover	x %
Ground cover	x %
Litter	x %
Exposed Soil	x %
Total	100%

Soil colour: in *absence of Mansell colour chart, do your best as describing the colour.*

Shadow (% on ground): *this may be difficult if it is early morning of midday, so try to imagine the shadow cast at 10.30am.*

Site Measurements
Within each homogenous area, three representative 5 by 5m plots will be selected randomly within the mangrove. In the absence of 5 m poles cross the 4m poles in the centre and imagine adding ½ a meter on the end of the poles to make a 5 by 5m plot area.

Each plot (5m by 5m area) is used to estimate canopy cover, site vegetation cover, vegetation height and take photos of canopy and site.

Site 1 - Waypoint ID	*Record from GPS*		
Take GPS Waypoint from the centre of the plot (cross of poles).See figure 1.			
Latitude/Northing *Of Waypoint*	*Record from GPS*	**GPS Quality - PDOP** *At waypoint*	*Record from GPS*
Longitude/Easting *Of Waypoint*	*Record from GPS*	**Vegetation Height**	*Use the poles to estimate*
Canopy Cover % *(Just live canopy cover)*	*Look directly up through the crown and use Crown Types Keys 1 or 2*	**Canopy Photo ID** *Turn camera skyward so that it is as level (use a tripod with level if can) and place under canopy. Use the timer to take photo. Try to take a photo that is representative of the canopy, See Figure 2.*	*Record from camera filename*
Site Vegetation Cover % *(all live vegetation cover including understorey and ground cover)*	*Use Crown Types Keys 1 or 2 and imagine a birds eye view of the site*	**Photo ID & Direction** *Take a few steps back and take a photo of the whole plot if possible. Use a compass for direction (not GPS)*	*Record from camera filename and compass direction*

If there is the opportunity:

Random Validation: Select areas outside the pre-selected homogenous sites. At each plot the site description (species composition), GPS location, shadow percentage (%), soil colour, canopy cover (%) and photos will be recorded, for use as validation for post processing and future mangroves monitoring work. Preferably these sites should be located in homogeneous areas.

Figure 1: Example of plot photo and GPS waypoint position.

Example 2: Example of a canopy photo.

Appendix 4. *Ground truthing field data.*

Table 9. Sample site canopy cover data, validation data, and corresponding coordinates gathered on site.

OBJECT ID	Homogenous site	Homogenous site code	WAYPOINT	Date	Vegetation height (m)	Site Vegetation Cover	Canopy Cover %	Densiometer	Comments	Canopy Photograph(s)	Canopy Photograph ID	Photo Canopy Cover	Site Photographs ID	Direction of Site Photograph	GPS EASTINGS	GPS NORTHINGS	Eastings	Northings	Latitude	Longitude
116	Withnell 4	I_With_4_50	WP28	12/5/2009	2	40	35	0		P5120110, P5120112, P5120113	P5120113. JPG	46	P5120114 - P5120115	SE, SW	478931	7725196	478931.00	7725196.00	-20.572091	116.797846
119	Withnell 1	I_With_1_85	WP26	12/5/2009	5.5	75	75	0		P512095	P5120095. JPG	90	P5120096 - P5120097	E	478866	7724792	478864.13	7724785.53	-20.575799	116.797199
120	Withnell 1	I_With_1_85	WP27	12/5/2009	4.5	80	80	0		P5120100	P5120100. JPG	88	P5120101 - P5120104	NE, E	478865	7724795	478871.81	7724796.53	-20.575700	116.797273
121	Withnell 2	I_With_2_85	WP23	12/5/2009	4	60	50	0		P5120085 - P5120086	P5120086. JPG	68	P5120087	NW	478728	7724690	478728.00	7724690.00	-20.576661	116.795892
122	Withnell 2	I_With_2_85	WP24	12/5/2009	3.5	65	60	0		P5120088, P5120089 (71.7%)	P5120088. JPG	75	P5120094, P5120093	S, W	478742	7724693	478742.00	7724693.00	-20.576634	116.796026
123	King Bay 3	I_King_3_70	WP23	11/5/2009	2	60	50	22		P5110014	P5110014. JPG	79	P5110058. JPG Brett	N	475629	7718673	475629.00	7718673.00	-20.630993	116.766074
124	King Bay 4	I_King_4_90	WP26	11/5/2009	4	70	65	11		P5110036 - P5110039	P5110038. JPG	76	P5110040 - P5110041	NE	475349	7718396	475350.33	7718393.06	-20.633519	116.763395
125	King Bay 2	I_King_2_55	WP24	11/5/2009	3	31	30	49		P5110020	P5110020. JPG	66	P5110021, P5110022	W	475663	7718723	475663.00	7718723.00	-20.630541	116.766401
126	King Bay 2	I_King_2_55	WP25	11/5/2009	0.9	65	55	17		P5110023	P5110023. JPG	64	P5110024, P5110026		475659	7718733	475659.00	7718733.00	-20.630451	116.766362
184	Cowie Cove 1	UI_C_1_60	WP26	13/5/2009	2.5	55	50	22		P5130175 (76%),P5130176 (70%)	P5130176. JPG	70	P5130177 - P5130179	S	480316	7722058	480314.49	7722057.18	-20.600468	116.811085
186	Cowie Cove 1	UI_C_1_60	WP28	13/5/2009	3	40	35	30		P5130180 subset (49%)	P5130180. JPG	49	P5130181, P5130182	SE	480318	7722046	480315.37	7722045.37	-20.600575	116.811093
187	Cowie Cove 2	UI_C_2_65	WP23	14/5/2009	3	40	35	32		P5140220 (52%), 222 (38%) 223 (44.5%)	P5140223. JPG	44	P5140224 - P5140225	N	480097	7721436	480096.91	7721437.00	-20.606070	116.808990
188	Cowie Cove 2	UI_C_2_65	WP24	14/5/2009	2.5	50	40	28		227, 229(71.9%), P5140230 subset(70.4%) - P5140231,	P5140229. JPG	72	P5140233 - P5140232	233-232	480089	7721423	480090.50	7721422.79	-20.606198	116.808928
191	Cowie Cove 4	UI_C_4_45	WP25	14/5/2009	2	45	40	24		P5140234 - P5140236	P5140234. JPG	74	P5140237 - P5140239	W	479973	7721446	479971.86	7721446.81	-20.605980	116.807790
192	Cowie Cove 4	UI_C_4_45	WP26	14/5/2009	2	40	35	42		P5140240 - P5140241(53.9%)	P5140241. JPG	54	P5140242 - P5140243	SW	479955	7721452	479955.36	7721452.14	-20.605932	116.807632
201	Cowie Cove 5	UI_C_5_90	WP23	13/5/2009	5-Jun	66	65	10		P5130152 (72 all or 66 for subset)	P5130152. JPG	72	P5130153 - P5130154	SE	480639	7722063	480641.68	7722064.56	-20.600405	116.814225
202	Cowie Cove 5	UI_C_5_90	WP24	13/5/2009	4-May	80	75	5		P5130155	P5130155. JPG	89	P5130156 - P5130157	N	480635	7722070	480638.55	7722071.20	-20.600345	116.814195
203	Cowie Cove 6	UI_C_6_70	WP29	13/5/2009	3	40	35	30		186,187(looks very similar but has bare branches)	P5130186. JPG	44	P5130188, P5130189	NW	480257	7722005	480256.72	7722006.38	-20.600927	116.810530

OBJECT ID	Homogenous site	Homogenous site code	WAYPOINT	Date	Vegetation height (m)	Site Vegetation Cover	Canopy Cover %	Densiometer	Comments	Canopy Photograph(s)	Canopy Photograph ID	Photo Canopy Cover	Site Photographs ID	Direction of Site Photograph	GPS EASTINGS	GPS NORTHINGS	Eastings	Northings	Latitude	Longitude
204	Cowie Cove 6	UI_C_6_70	WP30	13/5/2009	3	45	35	20	densiometer second reading 33	P5130190(38.5%), P5130191 (39.2%) - P5130192 (35.7%)	P5130192.JPG	36	P5130193, P5130194	SW	480239	7721997	480240.75	7721997.33	-20.601008	116.810377
205	Cowie Cove 7	UI_C_7_45	WP31	13/5/2009	1	30	30	47		P5130195 - P5130197	P5130196.JPG	46	P5130198 - P5130199	SW	479997	7721829	479997.12	7721829.75	-20.602520	116.808037
206	Cowie Cove 7	UI_C_7_45	WP32	13/5/2009	1.2	25	25	44		P5130200	P5130200.JPG	38	P5130201	NE	480000	7721814	480001.12	7721814.26	-20.602660	116.808075
209	King Bay 1	I_KING_1_85	WP31	14/5/2009	5.5	70	65	16		P5130250	P5140250.JPG	76	P5140251 - P5140253	E	475047	7718100	475046.58	7718097.16	-20.636188	116.760475
210	King Bay 1	I_KING_1_85	WP32	14/5/2009	3	65	65	19		P5130254	P5140254.JPG	80	P5140255, P5140256	S	475056	7718126	475055.39	7718125.95	-20.635928	116.760560
Validation sites																				
118		I_With_4_50	WP31	12/5/2009	3	30	30	0	Validation, last mangrove tree in tidal creek.	P5120128, P5120127subset	P5120127.JPG	33	P5120125, P5120126	W, E	479375	7725318	479375.00	7725318.00	-20.570993	116.802107
117		I_With_4_50	WP30	12/5/2009	3	50	50	0	Validation, Ceria australis, inner edge of stand.	P5120122	P5120122.JPG	61	P5120123 - P5120124	E	478951	7725336	478951.00	7725336.00	-20.570826	116.798039
207		UI_C_7_45	WP30	13/5/2009	1	25	25	0	Validation, Cowie cover, GPS died while writing coordinates	P5140247	P5140247.JPG	47	P5140248, P5140249	E	479755	7721463	479924.95	7721750.54	-20.603235	116.807343
Additional Ground Truthing Waypoint for Extent																				
193	Cowie Cove		WP27	14/5/2009					Last mangrove in tidal creek Cowie cove						479785.57	7721254.2	479785.57	7721254.21	-20.607718	116.806000
194	Cowie Cove		WP28	14/5/2009					Last mangrove in tidal creek Cowie cove						479787.13	7721253.7	479787.14	7721253.66	-20.607723	116.806015
195	Cowie Cove		WP29	14/5/2009					Looking at mud site				P5140246	N	479761.6	7721253.8	479761.61	7721253.81	-20.607722	116.805770

Table 10. Homogenous site general description and characteristics, including the general site canopy cover at all levels of the canopy, soil colour, shadow estimate, species type, and slope.

OBJECT ID	Homogenous site	Homogenous site code	Canopy Estimate (%)	Mid Storey Estimate (%)	Ground Cover Estimate (%)	Litter Estimate (%)	Exposed Soil (%)	Shadow Estimate (%)	Soil Colour	Location	Vegetation	Slope	Other
40	King Bay 1	I_KING_1_85	65	5	0	1	29	70	grey brown	intertidal mangrove	Avicenna marina 5-6m, old with many large hollows with small young Rhizophora stylosa	1%	uneven ground, e site sand bar (shells 1 inch), w pools- not used
41	King Bay 2	I_KING_2_55	40	10	0	1	49	95	dark brown	intertidal mangrove	Avicenna marina 3-3.5m, air holes in mud, few young mangroves	2	muddy exposed, some shells, sea eagle, green budgies fly over
42	King Bay 3	I_KING_3_70	64	30	0	1	5	90	dark brown	intertidal mangrove	Rhizophora stylosa 1-2.5m, dense roots and canopy, difficult to move , low tide	1	part site has white beach sand slope up to land, but most has is over mud and flat
43	King Bay 4	I_KING_4_90	55	15	10	10	10	75	brown	mangrove intertidal	Avicenna marina, many phophores, high leaf litter, high# seedlings, drift wood and rubbish	flat	uneven ground (Mud), little puddles, shells in mud
37	Withnell 1	I_With_1_85	85	0	0	5	10	80	grey/cream & shell	intertidal mangrove, tidal creek, west of site	Avicenna marina 5.5m, no understorey, some leaf litter, birds present, oysters amongst shells	flat	
38	'Withnell 2	I_WITH_2_85	50	15	0	5	30	40	light brown, cream & dark pebble	intertidal mangrove	Avicenna marina 2.5-4m high, some small mangroves, some gastropods,	1%	shells in course sand
39	'Withnell 4	I_WITH_4_50	5	35	0	1	59	35	light brown/ yellow	intertidal mangrove	Low Avicenna marina 1.5-2m, some seedlings	1%	pebbles 1inch square dark
18	Cowie Cove 1	UI_C_1_60	25	20	0	0	54	60	brown/grey	intertidal mangrove	Patchy Avicenna marina 2.5m, quite eaten a few seedlings	1%	muddy
32	Cowie Cove 2	UI_C_2_65	30	30	0	1	39	50	dark grey & creamy specs	intertidal mangrove,176m from road	Avicenna marina 3-3.5m, with few small young Rhizophora stylosa	1%	wet mud with phorohores
33	Cowie Cove 4	UI_C_4_45	10	30	0	1	59	50	grey brown	intertidal mangrove, 100m from track	Avicenna marina 1.5-2m, sparser apart but denser leaves, many bare branches, some sincessing	flat	uneven mud
34	Cowie Cove 5	UI_C_5_90	65	10	0	1	24	70	cream sand and grey brown shell	intertidal mangrove	Rhizophora stylosa 5-6m, really dense, lots roots, difficult to move	flat	mud
35	Cowie Cove 6	UI_C_6_70	40	10	0	1	49	60	grey brown & shells	intertidal mangrove	Avicenna marina 2.5-3m, few branches on ground, large conical gastropods,	<5	course sand white and red, large grasshoppers, dragonfly, sea eagles
36	Cowie Cove 7	UI_C_7_45	0	50	0	1	49	30	light grey brown tinge	intertidal mangrove, 200m from track	Stunted Avicenna marine <1m in height, seedlings present	flat	uneven ground, mud with shells and lots of holes- bioturbulation

Table 11. Sample site canopy cover data for each field method averaged per homogenous site, including the calculated PFC(f) values.

Homogenous site	Homogenous site code	Air Photo Estimate	Air Photo Estimate 2	Vegetation Cover	PFC(cc)	PFC(vc)	Average Canopy Cover	Densiometer	Densiometer corrected	Densiometer cover	Canopy Photo(%)	PFC(pvc)	PFC(p
King Bay 1	I_KING_1_85	85.0	90.0	67.5	55.3	43.9	65.0	17.5	18.2	81.8	78.0	52.7	66.3
King Bay 2	I_King_2_55	55.0	60.0	48.0	23.4	20.4	42.5	33.0	34.3	65.7	65.0	31.2	35.8
King Bay 3	I_King_3_70	70.0	75.0	60.0	35.0	30.0	50.0	22.0	22.9	77.1	79.0	47.4	55.3
King Bay 4	I_King_4_90	90.0	80.0	70.0	58.5	45.5	65.0	11.0	11.4	88.6	76.0	53.2	68.4
Withnell 1	I_With_1_85	85.0	85.0	77.5	65.9	60.1	77.5	0.0	0.0	0.0	89.0	69.0	75.7
'Withnell 2	I_With_2_85	85.0	80.0	62.5	46.8	34.4	55.0	0.0	0.0	0.0	71.5	44.7	60.8
'Withnell 4	I_With_4_50	50.0	45.0	40.0	17.5	14.0	35.0	0.0	0.0	0.0	46.0	18.4	23.0
Cowie Cove 1	UI_C_1_60	60.0	60.0	47.5	25.5	20.2	42.5	26.0	27.0	73.0	59.5	28.3	35.7
Cowie Cove 2	UI_C_2_65	65.0	75.0	45.0	24.4	16.9	37.5	30.0	31.2	68.8	58.0	26.1	37.7
Cowie Cove 4	UI_C_4_45	45.0	40.0	42.5	16.9	15.9	37.5	33.0	34.3	65.7	64.0	27.2	28.8
Cowie Cove 5	UI_C_5_90	90.0	90.0	73.0	63.0	51.1	70.0	7.5	7.8	92.2	80.5	58.8	72.5
Cowie Cove 6	UI_C_6_70	70.0	65.0	42.5	24.5	14.9	35.0	25.0	26.0	74.0	40.0	17.0	28.0
Cowie Cove 7	UI_C_7_45	45.0	50.0	27.5	12.4	7.6	27.5	45.5	47.3	52.7	42.0	11.6	18.9

Appendix 5. Imagery data values per homogenous site.

Table 12. Averaged DMSI imagery values for each band and indices applied per homogenous site. Values were extracted from edited boundaries of the homogenous site.

DMSI

SITE	Band1	Band2	Band3	Band4	Band4-Band3	NDVI
I_KING_1_85	441.4	552.1	365.7	1113.5	747.9	0.51
I_King_2_55	417.1	508.6	352.3	1126.0	773.7	0.52
I_King_3_70	367.1	416.3	267.8	1054.3	786.5	0.59
I_King_4_90	406.0	528.5	324.9	1133.7	808.8	0.55
I_With_1_85	401.9	476.4	304.6	988.6	684.0	0.53
I_With_2_85	362.5	424.1	263.5	911.9	648.4	0.55
I_With_4_50	462.4	574.1	406.4	974.2	567.8	0.41
UI_C_1_60	416.5	522.3	330.5	1095.4	764.9	0.54
UI_C_2_65	413.6	517.0	331.3	1080.3	749.0	0.53
UI_C_4_45	467.2	585.2	409.3	1017.0	607.7	0.43
UI_C_5_90	330.3	359.8	214.1	1015.4	801.4	0.65
UI_C_6_70	413.7	498.1	319.1	976.2	657.1	0.51
UI_C_7_45	609.2	767.3	598.8	929.8	331.0	0.22

Table 13. Averaged QB2 imagery values for each band and indices applied per homogenous site.

QB2

SITE	Band1	Band2	Band3	Band4	Band4-Band3	NDVI
I_KING_1_85	261.3	376.2	233.9	557.3	323.5	0.41
I_King_2_55	270.6	394.8	262.9	488.1	225.2	0.30
I_King_3_70	254.3	348.4	220.8	405.4	184.5	0.29
I_King_4_90	267.0	396.8	252.5	608.6	356.1	0.41
I_With_1_85	268.4	394.7	241.2	641.4	400.2	0.45
I_With_2_85	272.8	402.8	248.8	607.6	358.8	0.42
I_With_4_50	283.5	421.0	279.3	518.3	239.0	0.30
UI_C_1_60	279.1	412.1	258.8	591.8	333.0	0.39
UI_C_2_65	284.6	426.6	274.0	607.8	333.8	0.38
UI_C_4_45	293.9	433.4	292.4	485.9	193.5	0.25
UI_C_5_90	245.3	334.8	188.5	529.4	340.9	0.47
UI_C_6_70	283.2	416.6	265.8	560.6	294.8	0.36
UI_C_7_45	332.8	518.7	372.8	548.3	175.5	0.19

AVNIR 2

SITE	Band1	Band2	Band3	Band4	Band4-Band3	NDVI
I_KING_1_85	85.4	66.3	49.5	68.8	19.3	0.16
I_King_2_55	86.3	67.0	55.6	51.3	-4.2	-0.04
I_King_3_70	80.5	57.3	42.5	48.3	5.8	0.06
I_King_4_90	85.0	66.5	51.2	67.2	16.0	0.14
I_With_1_85	84.7	66.2	47.7	75.6	27.9	0.23
I_With_2_85	85.3	66.7	49.3	68.3	19.0	0.16
I_With_4_50	88.6	72.4	60.8	55.0	-5.8	-0.05
UI_C_1_60	87.3	70.2	53.5	61.5	8.0	0.07
UI_C_2_65	88.7	72.8	55.5	65.3	9.8	0.08
UI_C_4_45	96.4	81.4	71.8	53.0	-18.8	-0.15
UI_C_5_90	80.5	55.2	36.7	65.5	28.8	0.28
UI_C_6_70	88.9	70.4	55.8	57.0	1.3	0.01
UI_C_7_45	105.9	98.7	93.4	62.6	-30.9	-0.20

Table 14. Mangrove transect raw data.

Study Site	Site	Transect	Date	GPS start Lat			GPS start Long			GPS end Lat			GPS end Long			<1m	1-2m	>2m	# healthy	# sick	# dead	primary species	secondary species	Photo #'s
				Degrees	Minutes	Seconds	Degrees	Minutes	Seconds	Degrees	Minutes	Seconds	Degrees	Minutes	Seconds									
Withnell Bay	WB2	1	12 May 2009	20	34	35.9	116	47	45.1	20	34	35.9	116	47	45.3	1	0	4	5	0	0	Avicennia marina	-	75-82
Withnell Bay	WB2	2	12 May 2009	20	34	35.8	116	47	45.6	20	34	35.9	116	47	45.6	0	0	4	4	0	0	Avicennia marina	-	83-89
Withnell Bay	WB1	1	12 May 2009	20	34	32.8	116	47	50.0	20	34	32.9	116	47	50.0	0	0	2	1	1	0	Avicennia marina	-	90-100
Withnell Bay	WB1	2	12 May 2009	20	34	32.6	116	47	50.2	20	34	32.4	116	47	50.1	0	0	9	9	0	0	Avicennia marina	-	101-115
Withnell Bay	WB4	1	12 May 2009	20	34	19.6	116	47	52.3	20	34	19.5	116	47	52.2	52	1	1	54	0	0	Avicennia marina	-	116-128
Cowrie Cove	CC5	1	13 May 2009	20	36	1.5	116	48	51.3	20	36	1.3	116	48	51.2	14	0	6	19	1	0	Rhizophora stylosa	Avicennia marina	132-139
Cowrie Cove	CC5	2	13 May 2009	20	36	1.2	116	48	51.0	20	36	1.2	116	48	51.1	0	0	5	5	0	0	Rhizophora stylosa	-	140-149
Cowrie Cove	CC1	1	13 May 2009	20	36	1.6	116	48	39.9	20	36	1.8	116	48	40.0	0	0	12	12	0	0	Avicennia marina	-	150-158
Cowrie Cove	CC1	2	13 May 2009	20	36	2.1	116	48	40.0	20	36	2.0	116	48	39.8	0	0	5	5	0	0	Avicennia marina	-	159-167
Cowrie Cove	CC6	1	13 May 2009	20	36	3.4	116	48	38.0	20	36	3.3	116	48	37.9	0	2	10	11	1	0	Avicennia marina	-	168-173
Cowrie Cove	CC6	2	13 May 2009	20	36	3.5	116	48	37.4	20	36	3.6	116	48	37.2	3	11	6	20	0	0	Avicennia marina	-	174-181
Cowrie Cove	CC7	1	14 May 2009	20	36	9.0	116	84	29.1	20	36	9.1	116	48	28.9	42	0	0	42	0	0	Avicennia marina	-	182-187
Cowrie Cove	CC7	2	14 May 2009	20	36	9.5	116	48	29.0	20	36	9.6	116	48	29.2	37	0	0	32	1	4	Avicennia marina	-	188-192
Cowrie Cove	CC2	1	14 May 2009	20	36	22.0	116	48	32.4	20	36	21.8	116	48	32.4	1	2	23	21	5	0	Avicennia marina	Rhizophora stylosa	197-204
Cowrie Cove	CC2	2	14 May 2009	20	36	22.2	116	48	32.1	20	36	22.3	116	48	32.1	28	50	9	80	1	6	Avicennia marina	Rhizophora stylosa	205-216
Cowrie Cove	CC4	1	14 May 2009	20	36	21.5	116	48	28.0	20	36	21.6	116	48	28.1	3	10	2	14	0	1	Avicennia marina	-	217-229
Cowrie Cove	CC4	2	14 May 2009	20	36	21.2	116	48	27.5	20	36	21.4	116	48	27.4	1	13	4	16	2	0	Avicennia marina	-	230-238
King Bay	KB1	1	14 May 2009	20	38	10.2	116	54	37.8	20	38	10.1	116	45	37.7	3	0	4	7	0	0	Avicennia marina	-	239-251
King Bay	KB1	2	14 May 2009	20	38	9.4	116	45	37.9	20	38	9.2	116	45	38.1	15	0	5	20	0	0	Avicennia marina	Rhizophora stylosa	252-259
King Bay	KB3	1	11 May 2009	20	37	51.6	116	45	57.8	20	37	51.6	116	45	57.8	0	0	10	10	0	0	Rhizophora stylosa	Avicennia marina	51-58
King Bay	KB2	1	11 May 2009	20	37	50.0	116	45	59.1	20	37	49.9	116	45	59.1	21	1	2	23	1	0	Avicennia marina	-	58-65
King Bay	KB2	2	11 May 2009	20	37	49.7	116	45	58.9	20	37	49.7	116	45	58.9	13	2	7	21	1	0	Avicennia marina	-	65-69
King Bay	KB4	1	11 May 2009	20	38	0.7	116	45	48.3	20	38	0.7	116	45	48.3	186	0	2	188	0	0	Avicennia marina	-	69-74

Table 15. Water and sediment sample data from mangrove transects.

Site	Transect	Water Quality														Sediment quality									
		Time	°C	pH	pH mV	ORP	DO %	DO mg/l	mS/cm	mS/cm A	TDS mg/l	Salinity	sigma t	mbar	Moisture %	TPH C6-C9 mg/kg	TPH C10-C14 mg/kg	TPH C15-C28 mg/kg	TPH C29-C36 mg/kg	Total TPH mg/kg	Cd mg/kg	Cr mg/kg	Cu mg/kg	Fe mg/kg	Pb mg/kg	Ni mg/kg	Zn mg/kg
WB2	1	07:29:00	22.08	6.58	16.8	-126.4	13.9	0.89	88.440	83.530	44220	62.91	45.6	1062.7	44	<25	<50	<100	<100	<275	<1	17.0	2.8	6500.0	1.8	7.5	11.0
WB2	2	07:51:39	20.91	6.90	-2.7	-25.0	45.7	3.07	80.720	74.450	40360	56.57	41.1	1063.1													
WB1	1	08:14:55	19.67	6.93	-4.5	-124.4	21.4	1.57	67.260	60.460	33630	45.88	33.2	1063.4	29	<25	<50	<100	<100	<275	<1	5.5	1.2	3100.0	1.7	2.6	6.6
WB1	2	08:45:45	21.32	6.79	3.9	-369.7	0.0	0.00	64.230	59.740	32120	43.52	30.9	1063.4													
WB4	1	09:40:39	21.11	6.43	25.2	-161.6	7.7	0.51	84.260	78.020	42130	59.45	43.2	1064.8													
CC5	1	07:05:16	22.94	6.91	-3.3	-304.9	19.5	1.41	57.130	54.890	28560	38.08	26.3	1062.4	58	<25	<50	<100	<100	<275	<1	55.0	11.0	17000.0	3.0	20.0	18.0
CC5	2	07:34:17	22.45	6.62	14.4	-313.9	17.3	1.24	62.510	59.480	31250	42.18	29.6	1063.4													
CC1	1	08:25:33	21.63	6.72	8.0	-166.4	16.3	1.10	77.140	72.210	38570	53.67	38.6	1063.9	41	<25	<50	<100	<100	<275	<1	56.0	8.4	16000.0	3.2	21.0	18.0
CC1	2	08:41:07	21.93	6.73	7.5	-87.3	18.5	1.28	70.650	66.540	35330	48.51	34.5	1063.9													
CC6	1	09:05:53	21.56	6.71	8.6	-150.5	8.4	0.60	66.150	61.830	33080	45.00	32.0	1064.8													
CC6	2	09:36:35	22.23	6.65	12.5	-213.3	15.7	1.05	77.700	73.610	38850	54.11	38.8	1065.4													
CC7	1	10:03:31	21.79	7.30	-24.9	-66.7	25.0	1.69	77.760	73.030	38880	54.17	38.9	1066.2	35	<25	<50	<100	<100	<275	<1	47.0	6.3	13000.0	2.1	17.0	15.0
CC7	2	10:22:03	20.87	6.98	-7.3	-201.1	18.7	1.21	89.860	82.800	44930	64.10	46.9	1067.1													
CC2	1	07:01:38	21.69	6.62	3.8	-31.2	3.2	0.23	65.130	61.040	32570	44.21	31.3	1063.2	32	<25	<50	<100	<100	<275	<1	34.0	5.6	9500.0	2.3	14.0	12.0
CC2	2	07:28:08	19.67	6.89	-12.3	-39.6	9.8	0.72	66.570	59.820	33280	45.34	32.8	1063.2													
CC4	1	08:00:06	20.70	6.59	5.1	-254.3	1.8	0.11	91.070	83.630	45540	65.11	47.7	1063.5													
CC4	2	08:20:53	19.85	6.57	6.3	-192.5	2.3	0.15	94.280	85.050	47140	67.81	50.0	1064.3													
KB1	1	10:28:01	20.78	6.91	-14.0	-333.6	0.0	0.00	64.860	59.660	32430	44.01	31.4	1065.9													
KB1	2	10:38:11	20.48	6.70	-1.0	-256.8	0.0	0.00	66.710	60.980	33360	45.45	32.6	1065.7													
KB3	1	07:53:49	19.64	7.28	-25.5	223.9	0.0	0.00	60720	54540	30360	40.85	29.3	101.49	50	<25	<50	<100	<100	<275	<1	63.0	18.0	29000.0	7.1	25.0	38.0
KB2	1	08:54:18	16.94	8.66	-93.6	232.1	70.1	5.25	63240	53550	31620	42.75	31.5	101.53	44	<25	<50	<100	<100	<275	<1	40.0	11.0	23000.0	5.2	18.0	27.0
KB2	2	09:25:51	19.97	7.13	-18.0	208.7	0.0	0.00	72440	65520	36220	49.94	36.2	101.64													
KB4	1	10:26:53	20.76	7.82	-52.2	156.3	15.4	1.06	65990	60670	32990	44.88	32.1	101.66													

Table 16. Flagged tree transects.

Study Site	Site	Date	GPS Lat			GPS Long			trunk diam @1m (cm)	% herbivory	# propagule	leaves		
			Degrees	Minutes	Seconds	Degrees	Minutes	Seconds				% healthy	% sick	% dead
Withnell Bay	WB2	12 May 2009	20	34	35.8	116	47	45.2	30.7	80	0	90	5	5
Withnell Bay	WB1	12 May 2009	20	34	32.8	116	47	49.9	39.4	100	0	40	50	10
Withnell Bay	WB4	12 May 2009	20	34	19.6	116	47	52.3	17.0	60	0	80	10	10
Cowrie Cove	CC5	13 May 2009	20	36	1.4	116	48	51.3	21.0	75	6	90	5	5
Cowrie Cove	CC1	13 May 2009	20	36	1.6	116	48	39.9	20.5	90	0	90	5	5
Cowrie Cove	CC6	13 May 2009	20	36	3.3	116	48	37.9	15.0	60	0	80	15	5
Cowrie Cove	CC7	14 May 2009	20	36	9.1	116	48	29.1	4.0	50	0	90	5	5
Cowrie Cove	CC2	14 May 2009	20	36	21.9	116	48	32.4	26.0	60	0	100	0	0
Cowrie Cove	CC4	14 May 2009	20	36	21.6	116	48	28.1	12.0	80	0	90	5	5
King Bay	KB1	14 May 2009	20	38	10.3	116	45	37.8	42.0	80	0	75	15	10
King Bay	KB3	11 May 2009	20	37	51.8	116	45	57.7	26.0	70	0	10	70	20
King Bay	KB2	11 May 2009	20	37	50.0	116	45	59.1	25.8	70	0	10	80	10
King Bay	KB4	11 May 2009	20	38	0.6	116	45	48.3	71.0	30	0	25	50	25

Table 17. Intertidal mudflat transect raw data.

Study Site	Site	Date	GPS start Lat			GPS start Long			GPS end Lat			GPS end Long			Grain size		
			Degrees	Minutes	Seconds	Degrees	Minutes	Seconds	Degrees	Minutes	Seconds	Degrees	Minutes	Seconds	% >2mm	% 1-2mm	% <1mm
Withnell Bay	WB mud	12 May 2009	20	34	12.6	116	47	51.8	20	34	17.5	116	47	54.8	10	25	65
Cowrie Cove	CC mud1	14 May 2009	20	36	26.9	116	48	20.9	20	36	27.3	116	48	16.9	10	0	90
Cowrie Cove	CC mud2	14 May 2009	20	36	8.1	116	48	24.8	20	36	4.5	116	48	27.8	35	45	20
King Bay	KB mud	11 May 2009	20	37	47.2	116	46	4.1	20	37	47.5	116	46	7.1	10	10	80

Table 18. Water and sediment sample data from intertidal mudflat transects.

Site	Time	Water Qualiity												Sediment Quality								
		°C	pH	pH mV	ORP	DO %	DO mg/l	mS/cm	mS/cm A	TDS mg/l	Salinity	sigma t	mbar	moisture %	TPH C6-C9 mg/kg	TPH C10-C14 mg/kg	TPH C15-C28 mg/kg	TPH C29-C36 mg/kg	Total TPH mg/kg	Cd mg/kg	Cr mg/kg	Cu mg/kg	Fe mg/kg	Pb mg/kg
WB mud	09:55:37	24.83	7.60	-41.4	-17.2	29.6	2.20	43.730	43.590	21860	28.19	18.3	1065.4	29	<25	<50	<100	<100	<275	<1	14.0	2.9	8700.0	1.7
CC mud1	08:55:51	20.59	7.53	-47.6	-2.7	20.8	1.03	140.600	128.800	70290	70.00	50.0	1065.4	19	<25	<50	<100	<100	<275	<1	41.0	8.3	16000.0	3.0
CC mud2	09:26:24	20.94	7.98	-72.1	-185.6	0.4	0.03	59.380	54.800	29690	39.82	28.2	1066.5	15	<25	<50	<100	<100	<275	<1	23.0	13.0	16300.0	2.2
KB mud	09:50:57	19.33	6.15	32.1	302.3	14.4	1.11	48600	43370	24300	31.81	22.5	101.64	27	<25	<50	<100	<100	<275	<1	33.0	10.0	22300.0	5.6

Appendix 7. Transect test results.

Table 19. Observations and ranking score from the transect validation test, investigating the suitability of images derived from the transformations of FPC (cc) to AVNIR -2 NDVI and QB-2 NDVI.

	Sensor			
	AVNIR-2		QB2	
Transects	Ranking	Comments	Ranking	Comments
‘Transect 1 Withnell Bay	0	Too low in high values too high in low.	0	Better than ALOS but too low
Transect 2 Withnell Bay	0	Too low	0	Good low and mid- bad high
Transect 3 Withnell Bay	0	Too low	0	Too low
‘Transect 1 King Bay	0	Too low	0	Too low
Transect 2 King Bay	0	Too low	1	Better than ALOS but Too low
Transect 3 King Bay	0	Too low	0	Too low
‘Transect 1 Cowrie Cove	0	Too low	0	Too low
Transect 2 Cowrie Cove	0	Too low	0	Too low
Transect 3 Cowrie Cove	0	-	1	Better than ALOS but too low
Total Ranking (excluding #0)	0		2	

Table 20. Observations and ranking score from the transect validation test, investigating the suitability of images derived from the transformations of FPC (cv) to AVNIR -2 NDVI, QB-2 NDVI and DMSI NDVI.

	Sensor					
	AVNIR-2		QB2		DMSI	
Transects	Ranking	Comments	Ranking	Comments	Ranking	Comments
‘Transect 1 Withnell Bay	0	Too low	0	Too low	0	Not high enough, but good on low values
Transect 2 Withnell Bay	1	Might be too low on high values	1	Ok	2	Maybe not high enough
Transect 3 Withnell Bay	0	Too low	0	Too low	1	Maybe not high enough
‘Transect 1 King Bay	0	Too low	0	Too low in high range	1	Maybe not high enough
Transect 2 King Bay	1	Might be too low on high values	0	Too low	0	Not high enough, but good on low values
Transect 3 King Bay	1	Ok	0	Too low	0	Not high enough, but good on low values
‘Transect 1 Cowrie Cove	0	Too low	1	Too low in low range and ok in high	1	Maybe not high enough
Transect 2 Cowrie Cove	0	Too low	0	Too low	0	Too low all over
Transect 3 Cowrie Cove	0	Too low	0	Too low	0	Too low all over
Total Ranking (excluding #0)	3		3		5	

Table 21. Observations and ranking score from the transect validation test, investigating the suitability of images derived from the transformations of FPC (p) to AVNIR -2 NDVI, QB-2 NDVI, DMSI NDVI.

	Sensors							
	AVNIR-2		QB2		DMSI- NDVI		DMSI- Band 3	
Transects	Ranking	Comments	Ranking	Comments	Ranking	Comments	Ranking	Comments
'Transect 1 Withnell Bay	1	Maybe too low on large values	1	Maybe a little too high at top and low at bottom	0	Too low in high range	1	Maybe too low
Transect 2 Withnell Bay	2		2		2		2	
Transect 3 Withnell Bay	2	Maybe too low on large values	1	Too low	1	Too low in high range	1	Maybe too low
'Transect 1 King Bay	2		1		1	Too low in high range	1	Too low in high range
Transect 2 King Bay	1		2		1	Too low in high range	0	Too low in high range and ranks shadow higher than tree
Transect 3 King Bay	2		1		1	Too low in high range	0	Too low in high range and ranks shadow higher than tree
'Transect 1 Cowrie Cove	2		2		2		0	Too low in high range and ranks shadow higher than tree
Transect 2 Cowrie Cove	1	'Maybe too low on high values	2		1	Too low in high range, very sparse not included but this could be samphire	0	Shadow has higher values
Transect 3 Cowrie Cove	2		2		2		0	Shadow has higher values
Total Ranking (excluding #0)	15	0	14	0	11	0	5	0

Table 22. Observations and ranking score from the transect validation test, investigating the suitability of images derived from the transformations of the densiometer cover to AVNIR -2 NDVI, QB-2 NDVI, DMSI NDVI and DMSI and Band 3.

	Sensors							
	AVNIR-2 NDVI		QB2 NDVI		DMSI NDVI		DMSI Band 3	
Transects	Ranking	Comments	Ranking	Comments	Ranking	Comments	Ranking	Comments
'Transect 1 Withnell Bay	1	Low values may not be low enough	1	Bit too high	0	Low range too high	1	Too high in low range
Transect 2 Withnell Bay	0	Too high	0	High in low areas	0	Low range too high	2	Too high in low range
Transect 3 Withnell Bay	2	Most high and med	1	High in zero areas	1		1	Values in water
'Transect 1 King Bay	0	Too high	1	High in zero areas	1	Low range too high	1	
Transect 2 King Bay	1	Low values may not be low enough	0	Too high	1	Low range too high	0	Too high in low range and ranks shadow higher than tree
Transect 3 King Bay	1	Low values may not be low enough	1	High in zero areas	1	Low range too high	0	Too high in shadows
'Transect 1 Cowrie Cove	0	Too high	0	Too high	0	All range too high	0	Too high
Transect 2 Cowrie Cove	0	Too high	0	High in zero areas	1	Bare is not 0	0	Low range good, but shadow in high range
Transect 3 Cowrie Cove	0	Too high	0	Too high in low areas	0	Too high	0	Low range good, but shadow in high range
Total Ranking (excluding #0)	5		4		5		5	

Table 23. Observations and ranking score from the transect validation test, investigating the suitability of images derived from the transformations of photo canopy estimate to DMSI NDVI and DMSI Band 3.

	Sensors			
	DMSI Photo % NDVI		DMSI Photo % Band 3	
Transects	Ranking	Comments	Ranking	Comments
'Transect 1 Withnell Bay	2		1	may be a little too high
Transect 2 Withnell Bay	1	may be a little too high in low range	1	may be a little too high in low range
Transect 3 Withnell Bay	1	may be a little too high in low range	1	may be a little too high in low range
'Transect 1 King Bay	1	may be a little too high in low range	2	
Transect 2 King Bay	2		1	may be a little too high in low range
Transect 3 King Bay	2	bare has values	1	but shadow higher
'Transect 1 Cowrie Cove	2	bare has values	1	but shadow higher
Transect 2 Cowrie Cove	2	bare is not 0, but very low	1	but shadow higher
Transect 3 Cowrie Cove	1	bare is not 0, but very low	0	
Total Ranking (excluding #0)	14	0	9	